

AD-751 862

IMPROVED MATERIALS AND MANUFACTURING
METHODS FOR GUN BARRELS. PART I

R. P. O'Shea, et al

IIT Research Institute

Prepared for:

Army Weapons Command

August 1972

DISTRIBUTED BY:

NTIS

National Technical Information Service
U. S. DEPARTMENT OF COMMERCE
5285 Port Royal Road, Springfield Va. 22151

AD 751862

AD

SWERR-TR-72-54

**IMPROVED MATERIALS AND MANUFACTURING
METHODS FOR GUN BARRELS
(PART I)**

August 1972



TECHNICAL REPORT

**Dr. R. P. O'Shea, IIT Research Institute
G. S. Allison, Battelle Northwest
and
J. D. DiBenedetto,
Dr. K. R. Iyer
USAWECOM**

RESEARCH DIRECTORATE

WEAPONS LABORATORY USAWECOM

RESEARCH, DEVELOPMENT AND ENGINEERING DIRECTORATE

U. S. ARMY WEAPONS COMMAND

Reproduced by
**NATIONAL TECHNICAL
INFORMATION SERVICE**

U.S. Department of Commerce
Springfield VA 22151

Approved for public release, distribution unlimited.

1047

DISPOSITION INSTRUCTIONS:

Destroy this report when it is no longer needed. Do not return it to the originator.

DISCLAIMER:

The findings of this report are not to be construed as an official Department of the Army position unless so designated by other authorized documents.

ACCESSION for	
NTIS	WHILE Section <input checked="" type="checkbox"/>
DIC	BUT Section <input type="checkbox"/>
UNANNOUNCED	<input type="checkbox"/>
JUSTIFICATION	
BY	
DISSEMINATION AVAILABLE COPIES	
DATE	
A	

Unclassified
Security Classification

DOCUMENT CONTROL DATA - R & D		
(Security classification of title, body of abstract and indexing annotation must be entered when the overall report is classified)		
1. ORIGINATING ACTIVITY (Corporate author) U. S. Army Weapons Command Research, Dev. and Eng. Directorate Rock Island, Illinois 61201		2a. REPORT SECURITY CLASSIFICATION Unclassified
		2b. GROUP
3. REPORT TITLE IMPROVED MATERIALS AND MANUFACTURING METHODS FOR GUN BARRELS (PART I) (U)		
4. DESCRIPTIVE NOTES (Type of report and inclusive dates)		
5. AUTHOR(S) (Last name, middle initial, first name) R. P. O'Shea - IIT Research Institute, Chicago, Illinois G. S. Allison - Battelle Northwest, Richland, Washington J. D. DiBenedetto and K. R. Iyer - USAWECOM, Rock Island, Illinois		
6. REPORT DATE August 1972	7a. TOTAL NO. OF PAGES 134	7b. NO. OF REFS 13
8a. CONTRACT OR GRANT NO. DAAFO1-70-C-0167	9a. ORIGINATOR'S REPORT NUMBER(S) SWERR-TR-72-54	
8b. PROJECT NO. AMS Code 4932.06.6784		
8c.	9b. OTHER REPORT NO(S) (Any other numbers that may be assigned this report)	
8d.		
10. DISTRIBUTION STATEMENT Approved for public release, distribution unlimited.		
11. SUPPLEMENTARY NOTES Details of illustrations in this document may be better studied on microfiche	12. SPONSORING MILITARY ACTIVITY U. S. Army Weapons Command	
13. ABSTRACT A multiphase program of the Research Directorate, Weapons Laboratory, USAWECOM, was conducted to utilize modern manufacturing methods for improved materials when used for rapid-fire 7.62mm gun barrels. An initial literature survey provided the state of the art and basis for preliminary screening of materials. Correlation of behavior of the materials in firing tests and vented bomb experiments, results of mechanical property tests, and economic limitations were used to select three materials - chrome-plated CG-27, chrome-plated H11, and a cobalt base metal powder alloy - for intensive evaluation. The hot extrusion/cold swaging production sequence was employed in barrel manufacture. The as-swaged bore surfaces were directly chrome plated to produce a finished bore. Chrome-plated CG-27 and chrome-plated H11 barrels were made. Unfortunately, the cobalt base metal powder barrels could not be fabricated. Barrels were test-fired under a controlled schedule and were evaluated by metallographic examination. Chrome-plated H11 steel barrels showed an improvement of one-third to twice the service life over the standard chrome-plated steel barrel; however, the chrome plated CG-27 barrels were inferior to the standard barrel. The outstanding performance of the chrome-plated H11 steel barrels was due to the hot strength, temper resistance, good toughness of the H11 steel, and the excellent adherence of the chromium plate. (U) (O'Shea, R. P., Allison, G. S., DiBenedetto, J. and Iyer, K.)		

DD FORM 1473

NOV 66

REPLACES DD FORM 1473, 1 JAN 64, WHICH IS OBSOLETE FOR ARMY USE.

Unclassified

Security Classification

1a

AD

RESEARCH DIRECTORATE
WEAPONS LABORATORY USAWECOM
RESEARCH, DEVELOPMENT AND ENGINEERING DIRECTORATE
U. S. ARMY WEAPONS COMMAND
TECHNICAL REPORT
SWERR-TR-72-54

IMPROVED MATERIALS AND MANUFACTURING
METHODS FOR GUN BARRELS
(PART I)

Dr. R. P. O'Shea
IIT Research Institute
Chicago, Illinois

G. S. Allison
Battelle Northwest
Richland, Washington

and

J. D. DiBenedetto
Dr. K. R. Iyer
Research Directorate
Weapons Laboratory USAWECOM

August 1972

Details of illustrations in
this document may be better
studied on microfiche

Contract DAAF01-70-C-0167

AMS Code 4932.66.6784

Approved for public release, distribution unlimited.

ABSTRACT

A multiphase program of the Research Directorate, Weapons Laboratory, USAWECOM, was conducted to utilize modern manufacturing methods for improved materials when used for rapid-fire 7.62mm gun barrels. An initial literature survey provided the state of the art and basis for preliminary screening of materials. Correlation of behavior of the materials in firing tests and vented bomb experiments, results of hot hardness and thermal fatigue tests, consideration of engineering and physical properties of the materials, and economic limitations were used to select three materials - chrome-plated CG-27, chrome-plated H11, and a cobalt base metal powder alloy - for intensive evaluation. The hot extrusion/cold swaging production sequence was employed in barrel manufacture. The as-swaged bore surfaces were directly chrome plated to produce a finished bore. Chrome-plated CG-27 and chrome-plated H11 barrels were made. Unfortunately, the cobalt base metal powder barrels could not be fabricated. Barrels were test-fired under a controlled schedule and were evaluated by metallographic examination. On the particular firing schedule the chrome-plated H11 steel barrels showed an improvement of one-third to twice the service life over the standard chrome-plated steel barrel; however, the chrome plated CG-27 barrels were inferior to the standard barrel. The poor performance of the chrome plated CG-27 alloy barrel was attributed to massive muzzle-end erosion which was probably induced by a high-temperature nickel-sulfur reaction. The outstanding performance of the chrome-plated H11 steel barrels was due to the hot strength, temper resistance, good toughness of the H11 steel, and the excellent adherence of the chromium plate.

FOREWORD

This report was prepared by Dr. R. P. O'Shea of IIT Research Institute, Chicago, Illinois, in compliance with Contract DAAF01-70-C-0167; by Mr. G. S. Allison of Battelle Northwest, Richland, Washington, in compliance with MIPR A1-9-30372-M1-W3; and by Mr. J. DiBenedetto and Dr. K. R. Iyer of the Research Directorate, Weapons Laboratory USAWECOM, U. S. Army Weapons Command.

The work was authorized as part of the Manufacturing Methods and Technology Program of the U. S. Army Materiel Command which is administered by the U. S. Army Production Equipment Agency.

CONTENTS

	<u>Page</u>
TITLE PAGE	i
ABSTRACT	ii
FOREWORD	iii
TABLE OF CONTENTS	iv
LIST OF FIGURES	vi
LIST OF TABLES	xiii
INTRODUCTION	1
EXPERIMENTAL WORK	2
PHASE I. Characterization of Erosion-Corrosion in the 7.62mm Barrels	2
Literature Survey	2
Gun Tests	2
Vented Bomb Tests	5
Mode of Failure of Chromium-Plated Barrels	12
PHASE II. Materials Evaluation	17
Vented Bomb-Gun Test Correlation	17
Correlation of Properties with Ma- terial Performance in Gun Barrels	31
Hot Hardness Determinations	31
Thermal Fatigue Testing	34
Summary	39
Vented Bomb Tests	48
PHASE III. Materials Selection	77

CONTENTS (Continued)

	<u>Page</u>
PHASE IV. Fabrication of Selected Materials into Gun Barrels and Test Firing	79
Fabrication	79
CG-27 Processing	79
H11 Processing	81
Cobalt-Iron Alloy Processing	82
Summary	82
Test Firing	83
PHASE V. Analysis	83
Post Analysis	83
Bore Measurements	83
Metallographic Examination	88
Chrome-Plated Gun Steel Barrels	88
Chrome-Plated H11 Steel Barrels	103
Chrome-Plated CG-27 Alloy Barrels	111
SUMMARY AND CONCLUSIONS	120
RECOMMENDATIONS	126
REFERENCES	128
DISTRIBUTION	130
DD FORM 1473 Document Control Data - R&D	133

FIGURES

	<u>Page</u>
1 Photomicrographs Showing Chromium Plate/Steel Interface of a Minigun Barrel After 300 Shots	13
2 Photomicrograph of a Longitudinal Section Showing Typical Chromium Plate/Steel Interface After Firing to Failure	14
3 Scanning Electron Micrograph Showing Typical Crack and Associated White Layer on Failed Gun Barrel	15
4 Scanning Electron Micrographs of Crack Tip and Associated White Layer	16
5 Photomicrograph Showing the Transverse Structure Along the Bore Surface of Unplated Gun Barrel After 300 Shots	18
6 Schematic View of the Vented Bomb Fixture	19
7 Typical Pressure-Time Pulse With a 23 1/2 g Charge of WC846 Ball Propellant	20
8 Photomicrograph Revealing the Transverse Structure Along the Bore Surface of an Unplated Rifled Insert After 5 Vented Bomb Shots With WC846 Propellant	23
9 Photomicrograph Revealing the Transverse Structure Along the Bore Surface of an Unplated Rifled Insert After 5 Vented Bomb Shots With IMR Propellant	23
10 Photomicrograph Revealing the Transverse Structure Along the Bore Surface of a Chromium-Plated Rifled Insert After 5 Vented Bomb Shots With WC846 Propellant	24
11 Photomicrograph Revealing the Transverse Structure Along the Bore Surface of a Chromium-Plated Rifled Insert After 5 Vented Bomb Shots With IMR Propellant	25
12 Photomicrograph Revealing the Transverse Structure Along the Bore Surface of a Haynes Stellite 21 Insert After 5 Vented Bomb Firings With WC846 Propellant	26
13 Photomicrograph Revealing the Transverse Structure Along the Bore Surface of a Haynes Stellite 21 Insert After 5 Vented Bomb Firings With IMR Propellant	27

FIGURES

		<u>Page</u>
14	Fixture and Test Specimens for the Mutual Indentation Hot Hardness Test	32
15	General View of Equipment for Mutual Indentation Hot Hardness Testing	33
16	Hot Hardness Data for Selected Alloys	36
17	Schematic View of Thermal Fatigue Facility	37
18	IITRI Thermal Fatigue Specimen	38
19	Crack Propagation in Notched Samples	42
20	Thermal Fatigue Specimen	43
21	Crack Propagation of First Crack in Each Unnotched Thermal Fatigue Sample	46
22	Dependence of Hardness and Impact Strength of D2 Steel on Tempering Temperature	51
23	Dependence of Hardness and Impact Strength of H11 on Tempering Temperature	53
24	Dependence of Hardness on H26 on Tempering Temperature	54
25	Dependence of Mechanical Properties of S-590 Alloy on Test Temperature	56
26	Dependence of Mechanical Properties of L605 Alloy on Test Temperature	57
27	Dependence of Mechanical Properties of HS-31 Alloy on Test Temperature	58
28	Photomicrographs Showing the Structure Along the Bore Surface of an H11 Alloy Insert After One Vented Bomb Shot With WC846 Propellant	61
29	Photomicrographs Showing the Structure Along the Bore Surface of an H11 Alloy Insert After Five Vented Bomb Shots With WC846 Propellant	62
30	Photomicrographs Showing the Structure Along the Bore Surface of an H26 Alloy Insert After One Vented Bomb Shot With WC846 Propellant	64
31	Photomicrographs Showing the Structure Along the Bore Surface of an H26 Alloy Insert After Five Vented Bomb Shots With WC846 Propellant	65

FIGURES

	<u>Page</u>
32 Photomicrographs Showing the Structure Along the Bore Surface of the D2 Alloy Insert After One Vented Bomb Shot With WC846 Propellant	66
33 Photomicrographs Showing the Structure Along the Bore Surface of the D2 Alloy Insert After Five Vented Bomb Shots With WC846 Propellant	67
34 Photomicrographs Showing the Structure Along the Bore Surface of the 446 Alloy Insert After One Vented Bomb Shot With WC846 Propellant	68
35 Photomicrographs Showing the Structure Along the Bore Surface of the 446 Alloy Insert After Five Vented Bomb Shots With WC846 Propellant	69
36 Photomicrographs Showing the Structure Along the Bore Surface of an L605 Alloy Insert After One Vented Bomb Shot With WC846 Propellant	70
37 Photomicrographs Showing the Structure Along the Bore Surface of an L605 Alloy Insert After Five Vented Bomb Shots With WC846 Propellant	71
38 Photomicrographs Showing the Structure Along the Bore Surface of an HS-31 Alloy Insert After One Vented Bomb Shot With WC846 Propellant	72
39 Photomicrographs Showing the Structure Along the Bore Surface of an HS-31 Alloy Insert After Five Vented Bomb Shots With WC846 Propellant	73
40 Photomicrographs Showing the Structure Along the Bore Surface of an S-590 Alloy Insert After One Vented Bomb Shot With WC846 Propellant	74
41 Photomicrographs Showing the Structure Along the Bore Surface of an S-590 Alloy Insert After Five Vented Bomb Shots With WC846 Propellant	75
42 Photomicrograph of a 50Co-29Fe-20W-1C Alloy Revealing the Transverse Structure Along the Bore Surface After Five Vented Bomb Firings With IMR Propellant	76
43 Bore Profile for CG-27 Material for Various Numbers of Total Rounds Fired	89
44 Bore Profile for CG-27 Material for 4036 Total Rounds Fired	90

FIGURES

	<u>Page</u>
57 Transverse Section at 2 Inches from the Chamber of a Standard Chrome-Plated Gun Barrel After Firing 12,068 Rounds and Being Declared Unserviceable	100
58 Transverse Section at 10 Inches from the Chamber of a Standard Chrome-Plated Gun Barrel After Firing 12,068 Rounds and Being Declared Unserviceable	100
59 Transverse Section at 17 1/2 Inches from the Chamber of a Standard Chrome-Plated Gun Barrel After Firing 12,068 Rounds and Being Declared Unserviceable	101
60 Transverse Section at 19 1/2 Inches from the Chamber of a Standard Chrome-Plated Gun Barrel After Firing 12,068 Rounds and Being Declared Unserviceable	101
61 Transverse Section at 1/2 Inch from the Chamber of a Chrome-Plated H11 Steel Gun Barrel After Firing 16,291 Rounds and Being Declared Unserviceable	104
62 Transverse Section at 1 1/2 Inches from the Chamber of a Chrome-Plated H11 Steel Gun Barrel After Firing 16,291 Rounds and Being Declared Unserviceable	104
63 Transverse Section at 2 Inches from the Chamber of a Chrome-Plated H11 Steel Gun Barrel After Firing 16,291 Rounds and Being Declared Unserviceable	105
64 Transverse Section at 10 Inches from the Chamber of a Chrome-Plated H11 Steel Gun Barrel After Firing 16,291 Rounds and Being Declared Unserviceable	106
65 Transverse Section at 17 1/2 Inches from the Chamber of a Chrome-Plated H11 Steel Gun Barrel After Firing 16,291 Rounds and Being Declared Unserviceable	106
66 Transverse Section at 19 1/2 Inches from the Chamber of a Chrome-Plated H11 Steel Gun Barrel After Firing 16,291 Rounds and Being Declared Unserviceable	106

FIGURES

	<u>Page</u>
67 Transverse Section at 1/2 Inch from the Chamber of a Chrome-Plated H11 Steel Gun Barrel After Firing 24,466 Rounds and Being Declared Unserviceable	108
68 Transverse Section at 1 1/2 Inches from the Chamber of a Chrome-Plated H11 Steel Gun Barrel After Firing 24,466 Rounds and Being Declared Unserviceable	108
69 Transverse Section at 2 Inches from the Chamber of a Chrome-Plated H11 Steel Gun Barrel After Firing 24,466 Rounds and Being Declared Unserviceable	109
70 Transverse Section at 10 Inches from the Chamber of a Chrome-Plated H11 Steel Gun Barrel After Firing 24,466 Rounds and Being Declared Unserviceable	109
71 Transverse Section at 17 1/2 inches from the Chamber of a Chrome-Plated H11 Steel Gun Barrel After Firing 24,466 Rounds and Being Declared Unserviceable	110
72 Transverse Section at 19 1/2 Inches from the Chamber of a Chrome-Plated H11 Steel Gun Barrel After Firing 24,466 Rounds and Being Declared Unserviceable	110
73 Transverse Section at 1/2 Inch from the Chamber of a Chrome-Plated CG-27 Alloy Barrel After Firing 4,036 Rounds and Being Declared Unserviceable	112
74 Transverse Section at 1 1/2 Inches from the Chamber of a Chrome-Plated CG-27 Alloy Barrel After Firing 4,036 Rounds and Being Declared Unserviceable	112
75 Transverse Section at 2 Inches from the Chamber of a Chrome-Plated CG-27 Alloy Barrel After Firing 4,036 Rounds and Being Declared Unserviceable	113
76 Transverse Section at 10 Inches from the Chamber of a Chrome-Plated CG-27 Alloy Barrel After Firing 4,036 Rounds and Being Declared Unserviceable	113

FIGURES

	<u>Page</u>
77 Transverse Section at 17 1/2 Inches from the Chamber of a Chrome-Plated CG-27 Alloy Barrel After Firing 4,036 Rounds and Being Declared Unserviceable	114
78 Transverse Section at 18 Inches from the Chamber of a Chrome-Plated CG-27 Alloy Barrel After Firing 4,036 Rounds and Being Declared Unserviceable	114
79 Transverse Section at 1/2 Inch from the Chamber of a Chrome-Plated CG-27 Alloy Barrel After Firing 7,324 Rounds and Being Declared Unserviceable	116
80 Transverse Section at 1 1/2 Inches from the Chamber of a Chrome-Plated CG-27 Alloy Barrel After Firing 7,324 Rounds and Being Declared Unserviceable	116
81 Transverse Section at 2 Inches from the Chamber of a Chrome-Plated CG-27 Alloy Barrel After Firing 7,324 Rounds and Being Declared Unserviceable	117
82 Transverse Section at 10 Inches from the Chamber of a Chrome-Plated CG-27 Alloy Barrel After Firing 7,324 Rounds and Being Declared Unserviceable	117
83 Transverse Section at 17 1/2 Inches from the Chamber of a Chrome-Plated CG-27 Alloy Barrel After Firing 7,324 Rounds and Being Declared Unserviceable	118
84 Transverse Section at 19 1/2 Inches from the Chamber of a Chrome-Plated CG-27 Alloy Barrel After Firing 7,324 Rounds and Being Declared Unserviceable	118
85 Typical Structure Showing the Morphology of Widmanstatten Precipitate in CG-27 Alloy Barrel	119
86 X-ray Pattern revealing Characteristic Radiation of Elements and Their Relative Concentration Near the Bore Surface of a CG-27 Alloy Barrel	121
87 X-ray Pattern Revealing Characteristic Radiation of Elements and Their Relative Concentration in the Base Material of a CG-27 Alloy Barrel	122

TABLES

	<u>Page</u>
1 Comparison of Conventional and Stellite Lined Cal .50 Barrels	4
2 Materials Evaluated in Vented Bomb Tests	6
3 Erosion Data for Metals Using the Criterion of Weight Loss Per Round	7
4 Erosion Data for Metals Using the Criterion of Diameter Increase, Inches Per Round	8
5 A Comparison of the Erosion Resistance of Materials With that of Gun Steel	9
6 Metallographic Observations of Fired Nozzles	10-11
7 Weight Loss of Gun Steel, Chromium-Plated Gun Steel, and Haynes Stellite 21 After 5 Shots in the Vented Bomb	21
8 Weight Loss Data of Selected Materials After 3 Firings in the Vented Bomb With WC846 Propellant	29
9 Summary of Performance of Selected Materials in Gun Tests	30
10 Hot Hardness Data of Selected Alloys	35
11 Propagation of Cracks in Notched Samples	40-41
12 Propagation of First Crack in Unnotched Thermal Fatigue Samples	44-45
13 Relative Thermal Fatigue Resistance	47
14 Chemical Composition of Candidate Materials	50
15 Weight Change Data of Selected Materials After Firings in the Vented Bomb With WC846 Propellant	59
16 Unit Weight Change for Selected Materials After Firings in the Vented Bomb With WC846 Propellant	60
17 Summary of Microexamination of Selected Alloys Subjected to Firings in the Vented Bomb With WC846 Propellant	78
18 Number of Rounds Fired on Schedule 1 Before Failure was Observed	84

TABLES

		<u>Page</u>
19	Bore Dimensional Measurements for Chrome-Plated CG-27 Barrels After Various Numbers of Total Rounds Fired on Schedule I	85
20	Bore Dimensional Measurements for Chrome-Plated H11 Barrels After Various Numbers Fired on Schedule I	86
21	Bore Dimensional Measurements for a Standard Gun Barrel After Various Numbers of Total Rounds Fired on Schedule I	87

INTRODUCTION

Erosion/corrosion of barrel materials limits the rate of fire of high-performance rapid-fire weapons, and thus limits service life. The objective of this program was to determine materials and/or surface treatments capable of providing improved performance in the 7.62mm barrels.

For achievement of the objective, the program comprised the following phases:

- I. Characterization of erosion/corrosion in the 7.62mm barrels.
- II. Material evaluation.
- III. Materials selection.
- IV. Fabrication of selected materials into gun barrels and test firing.
- V. Post analyses of the fired barrels.

Phase I consisted of a literature survey and an examination of the bore surface of chrome-plated standard steel gun barrels fired on a controlled schedule. The objective of this phase was to establish the state of the art and the baseline data.

In Phase II, a materials evaluation was made to assess various critical material and physical parameters, also a comparison was made of the results obtained by vented bomb tests and those obtained in gun tests for seven selected materials, and important mechanical and physical properties of the materials were determined. The objective of this phase of the work was to identify and correlate important material properties so that a rationale for selecting materials of improved performance could be established.

In the materials selection, Phase III, the information determined in Phase II was combined with economic considerations to form a basis for the selection of three materials for evaluation in gun tests. The objective of this phase was to select cost-effective materials which would provide improved performance as barrels in the Minigun.

Phase IV concerned the fabrication and the testing of barrels.

The post analyses of the fired barrels, Phase V, involved bore measurements and metallographic examination. In Phases IV and V, the objectives of the Research Directorate, Weapons Laboratory USAWECOM were to verify the performance and to rank the selected materials.

EXPERIMENTAL WORK

Phase I. Characterization of Erosion/Corrosion in the 7.62mm Barrels

Literature Survey

Two types of erosion studies have been made on selected barrel materials for small arms. These are the vented bomb test and the actual gun tests. The majority of the vented bomb tests were conducted during the 1940-1955 period and were centered on a peak pressure of 20,000 to 30,000 psi. In the actual firing tests, small caliber machine guns were used such as the Cal .50 or Cal .30 for the erosion studies. In most cases, the vented bomb test environments were designed to induce a large amount of erosion in a very few shots and, consequently, this type of test was usually more severe than the machine gun tests.

Gun Tests - Various metals and metal alloys have been evaluated in gun tests. These include chromium and chromium-base alloys, molybdenum and molybdenum alloys, tungsten alloys, tantalum, cobalt, cobalt-tungsten, stellites, and nickel alloys.

Cobalt and cobalt alloys have been considered for liners in gun barrels. Pure cobalt was tested as a liner in a Cal .30 gun. It showed excellent resistance to chemical attack and melting, but deformation of the rifling occurred.⁽¹⁾ Steel barrels plated with 0.005 inch thick pure cobalt were fired in a Cal .50 gun.⁽²⁾ In this instance, the cobalt adherence was satisfactory, but melting and deformation of the rifling occurred. Cobalt-tungsten alloys were plated onto the bore surface of a steel gun barrel and assessed in a Cal .50 gun. Melting occurred, and difficulties with adhesion were encountered. The cobalt-base stellites were also tested as liners. It was found that Stellite 21 was the most satisfactory member of this family. In tests in a Cal .50 machine gun, Stellite 21 showed outstanding performance as compared

to gun steel (see Table 1). However, in another investigation⁽²⁾ when Stellite 21 inserts were fired with double-base propellants, the bore surfaces melted.

Firing of nickel and nickel alloys as gun liners, showed that these materials, with the exception of the nichromes, were susceptible to severe intergranular attack by the propellant gases.⁽³⁾ The nickel-chromium alloys with more than 10% chromium were resistant to intergranular attack but were unable to withstand deformation by the projectile. A number of steels and other iron-base alloys have been evaluated. A 24Cr-5Ni-3Mo-0.45C-1Si steel was tested in a Cal .50 machine gun and showed much better resistance to erosion than regular 4150 gun steel.⁽⁴⁾

A 30Co-20Cr-4Mo-4W-2Ta-0.1C steel showed promise during firing with a Cal .50 machine gun, whereas a similar alloy incorporating 30 Ni instead of 30 Co was subject to severe thermochemical attack by the propellant gases.⁽⁵⁾

Both pure tantalum liners⁽²⁾ and steel with diffused-tantalum bore surfaces⁽⁶⁾ have been test fired. The tantalum liners were evaluated in a Cal .50 gun. The liners showed some transgranular cracking, but no other evidence of erosion. The diffused-tantalum coating on the bore surface of a steel barrel was tested in a Cal .30 machine gun. Barrels with coating thicknesses of 0.0005 inch and 0.001 inch were fired and performed better than gun steel.

A liner of chromium electroplate was evaluated,⁽⁷⁾ and it was found that cracking in the bore surface occurred after only a few rounds had been fired. The premature failure was attributed to a lack of cold ductility of chromium. Parke and Bens⁽⁸⁾ evaluated chromium alloys containing 20 to 30% iron and 10 to 15% molybdenum. When these alloys were fabricated into liners and test fired in a Cal .50 machine gun, they showed outstanding performance and did not crack or disintegrate despite their low ductility.

Pure molybdenum liners were investigated by Smith, and firing tests showed that the liners, as fabricated, were neither strong nor ductile enough to make a satisfactory liner.⁽²⁾ Other work⁽⁹⁻¹¹⁾ showed that these deficiencies can be overcome by addition of 0.1% to 0.2% cobalt, mechanical working, and proper heat treatment. In test firing, molybdenum alloys so modified showed outstanding performance. After firing 2024 rounds, the bore surface was examined and there was no evidence of erosion. There was, however, some cracking, swaging of the lands, and liner movement.

Table 1

COMPARISON OF CONVENTIONAL AND STELLITE LINED CAL .50 BARRELS (1)

Burst	Cooling, min	Barrel	Life, rounds	Reason for Failure	Velocity drop, fps
100	2	Conventional	885	Yaw	155
		Steel-Stellite	1,191	Yaw	26
5 x 100 ^a	1	Conventional	1,000	Yaw	183
		Steel-Stellite	2,000	Yaw	1
200	1 or 2	Conventional	1,929	Keyholing	142
		Steel-Stellite	10,554	Keyholing	124
200	Complete	Conventional	3,812	Velocity drop & dispersion	199
		Steel-Stellite	10,225	Dispersion	2

^a Five 100-round bursts with 1 min cooling between bursts and complete cooling after 500 rounds.

Tungsten-copper powder compacts⁽⁷⁾ were evaluated. It was found that these compacts were resistant to erosive effects of the powder gas but were unsuitable because of a lack of sufficient strength to resist deformation by the impact of the projectile.

Vented Bomb Tests - The vented bomb has been utilized for determining the erosion resistance of materials. In this type of test, a nozzle of the material of interest is mounted directly in front of the chamber and a blank is fired. The system is obturated so that all the burning gases flow through the test nozzle. By controlling the geometry of the system and the propellant, the internal ballistics of the system can be manipulated to simulate the pressure-time pulse of a specific weapon.

Vented bomb tests were reported in Reference 7. In this study the erosion resistance of pressed and sintered chromium-copper, molybdenum-copper, and tungsten-copper powder compacts were compared with gun steel. The best of the chromium compacts showed weight losses considerably less than gun steel but not as low as the molybdenum or tungsten compacts. The compacts were never considered for gun barrel liners because of the low melting point and hardness of copper.

Breitbart, in 1951,⁽¹²⁾ conducted the most comprehensive program of this type. A 37mm gun was modified so that a tapered nozzle could be placed directly in front of the chamber. The tapered nozzle had a bore which varied in size from 0.707 to 0.500 inch. Double-base M2 was the propellant, and charges usually consisted of 40, 50, 70, and 88 g, but other charges were also used, depending upon the results of the test. The 88 g load generated a pressure of 30,000 psi.

The rate of firing was limited to one round every 2 min in order to minimize any temperature effects from the preceding round. The materials which were evaluated are listed in Table 2. Erosion data from the vented bomb firings are given in Tables 3 and 4. A comparison of the erosion resistance, as determined by volume of metal lost per shot, of the candidate materials with that of gun steel is made in Table 5. Table 6 summarizes the metallographic observations which were made on the various materials after firing.

In general, the steels or special iron alloys tested have not shown outstanding promise as bore-surface materials. Chromium plating the bore surface improves the erosion resistance. Cobalt-base superalloys have shown satisfactory

Table 2
MATERIALS EVALUATED IN VENTED BOMB TESTS⁽¹²⁾

Pure Metals

Iron
Nickel
Titanium
Tungsten
Molybdenum
(Pressed and sintered,
Cast and forged)

Alloys

AISI 4140 Steel
25-20 Stainless Steel
Timken Alloy 16-25-6
Fe-24Cr-5Ni-2.75Mo-1.0Si-0.04C
Stellite 21
60Cr-25Fe-15Mo
68Cr-23Fe-9Mo
Mo-5W
WC + 13%Co

Table 3
EROSION DATA FOR METALS USING THE CRITERION OF WEIGHT LOSS PER ROUND (12)^a

Material	40 g	50 g	60 g	70 g	85 g	100 g	Special
Armco iron	-	-	-	-	.0156	-	.0058 (77 g)
Nickel	-	.0023	-	.0054	-	-	-
Tungsten	-	-	-	.0013	-	-	-
Mo (pressed & sintered)	-	-	-	.00982	.00214	.0029	.0036 (108 g)
Mo (cast and forged)	-	-	-	-	.00125	.0018	-
Mo (cast and forged)	-	-	-	.00044	.00135	.0021	-
Ti ^b	.7003	2.5012	-	4.2559	-	-	-
Gun Steel	.00029	.0011	-	.011	.028	-	d = .48"
	.00029	.0013	-	.0085	.0225	-	d = .51"
25-20 Stainless	.00012	-	-	.034	-	-	-
Timken 15-25-6	.00023	.00042	.023	.057	.097	-	-
0.40C-1Si-24Cr-2.75Mo-5Ni, Bal Fe	.00013	-	-	.042	-	-	-
Stellite 21	-	.0059	.024	.042	-	-	-
60Cr-25Fe-15Mo	c	.00013	.0054	.0156	.0387	-	-
68Cr-23Fe-9Mo	c	c	.0033	.0125	.031	.042	-
Mo + 5%W	-	-	-	-	.0016	.0022	.0027 (108 g, d = .52")
WC + 13%Co	.000050	.00043	.0014	.0093	.0249	.0331	-

^aThroat diameter of nozzle used in tests = 0.500", unless otherwise specified.

^bThese nozzles were of the new design.

^cIndicates no loss in weight.

Table 4

EROSION DATA FOR METALS USING THE CRITERION OF DIAMETER INCREASE, INCHES PER POUND⁽¹²⁾^a

Material	40 g	50 g	60 g	70 g	88 g	100 g	Special
Armco iron	-	-	-	-	.00212	-	.000692 (77 g)
Nickel	-	.00029	-	.00067	-	-	-
Tungsten	-	-	-	.00076	-	-	-
Mo (pressed & sintered)	-	-	-	b	.000264	c	.000414 (108 g)
Mo (cast and forged)	-	-	-	c	.000146	.000252	-
Mo (cast and forged)	-	-	-	-	c	.00027	-
Ti ^d	.0159	.0842	-	.1211	-	-	-
Gun Steel	b	b	-	.0016 .0016	.0035 .0027	-	d = .48" d = .51"
25-20 Stainless	b	-	-	.0047	-	-	-
Timken 16-25-6	b	c	.0031	.0053	.0065	-	-
0.40C-1Si-24Cr-2.75Mo- 5Ni, Bal Fe	b	-	-	.0033	-	-	-
Stellite 21	-	.0008	.003	.0052	-	-	-
60Cr-25Fe-15Mo	b	b	.0012	.0028	.0053	-	-
68Cr-23Fe-9Mo	b	b	.00085	.00195	.0044	.0047	.0028 (77 g)
Mo + 5%W	-	-	-	-	.00033	.00040 (108 g, d = .52")	.00042
WC + 13%Co	b	-	.00026	.0014	.0043	.0053	-

^aThroat diameter of nozzle used in tests
= 0.500", unless otherwise indicated.

^cData not sufficiently reliable.

^bIndicates no diameter increase.

^dThese nozzles were of the new design.

Table 5

A COMPARISON OF THE EROSION RESISTANCE OF MATERIALS
WITH THAT OF GUN STEEL (12)

Material	70 g Charge, 20,000 psi		88 g Charge, 30,000 psi	
	V_L/V_{LGS}	V_M/V_{LGS}	V_L/V_{LGS}	V_M/V_{LGS}
Armco iron	-	-	0.56	0.66
Nickel	0.49	0.41	-	-
Tungsten	0.12	0.16	-	-
Mo (pressed & sintered)	0.07	-	0.08	0.083
Mo (cast & forged)	0.04	-	0.04	0.045
Gun steel	1.00	1.00	1.00	1.00
25-20 Stainless	3.09	2.88	-	-
Timken 16-26-6	5.18	3.25	3.46	2.72
0.40C-1Si-24Cr-2.75Mo-5Ni, Bair Fe	3.82	3.25	-	-
Stellite 21	3.25	3.19	-	-
60Cr-25Fe-15Mo	1.42	1.72	1.38	1.69
68Cr-23Fe-9Mo	1.14	1.19	1.10	1.40
WC + 13%Co	0.85	0.86	0.89	1.39

V_L/V_{LGS} = ratio of volume loss per round for material to that for gun steel.

V_M/V_{LGS} = ratio of diameter increase per round for material to that for gun steel.

Table 6

METALLOGRAPHIC OBSERVATIONS OF FIRED NOZZLES (12)

Material	Results
<u>Pure Metals</u>	
Iron	Melting on bore surface occurred and some cracks. White layer was present.
Nickel	Intergranular attack and crack system.
Titanium	Excessive erosion probably caused by chemical reaction.
Tungsten	Bore surface showed "heat checking" with some evidence of spalling.
Molybdenum (pressed and sintered)	Material appeared to be chemically inert to the gases. Long longitudinal cracks were present and attributed to carbides in the test sample.
Molybdenum (cast and forged)	Similar to the pressed and sintered molybdenum.
<u>Alloys</u>	
4140 Gun Steel	At low charges bore surface showed "heat checking"; at high charges bore surface was smooth and shiny and assumed to have melted. White layer present.
25-20 Stainless	At 70 g charge, melting occurred.
Turken 16-25-6	This is a high-temperature alloy for gas turbine application. At 50 g charge, some melting. At charges below 50 g, deep intergranular cracks.
40C-1Si-24Cr-2.75Mo-5Ni, Bal Fe	No metallographic tests.

Table 6 (Continued)

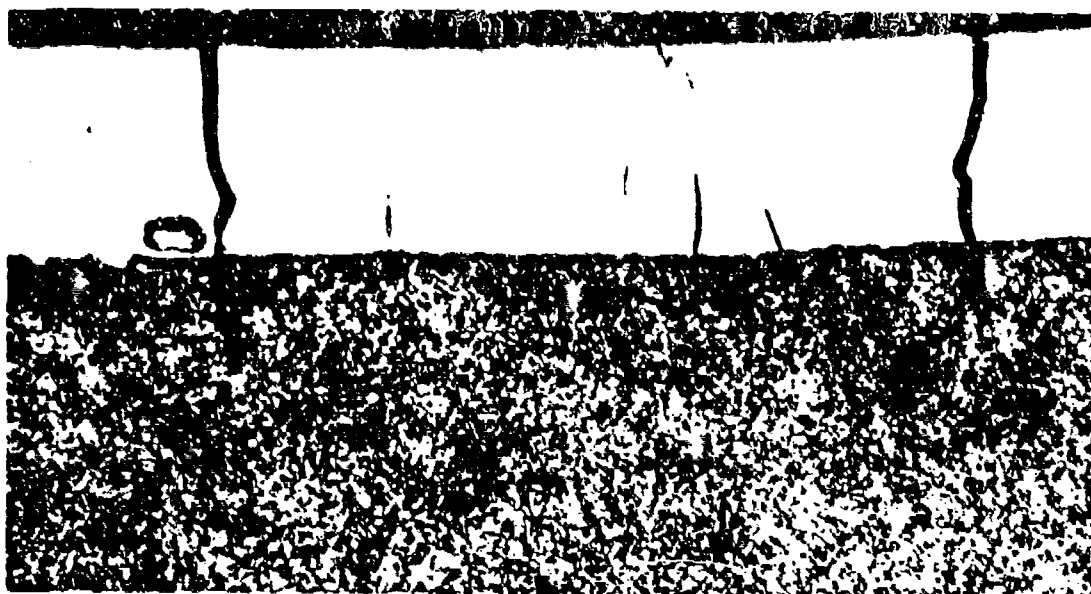
Material	Results
Steellite 21 60Cr-25Fe-15Mo	Melting on the bore surface. This material showed a pronounced tendency for "heat checking".
68Cr-23Fe-9Mo Mo-5W	Similar to 60Cr-25Fe-15Mo alloys, but more brittle. Similar to pure Mo.
WC + 13%Co	Material chemically inert to gases. Cracking not as excessive as in gun steel.

performance in applications in which single-base propellants are utilized. From the information presented in this survey, it appears that molybdenum-or tungsten-base materials with optimized mechanical properties would offer an improvement over cobalt-base alloys in the environments created by a double-base propellant; however, the cost and fabrication difficulties of these refractory metals do detract from their use.

Mode of Failure of Chromium-Plated Barrels

To determine the onset characteristics of erosion in the 7.62mm barrels, plated and unplated barrels were fired in continuous bursts for 1, 10, 50, 100, and 300 rounds. To establish the long-term characteristics a series of chromium-plated barrels which had been fired to rejection were examined. In the chromium-plated barrel, relatively large cracks are developed in the chromium plate after one shot. Each additional shot opens these cracks and causes them to propagate toward the steel. In a very short period (less than 300 rounds) the crack reaches the steel, the opening and closing of the crack is coupled to the steel at the chromium plate/steel interface, and the accompanying pressure and thermal excursions initiate a crack in the steel and propagation occurs. Figure 1 shows the plated barrel which was subjected to the 300-round burst. It should be noted that the crack in the steel is an extension of the crack in the chromium plate and that there is no white layer present. The cracks present in Figure 1 were examined at magnifications up to 20,000X, and no evidence of a white layer was seen. Figure 2 typifies a barrel which has been fired to failure. The cracking has significantly progressed into the steel, large regions of chromium plate and steel have been removed, and the cracks are encased in the white layer. Figures 3 and 4 are photomicrographs of a crack and associated white layer. Examination of Figure 4a and b reveals that cracking occurs around the white layer rather than through the layer. From this evidence, it appears that the white layer is produced after the crack has occurred. With continued firing the white layer flakes off and the crack widens.

Microscopic X-ray spectrographic analysis was performed on the white layer and the steel matrix. The spectrographic technique for each examination was closely controlled so that semiquantitative results could be obtained. Copper was found in the white layer area. The iron and chromium contents in the white layer were considerably lower than in the matrix. This indicates that there is a buildup of light elements in the white layer.



Nital Etch

(a) Transverse

500X

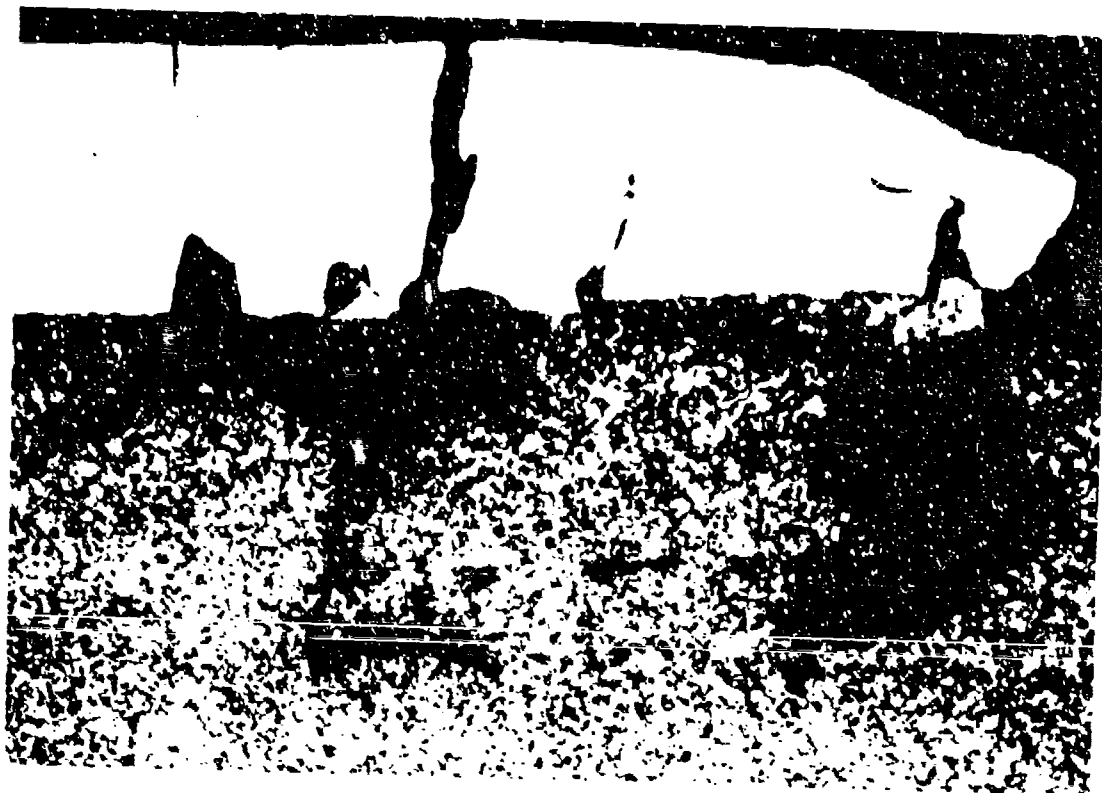


Nital Etch

(b) Longitudinal

500X

FIGURE 1 PHOTOMICROGRAPHS SHOWING CHROMIUM PLATE/STEEL
INTERFACE OF A MINIGUN BARREL AFTER 300 SHOTS.



Nital Etch

500X

FIGURE 2 PHOTOMICROGRAPH OF A LONGITUDINAL SECTION SHOWING
TYPICAL CHROMIUM PLATE/STEEL INTERFACE
AFTER FIRING TO FAILURE.

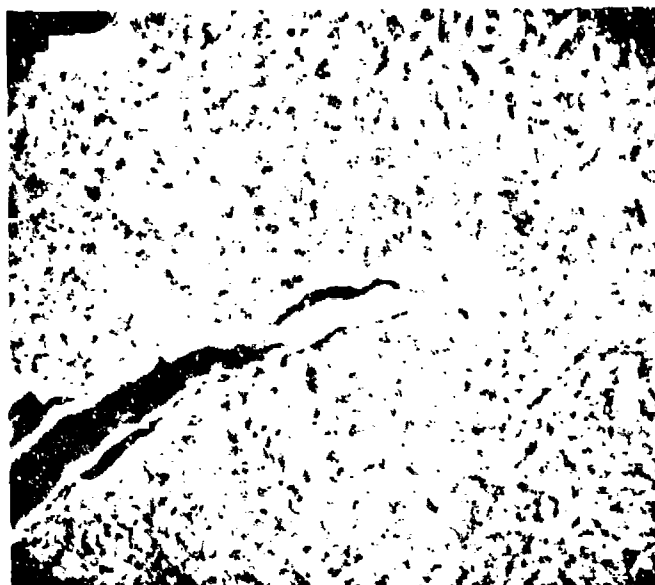


Nital Etch

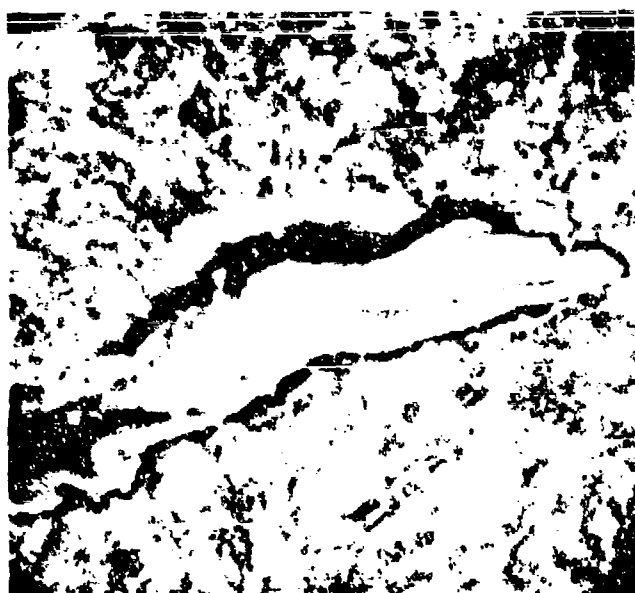
600X

FIGURE 3 SCANNING ELECTRON MICROGRAPH SHOWING TYPICAL CRACK AND ASSOCIATED WHITE LAYER ON FAILED GUN BARREL.

Reproduced from
best available copy.



Nital Etch (a) 2000X



Nital Etch (b) 6000X

FIGURE 4 SCANNING ELECTRON MICROGRAPHS OF
CRACK TIP AND ASSOCIATED WHITE LAYER.

Examination of the fired unplated barrels revealed that material removal or erosion was the prime mode of failure for gun steel. The lands are flattened considerably by firing. Figure 5 typifies the microstructure along the bore surface and shows the intersection of a land and groove.

Phase II - Materials Evaluation

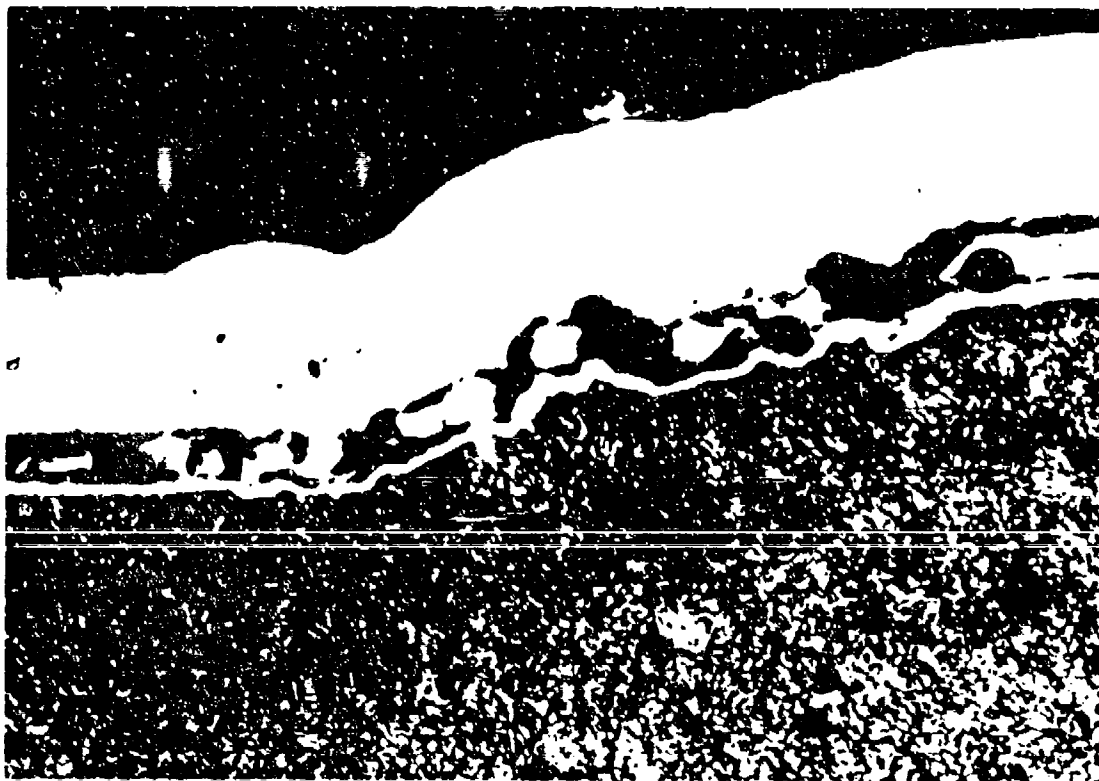
Vented Bomb-Gun Test Correlation

An improved gun barrel material must possess a combination of mechanical and physical properties which would enable it to resist the gun barrel environment. The material must have enough high-temperature strength to allow for sustained bursts without excessive wear; however, it also must have sufficient toughness so that it will not fail by cracking. It must have good mechanical and thermal fatigue properties. The material must not react excessively with the hot gas stream. This requires a reasonably high melting point and a low chemical reactivity potential with the propellant gases.

Much information is available on the mechanical and physical properties of materials under relatively controlled or known environments. However, little is available on how materials will respond to a gun barrel environment. The vented bomb (Figure 6) was utilized in this program to establish the response of materials to a gun-type environment. The test specimen in the vented bomb is 2 inches long and has a bore diameter of 7.62mm.

The first effort was to establish the level of correlation of material response in vented bomb firing with that observed in actual gun tests. A section of a rifled chromium-plated gun barrel, an unplated barrel, and a Haynes Stellite 21 gun barrel insert were subjected to five shots each in the vented bomb. Two propellants, IMR and WC846, were employed and the peak pressure was controlled at $50,000 \pm 2,000$ psi with a rise time of less than 1 millisecond. A typical pressure-time pulse is shown in Figure 7. The weight loss data are listed in Table 7. The ranking of materials in the vented bomb test, according to these data, is as follows:

1. Chromium-plated gun steel
2. Gun Steel
3. Haynes Stellite 21



Nital Etch

500X

FIGURE 5 PHOTOMICROGRAPH SHOWING THE TRANSVERSE STRUCTURE
ALONG THE BORE SURFACE OF UNPLATED GUN BARREL AFTER 300 SHOTS.
(Bore surface was nickel plated for metallographic examination.)

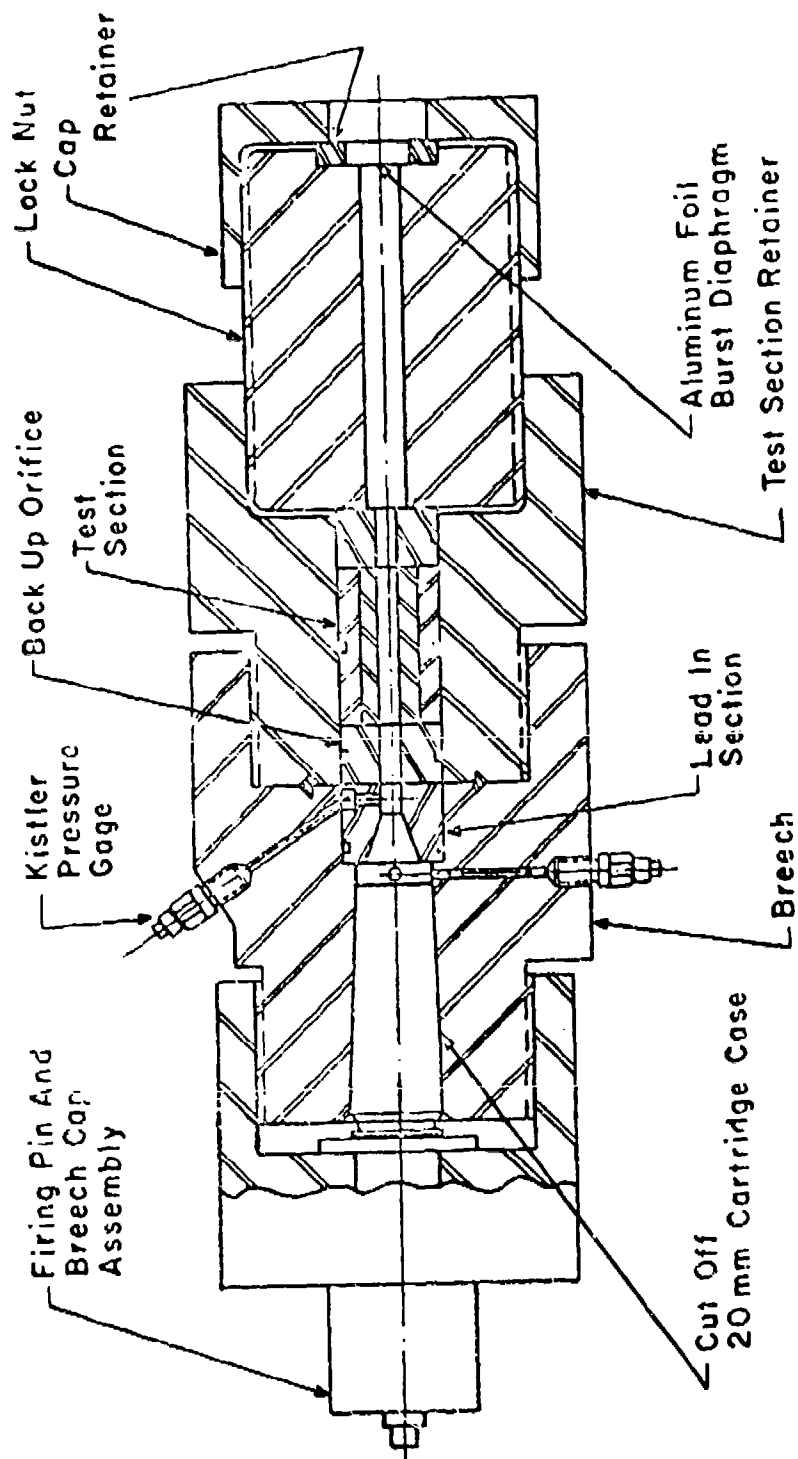


FIGURE 6 SCHEMATIC VIEW OF THE VENTED BOMB FIXTURE.

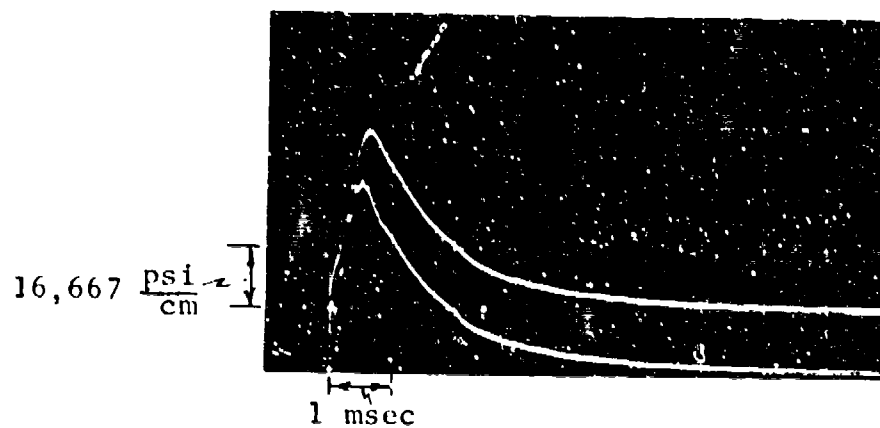


FIGURE 7 TYPICAL PRESSURE-TIME PULSE WITH A
23 1/2 g CHARGE OF WC846 BALL PROPELLANT.

Table 7

WEIGHT LOSS OF GUN STEEL, CHROMIUM-PLATED GUN STEEL,
AND HAYNES STELLITE 21 AFTER 5 SHOTS IN THE VENTED BOMB

<u>Material</u>	<u>Propellant</u>	<u>Weight loss, grams</u>
Cr-Mo-V gun steel	IMR	0.2345
	WC846	0.0059
Chromium-plated gun steel	IMR	0.0002
	WC846	0.0000
Haynes Stellite 21	IMR	0.5884
	WC846	0.0650

This ranking is not that observed in gun tests, in which the Haynes Stellite 21 outperforms the chromium-plated gun barrel, which in turn outperforms the gun steel.

The effects of propellant on erosion can also be deduced from Table 7. Both of these propellants have approximately the same flame temperature, 5235°F for the WC846 and 5160°F for the IMR 5010; however, because of differences in the burning rates 29 grams of IMR 5010 and 23-1/2 grams of WC846 were required to produce 50,000 psi peak pressure in 0.6 and 0.5 milliseconds, respectively. Consequently, the IMR 5010 propellant produces more gas and a longer thermal pulse than the WC846 propellant, and represents a more severe erosion condition.

The relative ranking of each material remains unchanged with each propellant; however, the large differences encountered for each alloy with the two propellants indicate that performance in a gun system would be greatly dependent upon the propellant and firing schedule employed.

Each of the three vented bomb fired materials was metallographically examined. Figures 8 and 9 show the bore surface of the unplated rifled inserts which were fired with IMR and WC846 propellants. The bore surface was plated with nickel to preserve surface effects. Both sections shown in these figures are at a land and groove intersection. Evidently in the vented bomb gun steel does not crack, but rather there appears to be a general removal of metal along the bore surface and a rather sharp heat-affected zone present. In both cases, the rifling is flattened but much more extremely with the IMR propellant. This mode of failure is similar to that encountered in gun tests.

Typical land and groove intersections of the rifled, chromium-plated inserts subjected to 5 firings in the vented bomb with WC846 and IMR propellants are shown in Figures 10 and 11. It is apparent that cracking from the chromium plate has progressed into the steel, but no spalling off has occurred. This mode of failure is similar to that encountered in gun tests.

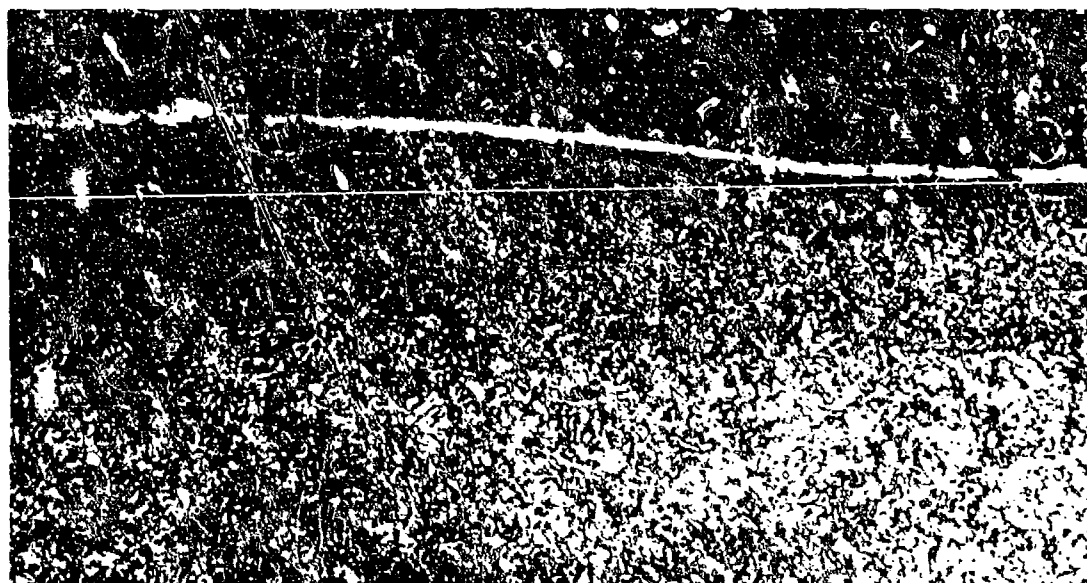
Figures 12 and 13 exhibit transverse microstructures along the bore of the Haynes Stellite 21 test insert after 5 firings in the vented bomb with IMR and WC846 propellants. The nickel plating did not adhere very well to the bore surfaces. The bore surfaces appear to be quite irregular, and chips of metal have been removed.



Nital Etch

500X

FIGURE 8 PHOTOMICROGRAPH REVEALING THE TRANSVERSE STRUCTURE
ALONG THE BORE SURFACE OF AN UNPLATED RIFLED INSERT AFTER
5 VENTED BOMB SHOTS WITH WC846 PROPELLANT.



Nital Etch

500X

FIGURE 9 PHOTOMICROGRAPH REVEALING THE TRANSVERSE STRUCTURE
ALONG THE BORE SURFACE OF AN UNPLATED RIFLED INSERT AFTER
5 VENTED BOMB SHOTS WITH IMR PROPELLANT.



Nital Etch

500X

FIGURE 10 PHOTOMICROGRAPH REVEALING THE TRANSVERSE STRUCTURE
ALONG THE BORE SURFACE OF A CHROMIUM-PLATED RIFLED INSERT
AFTER 5 VENTED BOMB SHOTS WITH WC846 PROPELLANT.



Nital Etch

500X

FIGURE 11 PHOTOMICROGRAPH REVEALING THE TRANSVERSE STRUCTURE
ALONG THE BORE SURFACE OF A CHROMIUM-PLATED RIFLED INSERT
AFTER 5 VENTED BOMB SHOTS WITH IMR PROPELLANT.



Nital Etch

500X

FIGURE 12 PHOTOMICROGRAPH REVEALING THE TRANSVERSE STRUCTURE
ALONG THE BORE SURFACE OF A HAYNES STELLITE 21 INSERT AFTER
5 VENTED BOMB FIRINGS WITH WC846 PROPELLANT.



Nital Etch

500X

FIGURE 13 PHOTOMICROGRAPH REVEALING THE TRANSVERSE STRUCTURE
ALONG THE BORE SURFACE OF A HAYNES STELLITE 21 INSERT AFTER
5 VENTED BOMB FIRINGS WITH IMR PROPELLANT.

To further examine the correlation between vented bomb tests and gun tests, test inserts of CG-27 alloy, A286 alloy, 22-4-9 alloy, and X-15 alloy were given 3 firings in the vented bomb with the WC846 and the IMR propellants. These materials were selected because Rock Island Arsenal had fired gun barrels of each and the relative performance had been established under closely controlled firing schedules. The vented bomb materials were furnished by Rock Island Arsenal, and the metallurgical analysis was performed there. The weight loss data are reported in Table 8.

In the gun tests the rate of fire was 650 rounds per minute on the following schedule:

After every 125 rounds allow for a
10 second cool.

After 6 bursts cool to ambient temperature.

Every 3000 rounds de-copper the barrel.

The gun test data are listed in Table 9. Comparison of these data with Table 8 reveals that there is not a one-to-one correlation between the vented bomb firings and the gun tests. There are several probable reasons why there is not a one-to-one correlation. The more obvious are:

1. In the vented bomb the duration of each single thermal pulse or shot is much longer than that encountered in the gun tests. Consequently, melting point can become more influential.
2. The vented bomb only presents a high-temperature gas stream; the effects of the projectile acting on the bore surface in a gun test would introduce swaging and wear. Consequently, the high-temperature mechanical properties are more important in a gun test than the vented bomb.
3. Thermal fatigue properties are of importance in the gun tests since a large number of cycles is induced. In the vented bomb, only a few cycles are encountered.

Table 8

WEIGHT LOSS DATA OF SELECTED MATERIALS
AFTER 3 FIRINGS IN THE VENTED BOMB
WITH WC846 PROPELLANT

<u>Material</u>	<u>Weight Loss, grams</u>
CG-27	0.636
A286	0.3047 ^a
22-4-9	0.0531
X-15	0.0017

^aInsert galled on removal from holder.

Table 9
SUMMARY OF PERFORMANCE OF
SELECTED MATERIALS IN GUN TESTS

<u>Material</u>	<u>Rounds to Failure</u>	<u>Failure Criterion</u>
CG-27	5,250	Yaw
A286	4,000	Yaw
22-4-9	4,250	Barrel fracture
X-15	4,250	Yaw
Cr-Mo-V steel	4,250	Yaw & velocity
Cr-Plated Cr-Mo-V steel	11,400	Velocity

4. The mode of failure between the gun tests and the vented bomb can be significantly different. For example, in gun tests chromium-plated barrels fail by cracking and not by washing or reacting with the propellant gas; therefore, if enough cycles are not induced in the vented bomb firings, no sections of chromium plate and steel will be cracked out and weight losses would be minimal.

In view of the above factors, the vented bomb firing can only give qualitative information on the performance in a propellant gas stream. The tests can be utilized to determine resistance to the gas stream, indicate thermal shock resistance, and observe tendencies for a material to fail in such an environment.

Correlation of Properties with Material Performance in Gun Barrels

Minigun gun barrels of CG-27, X-15, A286, and 22-4-9 were test fired by the Rock Island Arsenal. With the firing data as a base, a study was made to establish whether a correlation exists between the material performance as a gun barrel and the material properties. The vented-bomb tests were considered to evaluate the relative resistance to thermal shock, chemical reactivity, and erosion resistance to a hot gas stream. Hot hardness (strength) data and thermal fatigue data on the above alloys were not available in the literature so these properties had to be determined experimentally.

Hot Hardness Determinations - The test employed to measure hot hardness was a mutual indentation technique which involves the pressing together of two cylindrical specimens of the test material. These specimens are 1 cm in diameter by 1 cm long. A load of 500 to 3000 kg is employed. The area of the flat surface developed at the junction of the test specimens is measured, and from this area the hardness data are derived. The anvils, anvil holders, and test specimen are shown in Figure 14. These pieces of equipment are loaded into a furnace attached to a Brinell machine as shown in Figure 15. The necessary load is applied, then released, and the test specimens are removed from the furnace. The flat which is generated at the junction of the two specimens can be clearly seen. Brinell hardness can be calculated from measurement of the flattened area as follows:



FIGURE 14 FIXTURE AND TEST SPECIMENS FOR THE MUTUAL
INDENTATION HOT HARDNESS TEST. DISASSEMBLED (LEFT)
AND ASSEMBLED (RIGHT).

Reproduced from
best available copy.

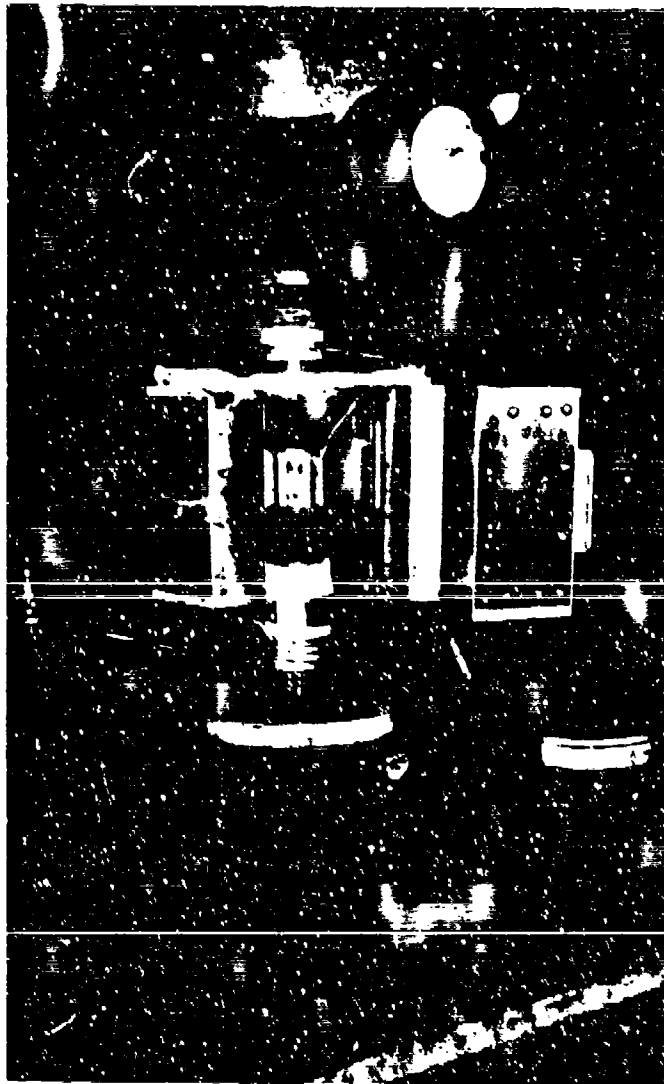


FIGURE 15 GENERAL VIEW OF EQUIPMENT FOR MUTUAL
INDENTATION HOT HARDNESS TESTING. LOADING DEVICE,
FURNACE (IN OPEN POSITION), AND TEST FIXTURE
WITH SPECIMENS ENCLOSED ARE SHOWN.

$$\text{BHN}_{\text{Mi}} = \frac{CP}{A} = \frac{CP}{(L)(W)}$$

where

C = constant (1.52)

P = load, in kg

A = area of impression of cylinders, in mm²

L = length of impression or flat, in mm

W = average width of impression or flat, in mm

The hot hardness data for the A286, X-15, 22-4-9, and Cr-Mo-V alloy are given in Table 10. The 22-4-9 alloy and the Cr-Mo-V steel deformed to such an extent at the 1800°F temperature that the test data were considered to be invalid. Figure 16 shows the hot hardness data. As can be seen, there is a cross-over point at approximately 1300°F, where the CG-27 alloy has a greater hot hardness, hence strength, than the other alloys.

Thermal Fatigue Testing - A schematic drawing of the thermal fatigue testing facility is shown in Figure 17. It consists of a 11.5 inch diameter high-temperature bed situated between two 14 inch diameter intermediate-temperature beds.

The specimens are cycled by means of automatically controlled pneumatic cylinders which are sequenced by timers and limit switches. The facility was cycled automatically for the number of cycles selected.

Each bed is fitted with four thermocouples for control, over-temperature protection, low-temperature test cutoff, and recording purposes.

The five alloys were tested over a temperature interval of 1500°F to 600°F. One specimen of each was prepared with a thermocouple in the edge of the fin. The configuration of the specimen is shown in Figure 18. The test conditions for each steel were established by varying the cycle times in the hot bed and the cold bed. The hot bed temperature was 2000°F, the cold bed 175°F. The test conditions established are given below:

Table 10
HOT HARDNESS DATA OF SELECTED ALLOYS

<u>Alloy</u>	<u>Test Temperature, °F</u>	<u>Load, kg</u>	<u>BHN</u>
A286	Room	3000	256
	1200	2000	235
	1400	1000	122
	1600	500	68
	1800	500	25
X-15	Room	3000	303
	1200	1500	190
	1400	500	110
	1600	500	73
	1800	500	24
22-4-9	Room	3000	341
	1200	1500	160
	1400	800	119
	1600	700	90
Cr-Mc-V	Room	3000	324
	1200	3000	93
	1400	500	49
	1600	500	20
CG-27	Room	3000	272
	1200	2000	200
	1400	1000	200
	1600	500	110

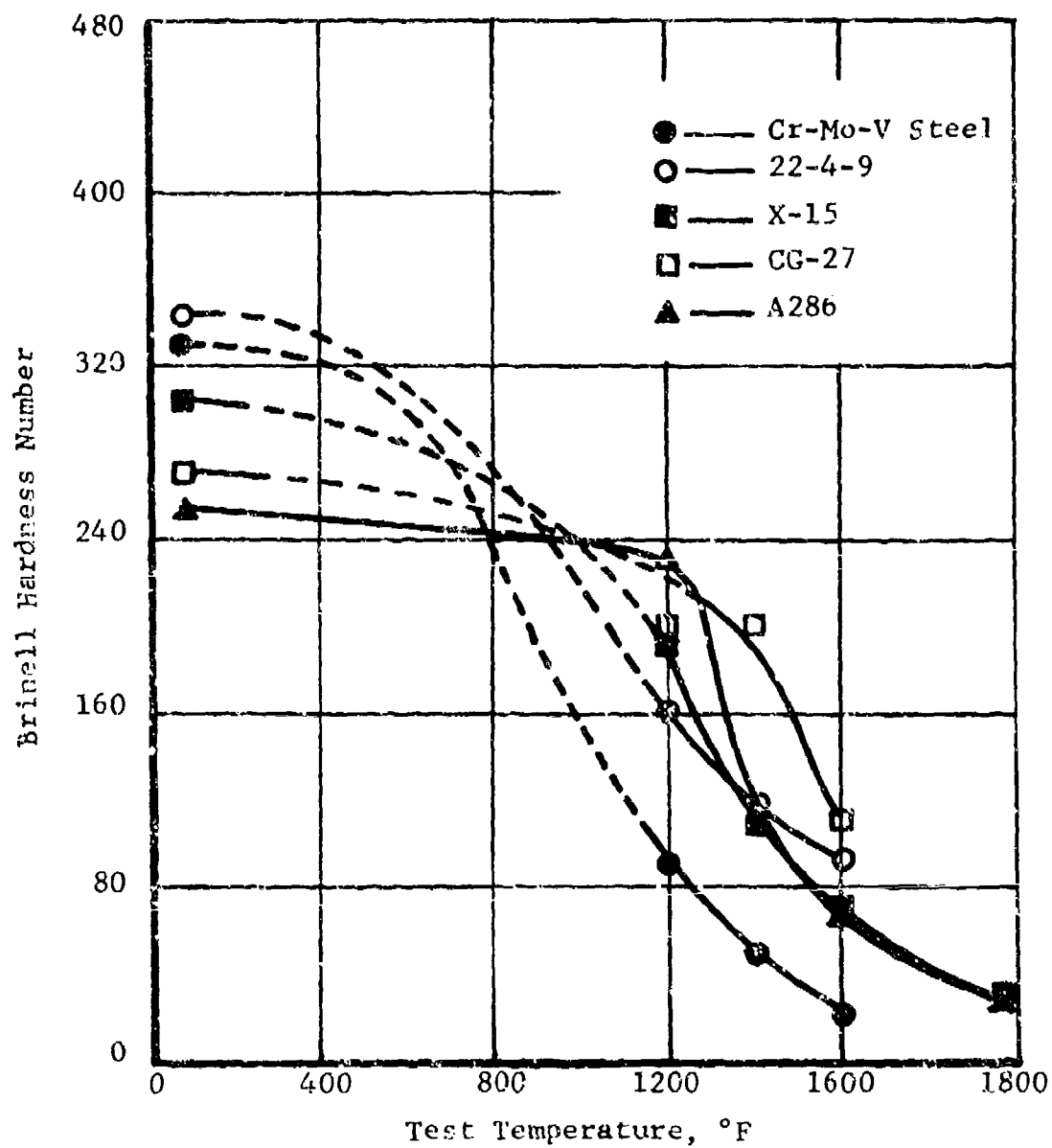


FIGURE 16 HOT HARDNESS DATA FOR SELECTED ALLOYS.

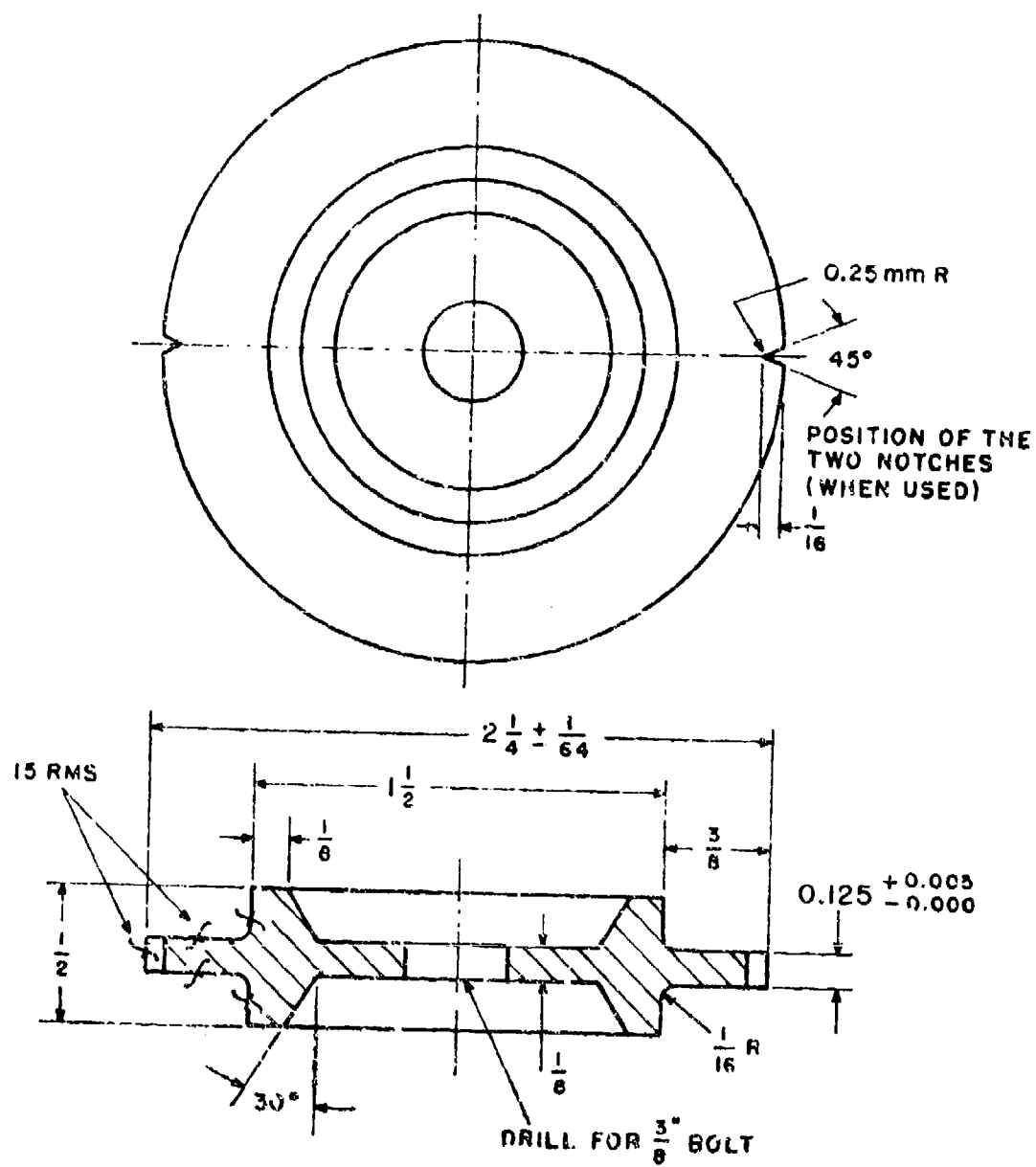


FIGURE 18 1:1 TRI THERMAL FATIGUE SPECIMEN.

<u>Steel</u>	<u>Time in Hot Bed, sec</u>	<u>Time in Cold Bed, sec</u>
X-15	18	35
22-4-9	14.5	24
CG-27	12	16
A286	13.5	22
Cr-Mo-V	12.5	19

Table 11 lists the propagation of cracks in the notched specimens of the five materials. These data are shown in Figure 19. The crack susceptibility of 22-4-9 alloy is readily apparent.

Thermal fatigue testing of unnotched specimens was also conducted. Figure 20 illustrates the test specimens. The test conditions for each alloy in the unnotched condition were similar to those employed on the notched specimens--i.e., hot bed temperature of 2000°F, cold bed temperature of 175°F, and a temperature interval of 1500°F to 600°F.

Table 12 lists the propagation of cracks in the unnotched specimens of the five materials. These data are shown in Figure 21. The CG-27 alloy exhibits the best resistance to crack initiation, followed by the A286 alloy. The X-15 alloy and the 22-4-9 alloy have the poorest resistance to crack initiation in this particular thermal cycle.

The relative ranking of thermal fatigue resistance is shown in Table 13.

Summary - The vented bomb tests ranked the gas erosion resistance of the materials in descending order as follows:

X-15 alloy
Cr-Mo-V steel
22-4-9 valve steel
A286 alloy
CG-27 alloy

Hot hardness resistance at 1600°F (in descending order) is ranked as:

CG-27 alloy
22-4-9 valve steel
X-15 alloy
A286 alloy
Cr-Mo-V steel

Table 11

PROPAGATION OF CRACKS IN NOTCHED SAMPLES
(Length in inches)

Cycles	1st Specimen				2nd Specimen				Avg
	Notch A		Notch B		Notch A		Notch B		
	Front	Back	Front	Back	Front	Back	Front	Back	
<u>X-15</u>									
100	.010	.009	.013	.011	.020	.015	.013	.015	.013
200	.042	.037	.042	.042	.053	.055	.045	.055	.047
300	.079	.070	.068	.071	.103	.098	.090	.102	.085
500	.192	.192	.184	.186	.218	.200	.185	.199	.196
<u>22-4-9</u>									
50	.003	.006	.005	.004	.016	.007	.005	.009	.007
150	.220	.227	.106	.107	.175	.161	.205	.199	.175
200	.281	.501	.256	.244	.300	.300	.300	.300	.285
<u>CG-27</u>									
100	0	0	.007	.010	.014	.011	0	.007	.006
200	.024	.025	.021	.030	.038	.038	.009	.018	.025
300	.050	.060	.050	.057	.077	.080	.035	.048	.057
500	.136	.148	.147	.150	.167	.166	.126	.135	.147
650	.210	.212	.220	.213	.235	.237	.197	.202	.216

Table 11 (Continued)

Cycles	1st Specimen				2nd Specimen			
	Notch A		Notch B		Notch A		Notch B	
	Front	Back	Front	Back	Front	Back	Front	Back
	<u>A286</u>							<u>Avg</u>
150	.022	.019	.017	.015	.018	.109	.015	.018
200	.036	.034	.025	.031	.034	.033	.029	.025
300	.069	.070	.055	.058	.066	.055	.058	.053
500	.145	.146	.137	.128	.136	.131	.124	.118
	<u>Gr-Mo-V</u>							
200	0	0	.028	.027	.034	.032	.032	.027
300	.047	.031	.052	.029	.044	.037	.040	.040
500	.090	.103	.112	.118	.137	.127	.113	.115

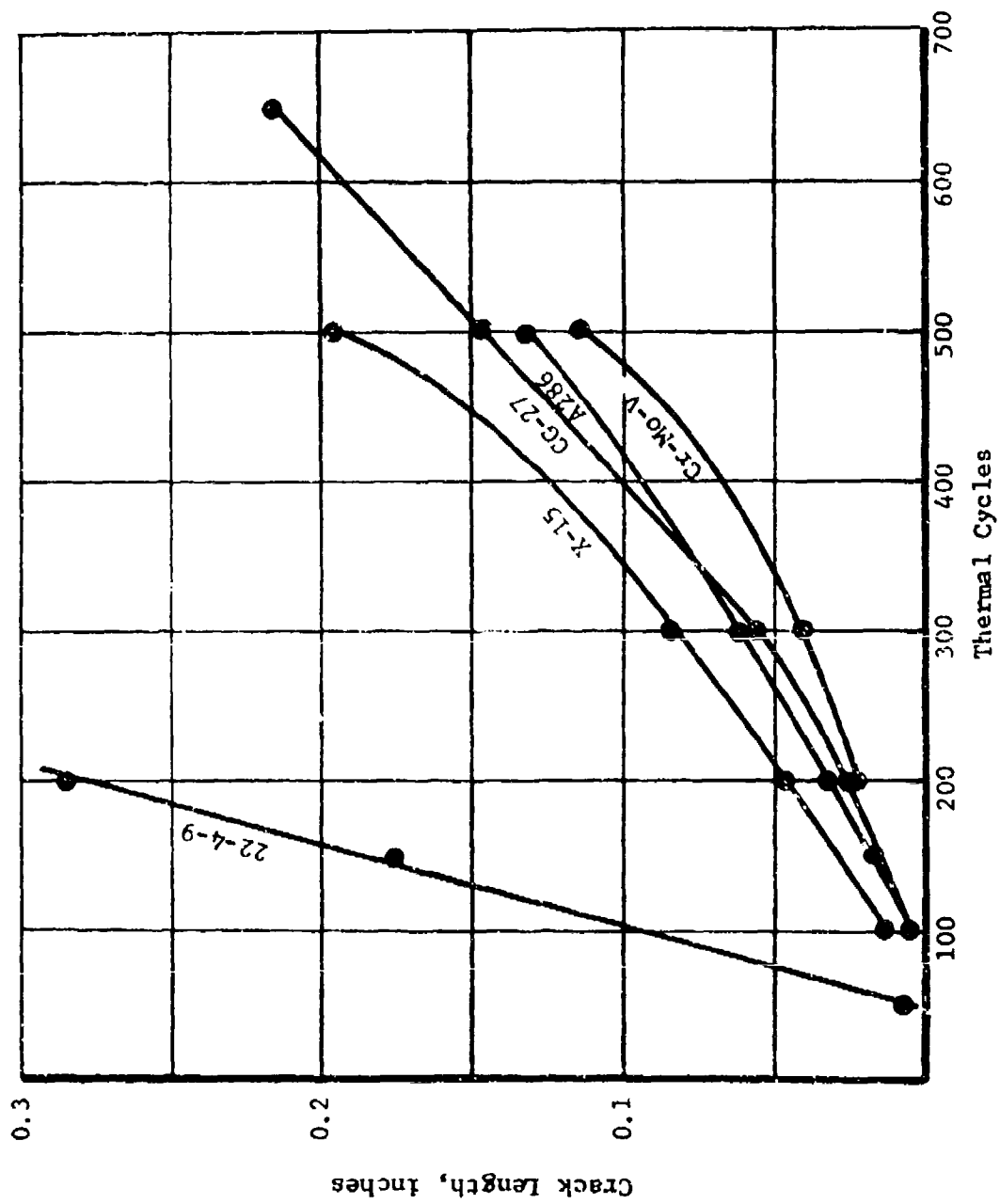


FIGURE 19 CRACK PROPAGATION IN NOTCHED SAMPLES.

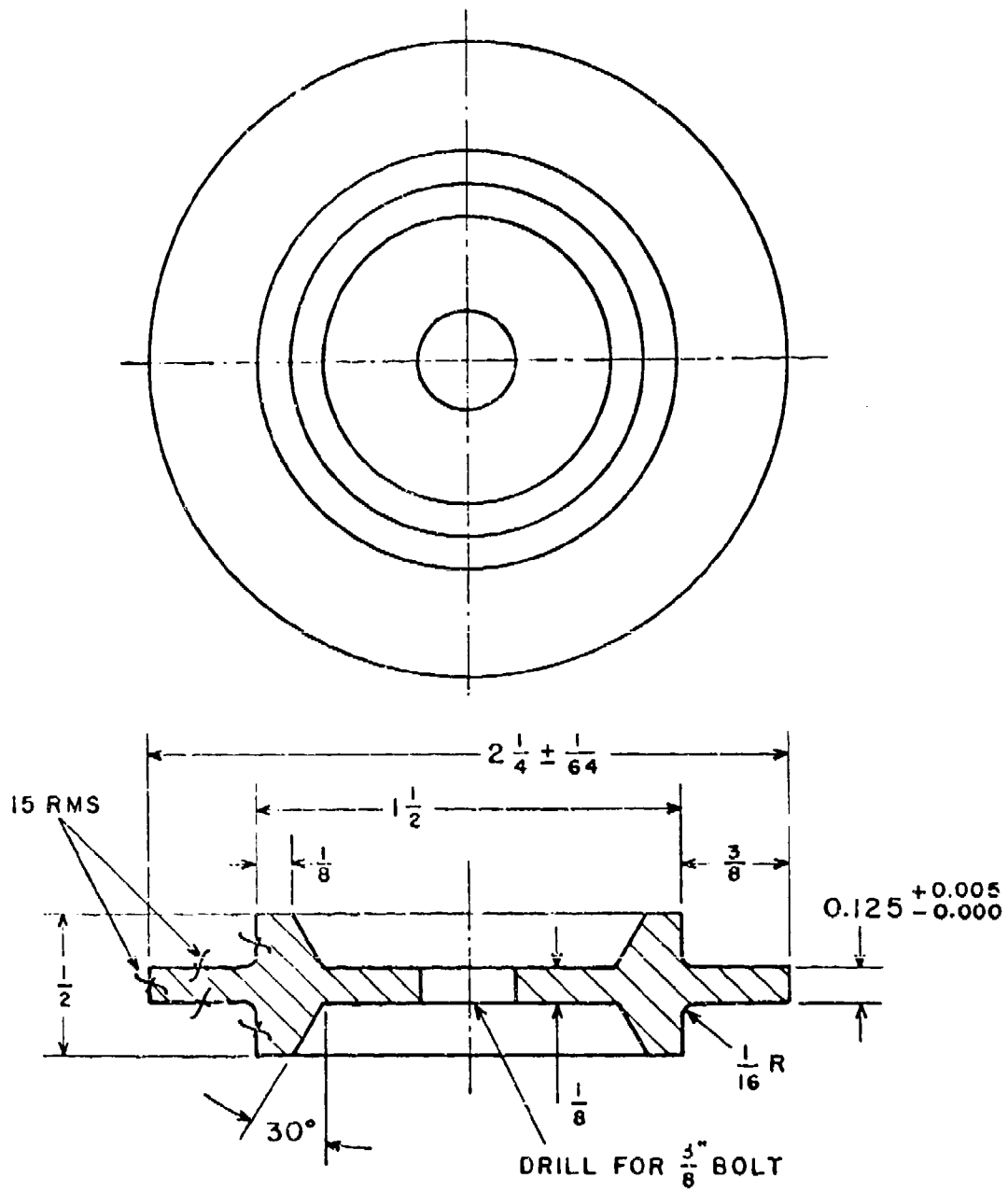


FIGURE 20 THERMAL FATIGUE SPECIMEN.

Table 12

PROPAGATION OF FIRST CRACK IN UNNOTCHED THERMAL FATIGUE SAMPLES

Cycles	1st Specimen			2nd Specimen			3rd Specimen			4th Specimen		
	Front	Back	Avg	Front	Back	Avg	Front	Back	Avg	Front	Back	Avg
X-15												
1400	Small cracks initiating 0			0	0	0	0	0	0	0	0	0
2000	.127	.136	.132	.189	.192	.191	.072	.047	.060	.049	.084	.067
2350	.291	.292	.292	> .400	> .400	> .400	.256	.248	.252	.145	.175	.160
22-4-9												
2000	> .400			> .400			Small cracks initiating			> .400		
2250	> .400			> .400			.065	0	.033	0	0	0
2500	> .400			> .400			.295	.297	.296	0	.065	.033
2750	> .400			> .400			> .400	> .400	> .400	> .400	> .400	> .400
3000	> .400			> .400			> .400			> .400		
3250	> .400			> .400			> .400			> .400		
3500	> .400			> .400			> .400			> .400		
3750	> .400			> .400			> .400			> .400		
CG-27												
2000	0	0	0	0	0	0	0	0	0	0	0	0
2500	.124	.037	.081	.116	.021	.069	0	.075	.038	0	0	0
3000	.244	.231	.238	.270	.280	.275	.121	.145	.133	.030	0	.015
3500	> .400	> .400	> .400	> .400	> .400	> .400	.301	.306	.304	.131	.125	.128
4000	> .400			> .400			> .400			> .400		
4500	> .400			> .400			> .400			> .400		
5000	> .400			> .400			> .400			> .400		

Table 12 (Continued)

Cycles	1st Specimen			2nd Specimen			3rd Specimen			4th Specimen		
	Front	Back	Avg	Front	Back	Avg	Front	Back	Avg	Front	Back	Avg
	A286											
2300	0	0	0	0	0	0						
2550	.082	0	.041	0	.066	.033						
2800	.155	.146	.150	.095	.115	.105	0	0	0			
3050	.247	.260	.254	.208	.197	.203	.095	0	.048			
3300							.145	.120	.133	0	0	0
3550							.191	.193	.192	.056	0	.028
3800							.255	.251	.253	.082	0	.041
Cr-Mo-V												
Testing concluded at 500 cycles due to circumferential fractures.												

Table 13
RELATIVE THERMAL FATIGUE RESISTANCE^a

<u>Material</u>	<u>Notched</u>	<u>Unnotched</u>
CG-27 alloy	3	1
A286 steel	2	2
X-15 steel	4	3
22-4-9 Stainless Steel	5	4
Cr-Mo-V steel	1	-

^aBest resistance is designated by 1.

Unnotched thermal fatigue tests ranked the materials, in descending order:

CG-27 alloy
A286 alloy
X-15 alloy
22-4-9 valve steel

These data appear to correlate quite well with the gun tests. The erosion tests (vented bomb) show that the CG-27 alloy will fail by reaction with the propellant gas stream if the firing sequence and barrel dimensions are such that sufficient heat is generated to allow the nickel in the CG-27 to react with the sulfur in the gas stream. The other alloys will fail either by cracking or flattening of the lands if the conditions of the firing test are such that the barrels attain high temperature.

Vented Bomb Tests

Based on the information obtained in the correlation study, it was established that the vented bomb test can only simulate the pressure, gas erosion, and thermal shock encountered in a gun test. The vented bomb was therefore utilized to evaluate the resistance of candidate materials to the above effects.

A variety of steels and superalloys offer potential as gun barrel materials. Included in the steels are the high-carbon, high-chromium cold work steels, chromium hot work tool steels, tungsten hot work tool steels, iron-nickel-chromium-molybdenum alloys, ferritic stainless steels, and the austenitic valve alloys. Among the superalloys, the iron-base and cobalt-base materials should provide better erosion resistance than the nickel-base materials because of the tendency of nickel to react with sulfur in the propellant gases.

Typical materials from the above classes were selected for testing in the vented bomb:

1. A286, an iron-nickel-chromium-molybdenum alloy.
2. 22Cr-4Ni-9Mn, an austenitic valve alloy
3. CG-27, an iron-base superalloy
4. X-15, an iron-base alloy
5. Cr-Mo-V steel, the current gun steel

6. Chromium-plated gun steel
7. Haynes Stellite 21, a cobalt alloy
8. 50Co-29Fe-20W-1C, a cobalt alloy
9. H11, a chromium hot work tool steel
10. D2, a high-carbon, high-chromium cold work steel
11. H26, a tungsten hot work tool steel
12. 446, a ferritic stainless steel
13. L605, a cobalt superalloy
14. HS-31, a cobalt-chromium-nickel-iron superalloy
15. S-590, a cobalt superalloy

Materials 1 through 7 were examined in the correlation study, and only the weight loss data will be considered in this section. The chemical compositions of the remaining alloys are listed in Table 14.

The 50Co-29Fe-20W-1C alloy has been evaluated at IITRI for a tool application. This material shows unusual wear resistance in the application. The material was solution-treated and quenched to a hardness of Rc 32 and then aged at 950°F to a hardness of Rc 45. In this condition, the material had a metallurgical structure of carbides dispersed in an alloy matrix.

The high-carbon, high-chromium cold work steels have chromium and carbon as the principal alloying elements, but they may also contain tungsten, molybdenum, cobalt, and vanadium. This class of steel is highly wear resistant with medium resistance to heat softening. D2 was selected to characterize the behavior of this type of steel. Hardness and unnotched Izod impact strength as a function of tempering temperature for D2 is shown in Figure 22. As can be seen, D2 undergoes a secondary hardening phenomenon at about 950°F and a tempered martensite embrittlement at 500°F. To avoid the limited ductility, a heat treatment consisting of austenitizing at 1850°F, air cooling, and a double temper at 1150°F was conducted for one set of vented bomb inserts. The resulting hardness was Rc 41.5. A second set of vented bomb inserts was heat treated as follows:

Austenitize at 1850°F

Air Cool

Table 14

CHEMICAL COMPOSITION OF CANDIDATE MATERIALS

Material	Composition, percent										
	C	W	Mo	V	Cr	Ni	Co	Mn	Si	Fe	Other
Cobalt alloy	1.3	20	--	--	--	--	50	--	--	28.7	--
H11	0.38	--	1.40	0.50	5.00	--	--	0.30	1.00	Ba1	--
D2	1.55	--	0.80	0.95	11.90	--	--	0.30	0.25	Ba1	--
H26	0.53	18.0	--	1.00	4.00	--	--	--	--	Ba1	--
446	0.20	--	--	--	25	--	--	1.5	1.0	Ba1	0.25N max
L605	0.15	15	--	--	20	10	Ba1	1.5	0.5	2.0	--
HS-31	0.45	7.0	--	--	25	10.5	Ba1	--	1.00	2	--
S-590	0.40	4	4	--	20	20	20	1.2	0.4	Ba1	4.0Cb

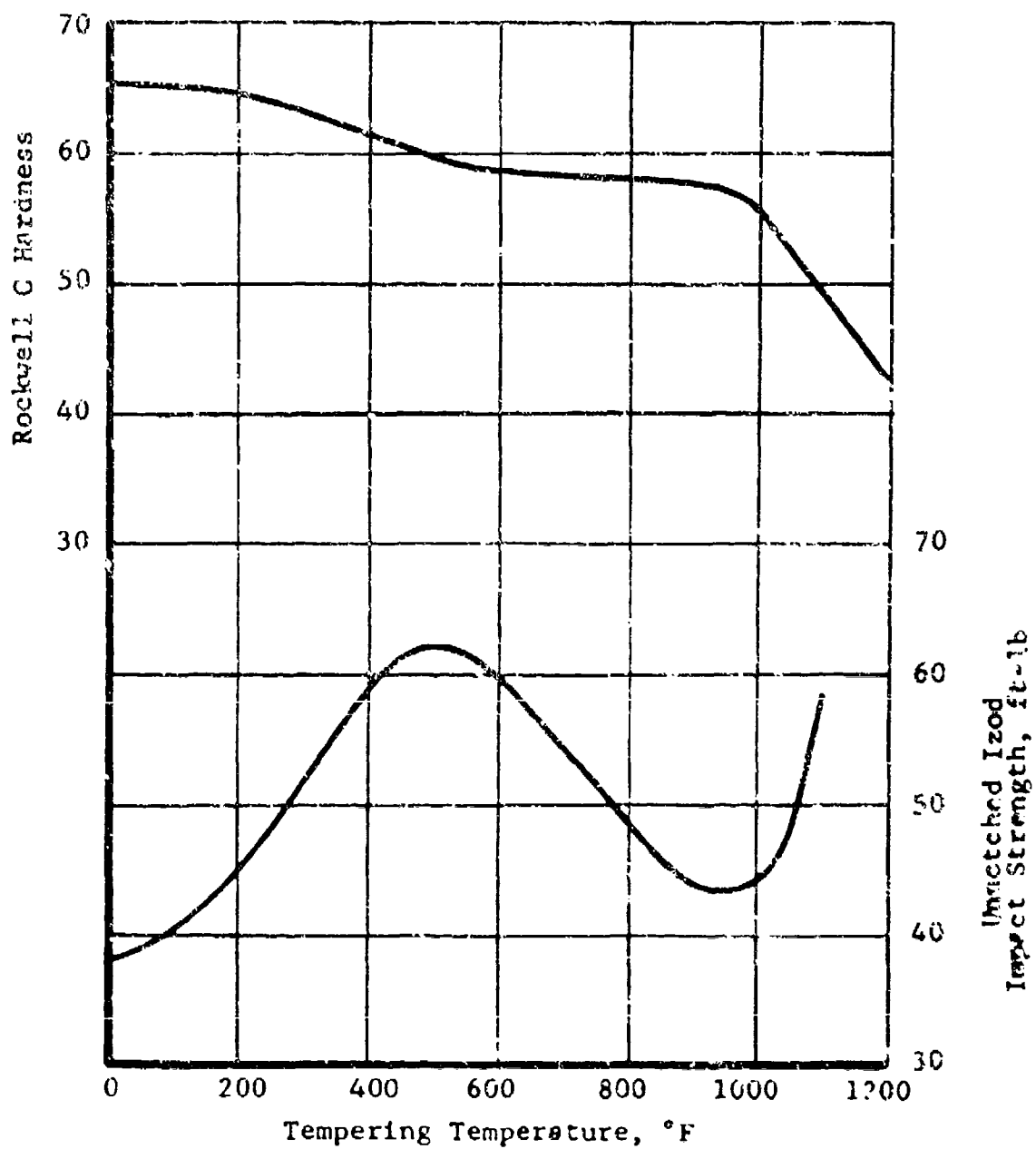


FIGURE 22 DEPENDENCE OF HARDNESS AND IMPACT STRENGTH OF D2 STEEL ON TEMPERING TEMPERATURE.

Spheroidize at 1550°F

Air Cool

Double temper at 1150°F

The spheroidizing treatment was given to improve the carbide morphology and toughness. The hardness of this set of samples was R_C 34.

H11 steel was selected to represent the chromium hot work class of alloys. This steel contains chromium and tungsten with additions of molybdenum and vanadium. It has good resistance to thermal softening because of the medium chromium content supplemented by the formation of tungsten, molybdenum, and vanadium carbides. The low carbon and relatively low total alloy content promote toughness in the hardness range of R_C 40 to 50. The H11 alloy has found use in highly stressed structural parts. It has above-average resistance to corrosion and oxidation as well as a relatively low coefficient of thermal expansion. Hardness and Charpy V-notch impact strength as a function of tempering temperature for H11 steel are shown in Figure 23. Hot hardness data for H11 hardened at 1850°F and double tempered at 1050°F are also shown in Figure 23. The vented bomb inserts were hardened at 1850°F and double tempered at 1150°F to provide a hardness of R_C 41.

The tungsten hot work steels are alloyed principally with carbon, tungsten, and chromium with some vanadium. The high alloy content increases resistance to high-temperature softening and washing; however, in the heat-treated state they possess low toughness. H26 was selected to typify this class of steel. Hardness as a function of tempering temperature for H26 is depicted in Figure 24. To assess the performance of the H26 in the vented bomb, inserts were hardened at 2100°F, oil quenched, and double tempered at 1250°F. After such treatment, the H26 had a hardness of R_C 41.

The ferritic stainless steel 446 typifies a class of materials which have excellent oxidation resistance at elevated temperatures. However, the strength of 446 is relatively low. The vented bomb inserts were austenitized at 1600°F, water quenched, and aged at 900°F for 16 hr. The aging treatment was conducted to increase strength; however, a hardness of only R_C 15 was obtained.

The wrought cobalt alloys have reasonably good mechanical properties and oxidation resistance at elevated temperature. To typify these materials S-590, L605, and HS-31

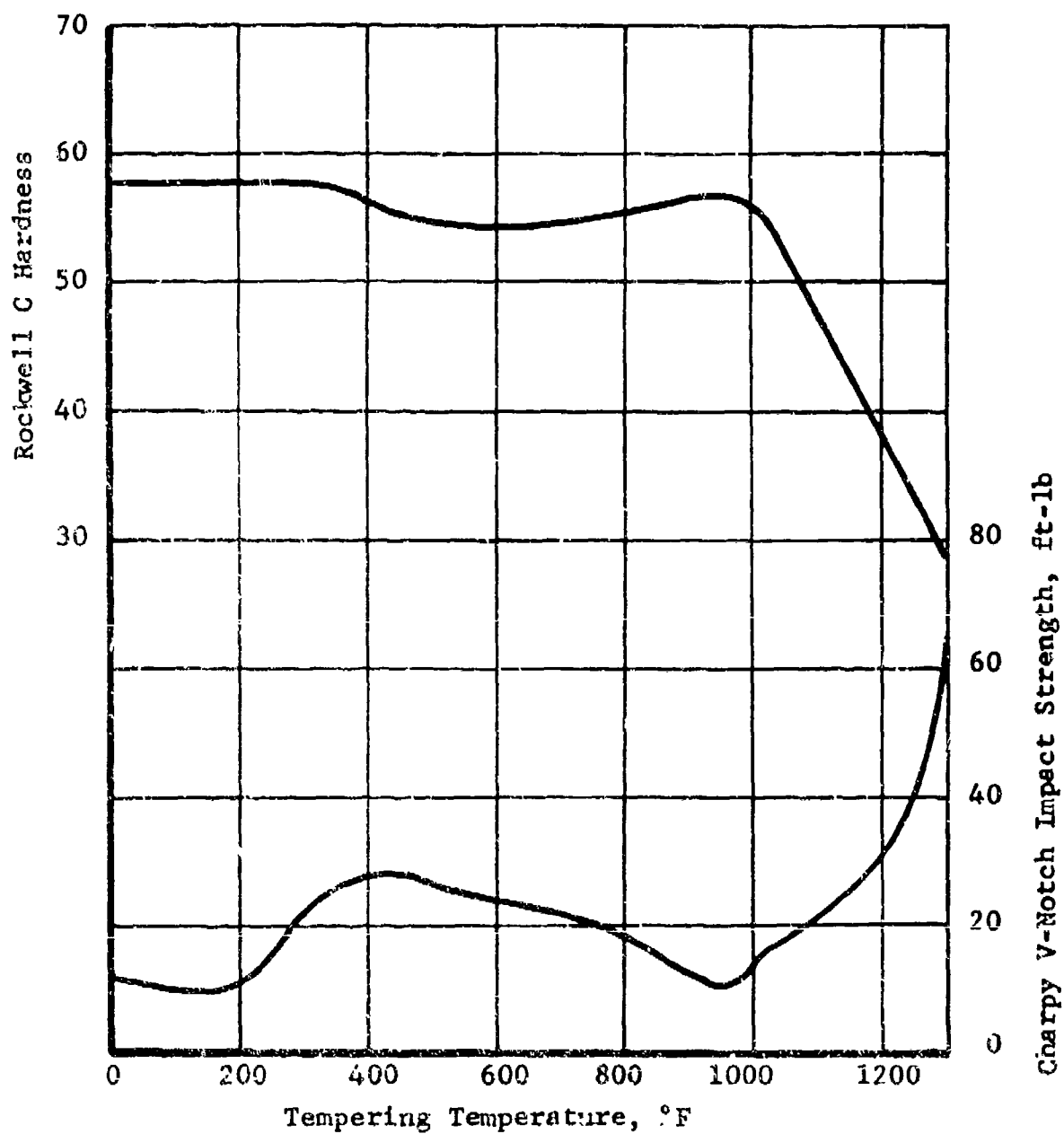


FIGURE 23 DEPENDENCE OF HARDNESS AND IMPACT STRENGTH OF H11 ON TEMPERING TEMPERATURE.

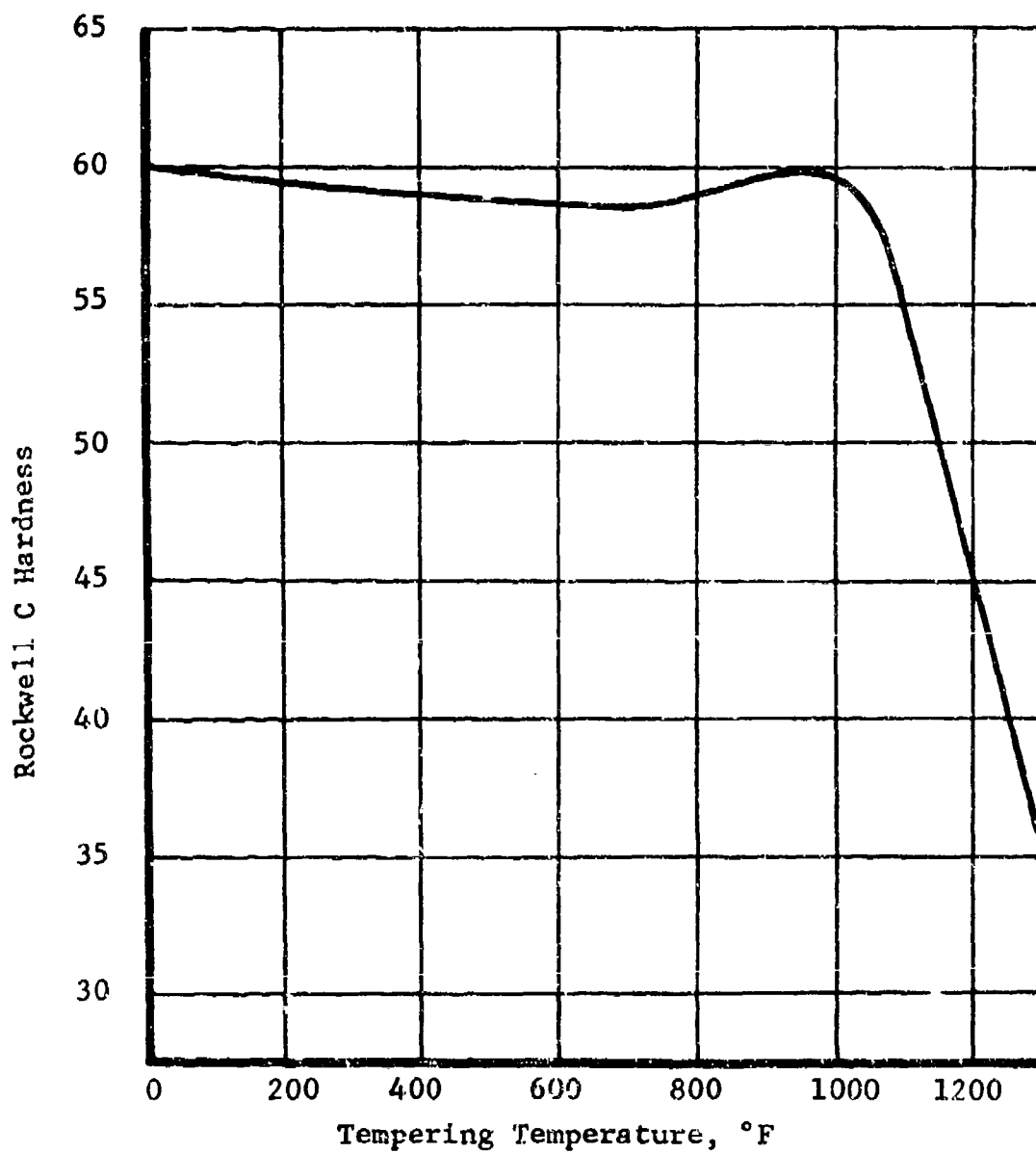


FIGURE 24 DEPENDENCE OF HARDNESS OF H26 ON TEMPERING TEMPERATURE.

were selected. S-590 is used for wheels and buckets for gas turbines and for forging operations to 1500°F. L605 is normally used in sheet form. Figure 25 shows the dependence of mechanical properties of S-590 on test temperature. The S-590 was solution treated at 2200°F, water quenched, aged at 1400°F for 16 hr and air cooled. The resulting hardness was R_C 30.

Figures 26 and 27 illustrate similar information for L605 and HS-31. The L605 alloy was solution treated at 2250°F, water quenched, aged at 1350°F for 50 hr, and air cooled. The hardness developed by the heat treatment was R_C 32. The HS-31 material was hot forged between 2250°F and 1800°F. The HS-31 inserts were fabricated from the as-forged material and had a hardness of R_C 38.

Bomb inserts, 2 inches long, of each material (Nos. 8 to 15) were fabricated with a 7.62mm bore. WC846 ball propellant was utilized at a load of 23 1/2 g to produce a peak pressure of $50,000 \pm 2,000$ psi at a rise time of approximately 0.5 millisecond. Each material was subjected to a one- and a five-shot sequence. The specific weight loss data are reported in Table 15.

Table 16 ranks the various materials on a weight change per shot based on the multiple firing data. This table indicates the resistance to the erosion and thermal shock which are encountered in the vented bomb. The ranking does not discriminate between weight loss due to erosion and that associated with cracking.

The H11 and the 446 alloys appeared to have gained weight during the firing. The S-590 lost considerable weight on one shot; however, the five-shot sequence indicates that on following shots a weight increase occurred. This indicates that a gas-metal reaction is probably occurring. The D2 appeared to gain weight slightly on the first shot and then lost weight during the five-shot sequence. The other alloys lost weight on the first shot and showed a continual loss on the five-shot schedule.

To characterize the mode of failure, extensive metallographic analysis on the fired inserts was performed.

In preparing the metallographic samples, a nickel plating was applied to the bore surface to preserve the edges. The transverse specimen was taken 1/2 inch from the inlet end and the longitudinal section from 1/2 to 1 1/2 inches from the inlet end. Figures 28 and 29 show the longitudinal

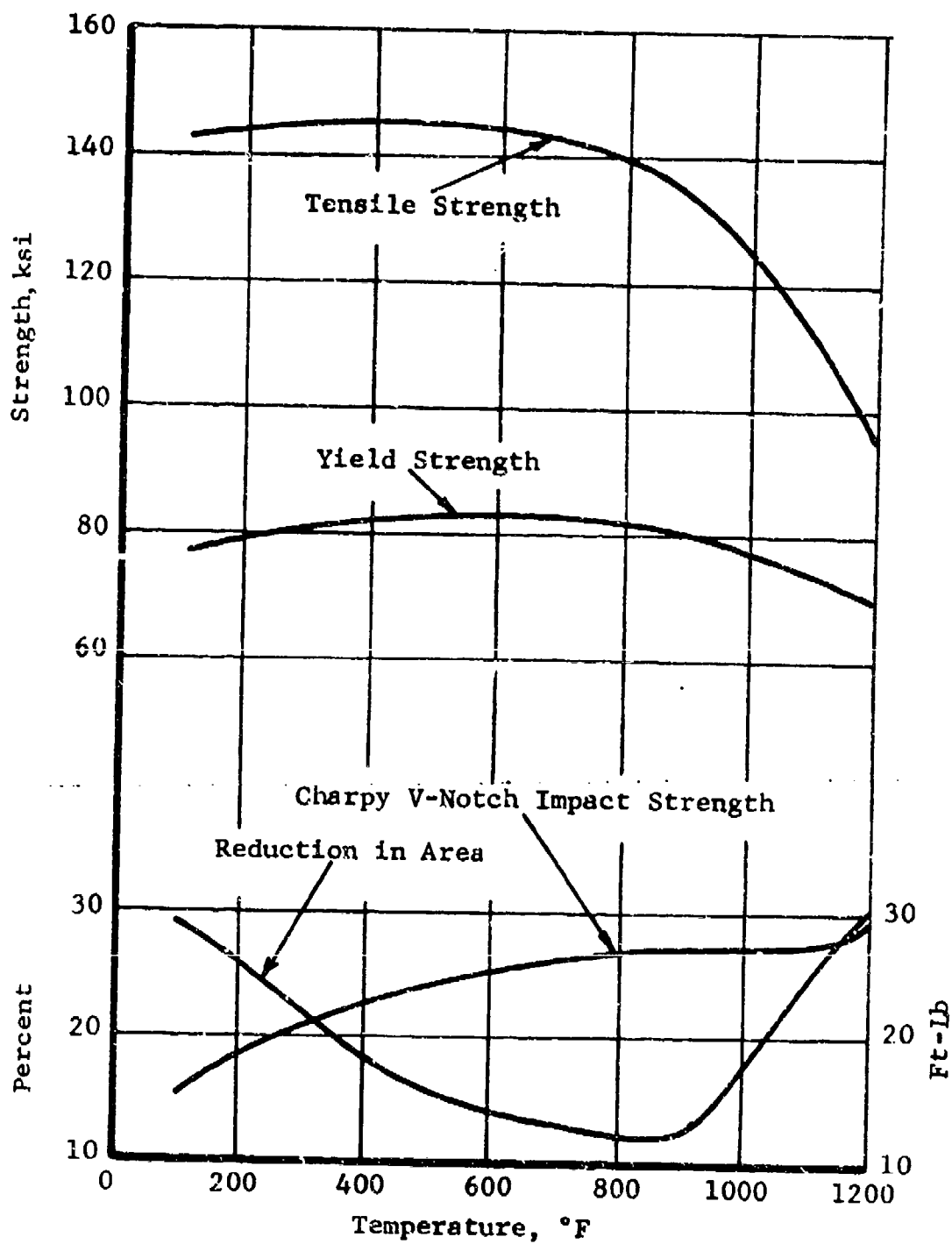


FIGURE 25 DEPENDENCE OF MECHANICAL PROPERTIES OF S-590 ALLOY ON TEST TEMPERATURE.

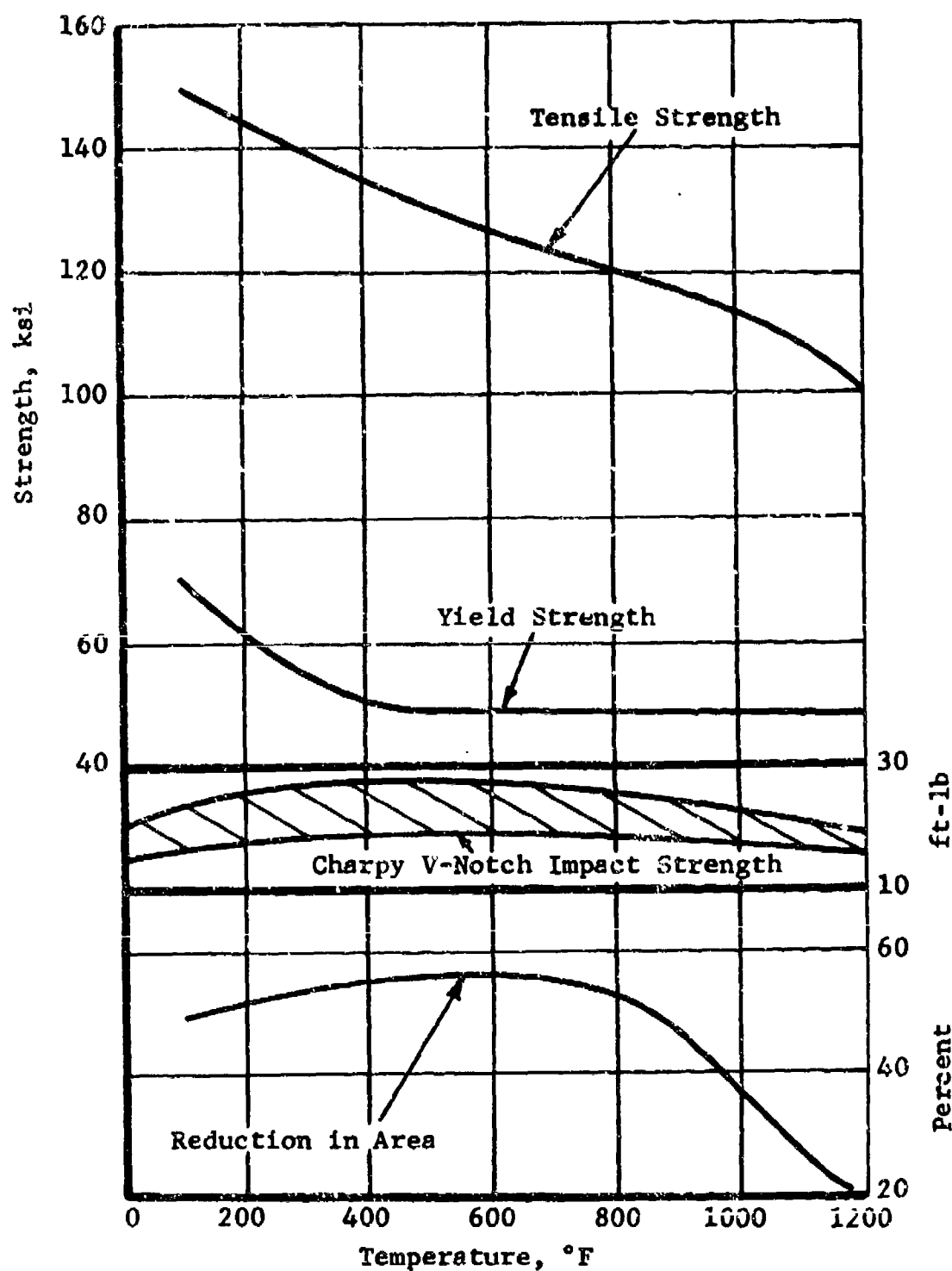


FIGURE 26 DEPENDENCE OF MECHANICAL PROPERTIES OF L605 ALLOY ON TEST TEMPERATURE.

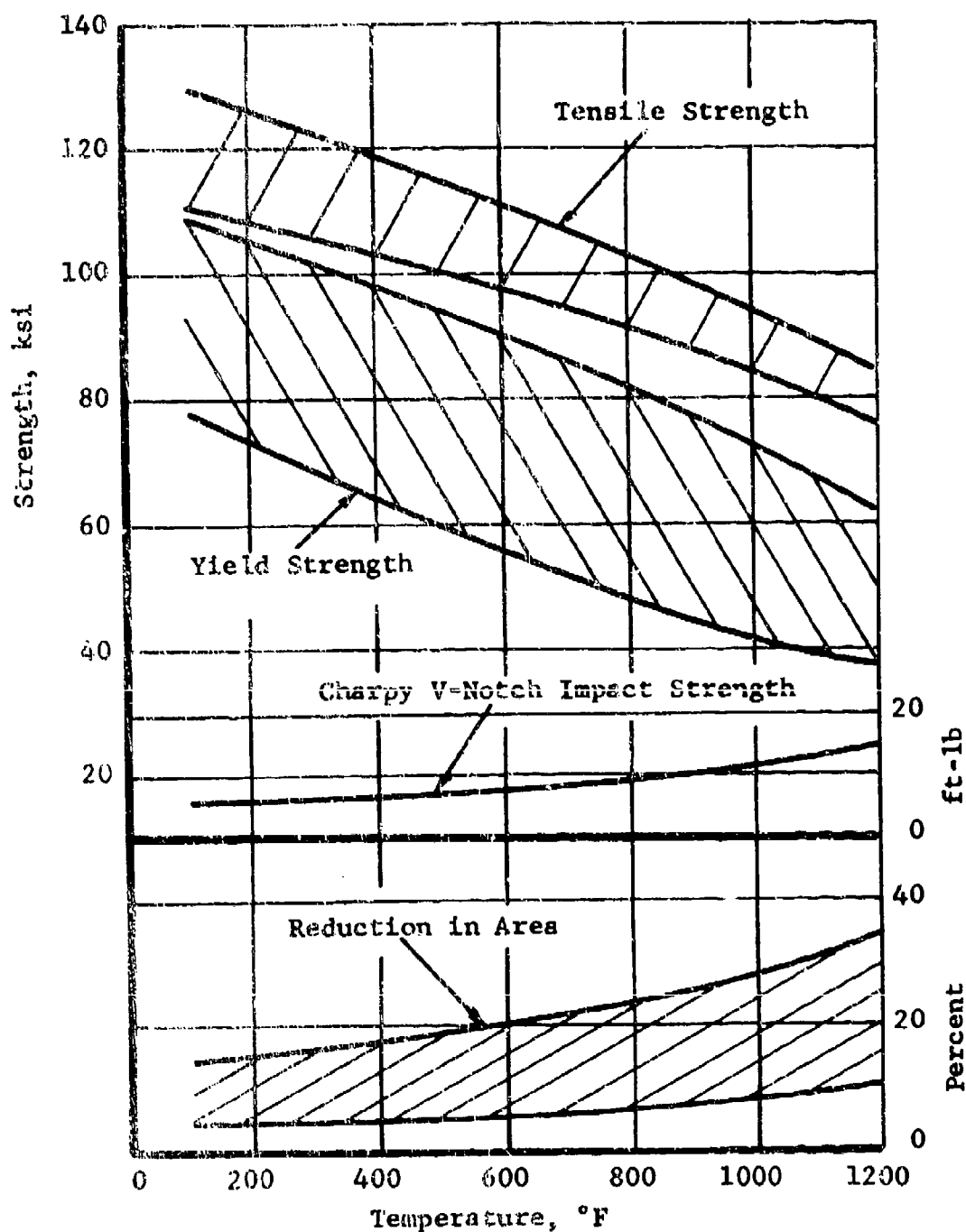


FIGURE 27 DEPENDENCE OF MECHANICAL PROPERTIES OF HS-31 ALLOY ON TEST TEMPERATURE.

Table 15

WEIGHT CHANGE DATA OF SELECTED MATERIALS AFTER FIRINGS
IN THE VENTED BOMB WITH WC846 PROPELLANT

Materials	Weight Change, grams		
	1 Shot	3 Shots	5 Shots
A285	-	-0.305 ^a	-
22Cr-4Ni-9Mn	-	-0.0531	-
CG-27	-	-0.636	-
X-15	-	-0.002	-
Cr-Mo-V	-	-	-0.0059
Chrome plated Cr-Mo-V	-	-	-0.0000
HS 21	-	-	-0.0650
50Co-29Fe-20W-1C	0.000	-	0.0000
H11	+0.0001	-	+0.001
D2	+0.002	-	-0.008
H26	+0.002	-	-0.011
446	+0.001	-	+0.008
L605	-0.001	-	-0.001
HS 31	-0.003	-	-0.008
S-590	-0.091	-	-0.009

^aInsert galled on removal from holder.

Table 16

UNIT WEIGHT CHANGE FOR SELECTED MATERIALS
AFTER FIRINGS IN THE VENTED BOMB
WITH WC846 PROPELLANT

Materials	Weight Change, grams	
	Based on 3 Shots	Based on 5 Shots
446 stainless steel	-	+0.0016
H11 steel	-	+0.0002
50Co-29Fe-20W-1C alloy	-	0.0000
Chrome plated Cr-Mo-V steel	-	0.0000
L605 alloy	-	-0.0005
X-15 steel	-0.0006	-
Cr-Mo-V	-	-0.0012
D2 steel	-	-0.0016
HS 31 alloy	-	-0.0016
S-590 alloy	-	-0.0018
H26 alloy	-	-0.0055
HS 21 alloy	-	-0.0130
22Cr-4Ni-9Mn steel	-0.0177	-
A286 steel	-0.1016	-
CG-27	-0.2120	-



(a) Longitudinal

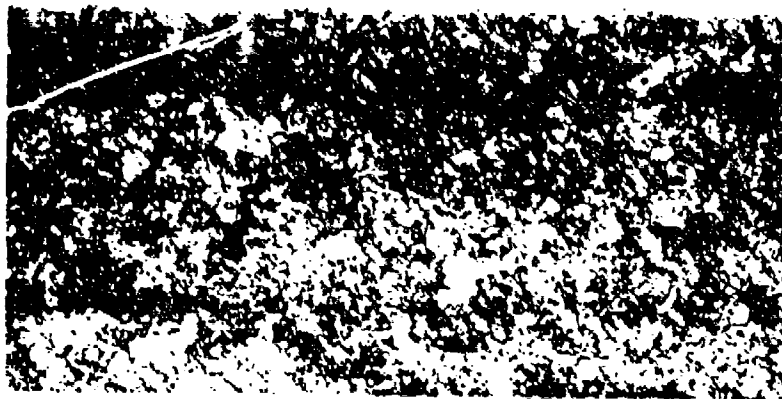
225X



(b) Transverse

225X

FIGURE 28 PHOTOMICROGRAPHS SHOWING THE STRUCTURE ALONG THE BORE SURFACE OF AN H11 ALLOY INSERT AFTER ONE VENTED BOMB SHOT WITH WC846 PROPELLANT. (PICRIC AND HYDROCHLORIC ACID IN ALCOHOL ETCH)



225X

(a) Longitudinal



225X

(b) Transverse

FIGURE 29 PHOTOMICROGRAPHS SHOWING THE STRUCTURE ALONG THE BORE SURFACE OF AN H11 ALLOY INSERT AFTER FIVE VENTED BOMB SHOTS WITH WC846 PROPELLANT. (PICRIC AND HYDROCHLORIC ACID IN ALCOHOL ETCH)

and transverse section of the H11 alloy after one and five shots. No cracking was observed anywhere along the bore surface, and this is indicative of the good thermal resistance of the hot work tool steels. In these photographs a heat-affected zone is present along the bore surface.

Figures 30 and 31 illustrate the bore surfaces of H26, the tungsten hot work tool steel, after one and five shots. There is no evidence of cracking on the bore surface of the inserts after either test series. There is, however, a small heat-affected zone present along the bore surface. This is more evident in the five-shot specimens.

The bore surfaces of the D2, the high-carbon, high-chromium cold work steel after one and five shots are shown in Figures 32 and 33. In the one-shot sequence one very fine crack was observed in microexamination. The specimen subjected to the five-shot cycle exhibited many cracks. The transverse section of Figure 33 shows two of them at a magnification of 500X.

Figures 34 and 35 depict the typical appearance of the bore surface of the 446 alloy inserts after one and five shots in the vented bomb. In these firing sequences one small crack was observed on the bore surface of the five-shot insert.

Figures 36 and 37 are typical photomicrographs along the bore surface of the L605 inserts which had received 1 and 5 shots. The surfaces have been nickel plated. Cracking is readily apparent in the insert which received 5 shots.

Figures 38 and 39 typify the metallurgical structure along the bore surface of the HS-31 alloy after 1 and 5 shots in the vented bomb. The surfaces were nickel-plated to preserve the as-fired bore surface. The cracks which occurred in these specimens were very fine and few in number. The areas shown do not have an appreciable evidence of cracking.

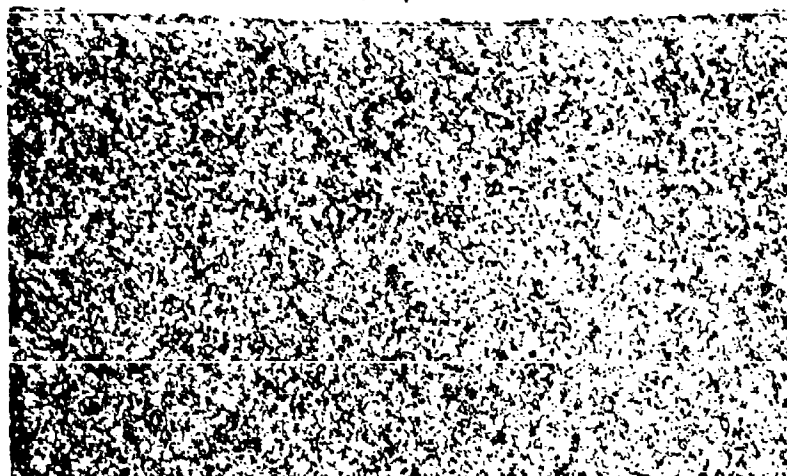
Figures 40 and 41 depict the bore surface of the S-590 alloy inserts which received 1 and 5 shots. Again, nickel plating was applied to the as-fired bore so as to protect the surface. Cracking which occurred during firing is apparent.

A photomicrograph showing the bore surface of a transverse section of the 50Co-29Fe-20W-1C alloy is presented in Figure 42. The structure of this material is a massive



(a) Longitudinal

225X



(b) Transverse

225X

FIGURE 30 PHOTOMICROGRAPHS SHOWING THE STRUCTURE ALONG THE BORE SURFACE OF AN H26 ALLOY INSERT AFTER ONE VENTED BOMB SHOT WITH WC846 PROPELLANT. (PICRIC AND HYDROCHLORIC ACID IN ALCOHOL ETCH)



(a) Longitudinal

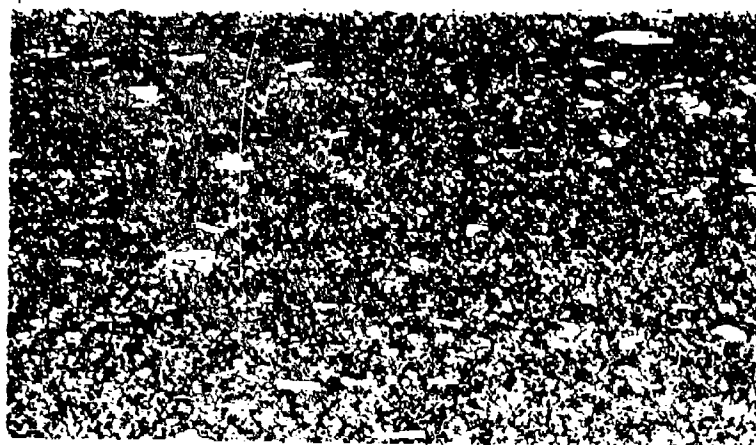
225X



(b) Transvers

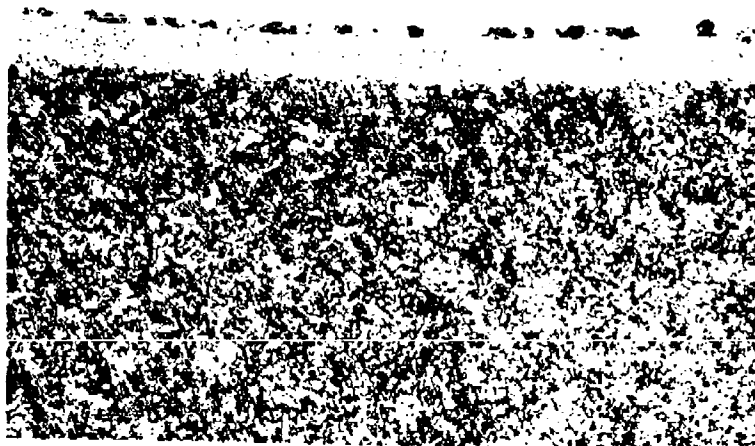
225X

FIGURE 31 PHOTOMICROGRAPHS SHOWING THE STRUCTURE ALONG THE BORE SURFACE OF AN H26 ALLOY INSERT AFTER FIVE VENTED BOMB SHOTS WITH WC846 PROPELLANT. (PICRIC AND HYDROCHLORIC ACID IN ALCOHOL, ETCH)



(a) Longitudinal

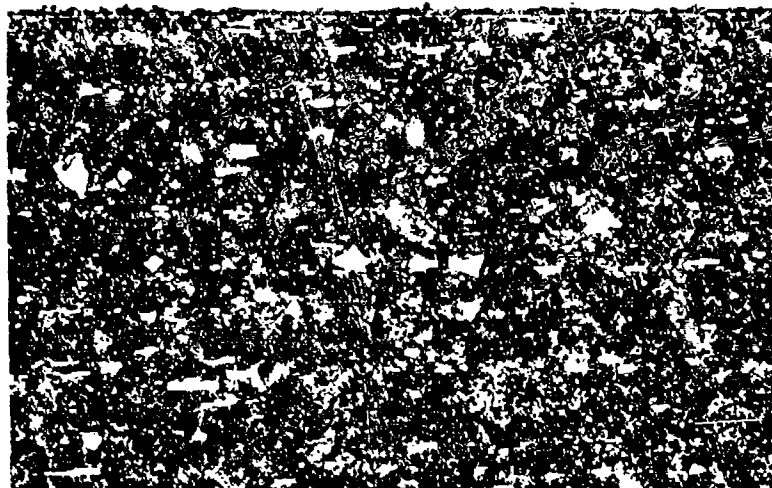
225X



(b) Transverse

225X

FIGURE 32 PHOTOMICROGRAPHS SHOWING THE STRUCTURE ALONG THE BORE SURFACE OF THE D2 ALLOY INSERT AFTER ONE VENTED BOMB SHOT WITH WC846 PROPELLANT. (PICRIC AND HYDROCHLORIC ACID IN ALCOHOL ETCH)



225X

(a) Longitudinal



225X

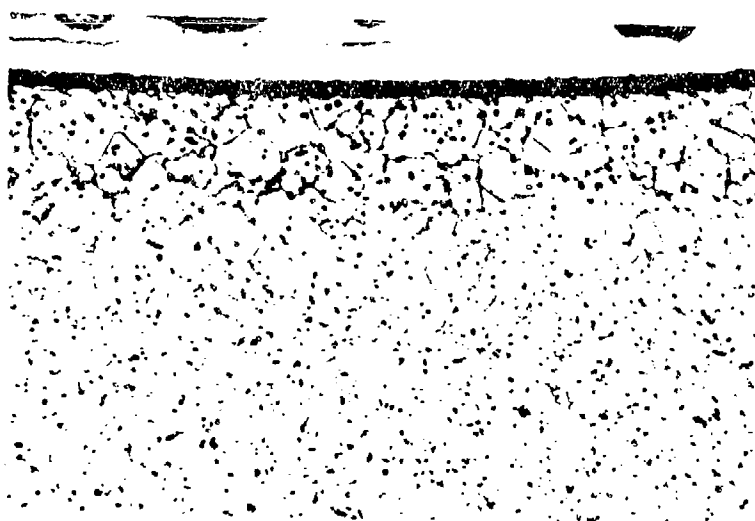
(b) Transverse

FIGURE 33 PHOTOMICROGRAPHS SHOWING THE STRUCTURE ALONG THE BORE SURFACE OF THE D2 ALLOY INSERT AFTER FIVE VENTED BOMB SHOTS WITH WC845 PROPELLANT. (PICRIC AND HYDROCHLORIC ACID IN ALCOHOL ETCH)



(a) Longitudinal

225X



(b) Transverse

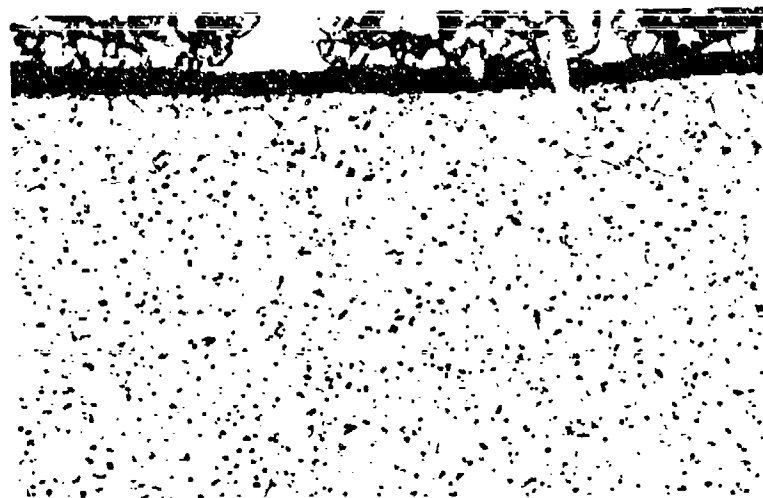
225X

FIGURE 34 PHOTOMICROGRAPHS SHOWING THE STRUCTURE ALONG
THE BORE SURFACE OF THE 446 ALLOY INSERT AFTER ONE
VENTED BOMB SHOT WITH WC846 PROPELLANT. (10%
SULFURIC ACID ELECTROLYTIC ETCH)



225X

(a) Longitudinal



225X

(b) Transverse

FIGURE 35 PHOTOMICROGRAPHS SHOWING THE STRUCTURE ALONG THE BORE SURFACE OF THE 446 ALLOY INSERT AFTER FIVE VENTED BOMB SHOTS WITH WC846 PROPELLANT. (10% SULFURIC ACID ELECTROLYTIC ETCH)



(a) Longitudinal

225X



(b) Transverse

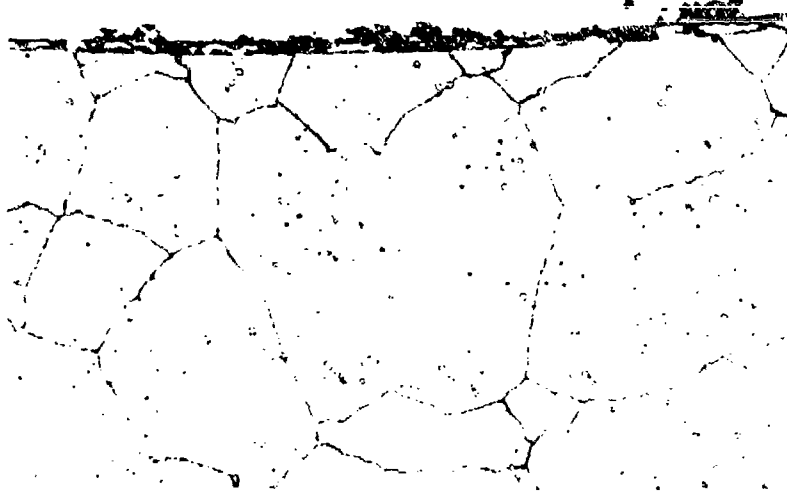
225X

FIGURE 36 PHOTOMICROGRAPHS SHOWING THE STRUCTURE ALONG THE BORE SURFACE OF AN I605 ALLOY INSERT AFTER ONE VENTED BOMB SHOT WITH WC846 PROPELLANT. (5% CHROMIC OXIDE ELECTROLYTIC ETCH)



(a) Longitudinal

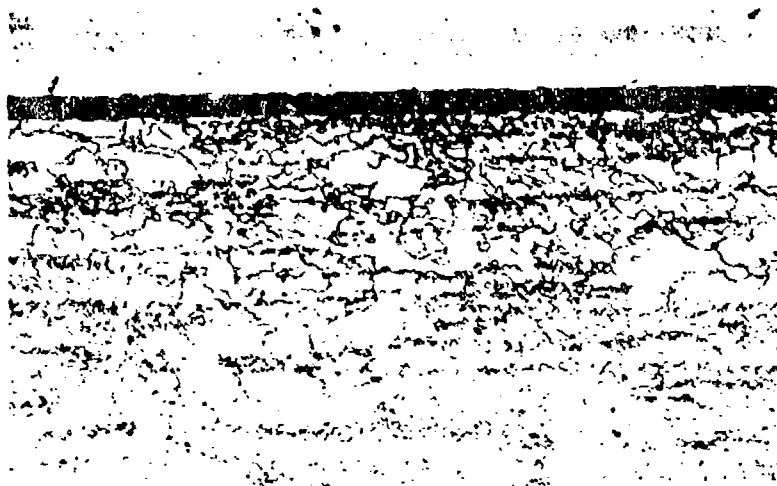
225X



(b) Transverse

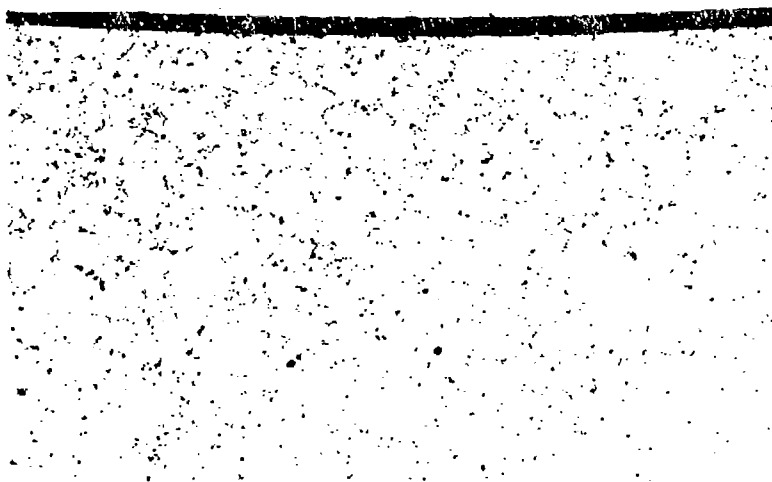
225X

FIGURE 37 PHOTOMICROGRAPHS SHOWING THE STRUCTURE ALONG THE BORE SURFACE OF AN L605 ALLOY INSERT AFTER FIVE VENTED BOMB SHOTS WITH WC846 PROPELLANT. (5% CHROMIC OXIDE ELECTROLYTIC ETCH)



(a) Longitudinal

225X



(b) Transverse

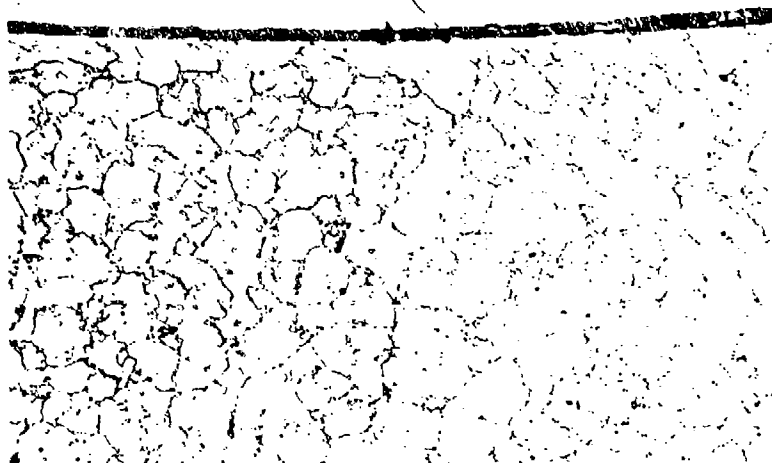
225X

FIGURE 38 PHOTOMICROGRAPHS SHOWING THE STRUCTURE ALONG THE BORE SURFACE OF AN HS-31 ALLOY INSERT AFTER ONE VENTED BOMB SHOT WITH WC846 PROPELLANT. (5% CHROMIC OXIDE ELECTROLYTIC ETCH)



(a) Longitudinal

225X



(b) Transverse

225X

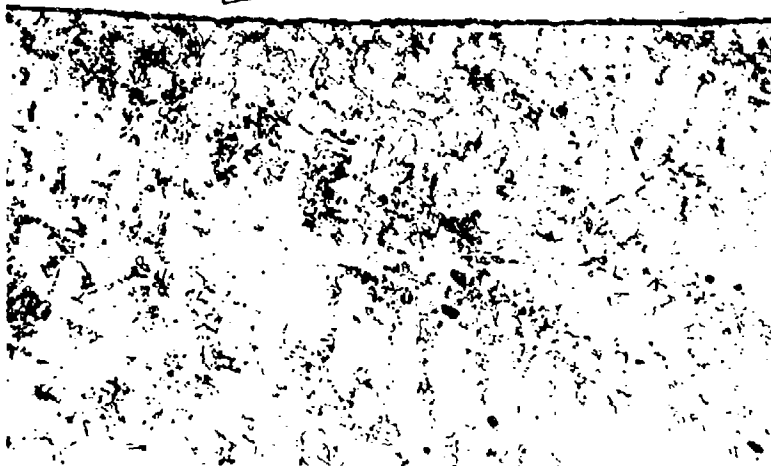
FIGURE 39 PHOTOMICROGRAPHS SHOWING THE STRUCTURE ALONG THE BORE SURFACE OF AN HS-31 ALLOY INSERT AFTER FIVE VENTED BOMB SHOTS WITH WC846 PROPELLANT. (5% CHROMIC OXIDE ELECTROLYTIC ETCH)



(a) Longitudinal

225X

Reproduced from
best available copy.



(b) Transverse

225X

FIGURE 40 PHOTOMICROGRAPHS SHOWING THE STRUCTURE ALONG THE BORE SURFACE OF AN S-590 ALLOY INSERT AFTER ONE VENTED BOMB SHOT WITH WC846 PROPELLANT. (5% CHROMIC OXIDE ELECTROLYTIC ETCH)



(a) Longitudinal

225X

Reproduced from
best available copy.



(b) Transverse

225X

FIGURE 41 PHOTOMICROGRAPHS SHOWING THE STRUCTURE ALONG
THE BORE SURFACE OF AN S-590 ALLOY INSERT AFTER FIVE
VENTED BOMB SHOTS WITH WC846 PROPELLANT. (5%
CHROMIC OXIDE ELECTROLYTIC ETCH)



Nital Etch

500X

FIGURE 42 PHOTOMICROGRAPH OF A 50Co-29Fe-20W-1C ALLOY
REVEALING THE TRANSVERSE STRUCTURE ALONG THE BORE SURFACE
AFTER FIVE VENTED BOMB FIRINGS WITH IMR PROPELLANT.

dispersion of carbides in a cobalt matrix. Again, nickel plating was employed to protect the bore surface during metallographic preparation. There are no apparent cracks along the bore surface.

Table 17 summarizes the microexamination of the selected alloys after being fired in the vented bomb. From the data it can be concluded that:

1. The cobalt-base superalloys tend to fail by cracking.
2. The 22Cr-4Ni-9Mn alloy exhibits brittle behavior in the vented bomb environment.
3. With the exception of D2 steel and 446 stainless steel, steel alloys do not tend to fail by cracking.
4. Chrome plate on steel produces crack starters which propagate into the steel outer element.
5. The 50Co-29Fe-20W-1C alloy and the CG-27 alloy do not appear to fail by cracking in the vented bomb.

Phase III - Materials Selection

The following material were selected for evaluation as gun barrels:

1. 50Co-29Fe-20W-1C alloy
2. Chrome-plated CG-27 alloy
3. Chrome-plated H11

The rationale for selecting these materials is as follows:

1. The 50Co-29Fe-20W-1C alloy showed good erosion resistance in the vented bomb test. There was no evidence of cracking, and the metallurgical structure of this material can be controlled to produce a dispersion of hard carbide precipitate in a tough matrix. In this condition a hardness of Rc 44 is obtained and the carbide precipitate will provide excellent wear resistance.

Table 17

SUMMARY OF MICROEXAMINATION OF SELECTED ALLOYS
SUBJECTED TO FIRINGS IN THE VENTED BOMB WITH WC846 PROPELLANT

Alloy	No. of of Shots	Cross Section 1/2 in. from Inlet	Longitudinal Center Section 1 in. Long
A286 steel ^c	3	No cracks	No cracks
22Cr-4Ni-9Mn ^a	3	Cracked	Cracked
CG-27 alloy ^a	3	No cracks	No cracks
X-15 steel ^a	3	No cracks	No cracks
Cr-Mo-V steel	5	No cracks	No cracks
Chrome-plated Cr-Mo-V	5	Many fine cracks	Many fine cracks
HS 21	5	Many fine cracks	Many fine cracks
50Co-29Fe-20W-1C alloy	5	No cracks	No cracks
H11 steel	1 5	No cracks No cracks	No cracks No cracks
D2 steel	1 5	1 small crack Many small cracks	No cracks No cracks
H26 steel	1 5	No cracks No cracks	No cracks No cracks
446 stainless steel	1 5	No cracks 1 small crack	No cracks No cracks
L605 alloy	1 5	1 large crack and a few very small cracks Many fine cracks	A few small cracks Many fine cracks
HS 31 alloy	1 5	A few very fine cracks A few very fine cracks	A few very fine cracks A few very fine cracks
S-590 alloy	1 5	A few very fine cracks Many small cracks	A few very fine cracks Many small cracks

^aAnalysis performed at Rock Island Arsenal.

2. The CG-27 alloy has good mechanical properties but has relatively poor erosion resistance as measured in the vented bomb. Chrome plating the CG-27 alloy theoretically will provide the erosion resistance, and the mechanical properties of the CG-27 alloy should provide sufficient support and crack resistance to obtain excellent performance as a gun barrel.
3. The H11 steel is a much tougher and wear resistant material than the Cr-Mo-V steel utilized in current gun barrels. The toughness and strength combination in conjunction with the erosion-resistant chrome plate would result in a good gun barrel system.

Sufficient quantities of the 50Co-29Fe-20W-1C alloy, CG-27 alloy, and H11 steel to fabricate 12 gun barrels of each material were obtained. The 50Co-29Fe-20W-1C alloy was made by the extrusion of powder into 2 inch rod by Federal-Mogul. The extruded rod was heat treated and shipped to Rock Island Arsenal. At the direction of Rock Island Arsenal 4 inch rounds of the H11 steel and the CG-27 alloy were shipped to Battelle-Northwest for fabrication into unplated 7.62mm barrels. Rock Island Arsenal chrome-plated the H11 and CG-27 barrels.

Phase IV - Fabrication of Selected Materials into Gun Barrels and Test Firing

Fabrication

The materials furnished by IITRI were to be fabricated into gun barrels by Battelle-Northwest. A formal report(13) was issued by Battelle-Northwest describing the fabrication methods. The CG-27 and H11 alloys were processed into barrels; however, the cobalt alloy could not be rifled by swaging. The following summarizes the Battelle-Northwest work:

CG-27 Processing - The CG-27 was supplied as solution treated, 4-1/4 inch diameter wrought bar. This material was machined into the 4 inch diameter extrusion billets. The billets were preheated to 2050°F inside stainless steel cans in a SiC resistance element powered air atmosphere furnace for 2-3 hr.

The extrusion step was performed on a 1250-ton press to produce a 1.35 inch diameter extrusion containing a mild steel sacrificial mandrel. The billet container and die were lubricated with "Oil Dag"* and "Phosphatherm RN."** The extrusion was conducted at a ram speed of approximately 300-330 inches per minute. The extrusion was rough straightened while cooling in air.

The extrusions were finish straightened on a Sutton five-roll rod and tube straightener and cut into 22-inch blanks. The extrusions were generally about 90 inches long and furnished three 22-inch blanks, one 13-inch rifling trial blank, plus several metallographic specimens.

Four CG-27 extrusions were performed, with preheat temperatures varied from 2040°F to 2075°F in an effort to select the optimum. It appears that 2050°F is optimum for this press. Lower temperatures increase the extrusion pressure above the practical maximum value. Higher temperatures result in a severe hot-short condition which precludes extrusion without rupture of the extrusion. Additionally, the higher temperatures are more prone to causing mandrel failure by necking.

Two extrusions were performed without incident. One of the extrusions whose mandrel failed was made into usable blanks by a combination of etching and drilling to remove the pieces of mandrel and prepare a bore for rifling. One extrusion was unsatisfactory.

Nine full length blanks and three shorter pieces (12-14 inches) were obtained from the three extrusions used. They were all solution annealed by heating in air at 1875°F for 1 hr prior to quenching in oil. The hardness was reduced from an average level in the air-cooled extrusion of 36 Rc to an average of 87 Rb after solution anneal. The warp in the blanks which was sustained in the anneal was removed by hand straightening in a press.

The pieces then had the sacrificial mild steel mandrel sleeve removed from the bore by machining. On subsequent extrusions of this nature this material was removed by acid dissolving. The bores of all pieces were polished by honing to remove sharp striations and scratches which would not be removed in the swaging operation.

*Proprietary graphite and oil suspension.

**Proprietary glass lubricant by Alpha Molycot Corporation.

The swaging operation was performed on a Ferro 47 four-die rotary swage. The four dies rotate inside a roll cage with hammer blocks riding on the rolls. The oscillating action of the hammer blocks riding over the rolls drives the dies in the radial direction to form the work.

The mandrel, was made of Grade 55B tungsten carbide and was brazed at the taper to a mild steel positioner rod which extends from the swage dies through the work, the work handle, and the feed chuck to a thrust bearing anchor at the rear of the power feed base.

The prepared rifling blank was welded to a hollow handle. The bore of the blank was lubricated with "Oil Dag," and the blank and handle assembly was placed into the power feed chuck fed over the mandrel and into the rotating and radially oscillating dies to produce the rifling. This step requires about 40 seconds. The power feed chuck brake applies a retarding torque to the work to prevent its seizing and flashing between the mating surfaces of the dies. The hardness of the blanks increased from 87 R_B to 103 R_B during the swage rifling.

The bores of the rifled blanks were cleaned and inspected by air gaging and boroscoping prior to heat treatment. They were aged in vacuum at 1450°F for 16 hr, then 1200°F for an additional 16 hr. Hardness after aging averaged 43 R_C. Reinspection of the bores revealed that the bore shrunk about 0.001 inch in diameter during the aging heat treatment. This resulted in the bores being on the minimum specified.

The acceptable rifled and heat treated blanks were chambered and externally machined in accordance with Arsenal Drawing 11701204, sheets 1 and 2, Rev. F conventional machining techniques.

H11 Processing - The processing of the H11 barrels was essentially the same as for the CG-27 except for heat treatment. Six extrusions were attempted with all but the first being successful. The first billet which was preheated to 2000°F stalled after 4 to 5 inches of extrusion and wiped all the ceramic coating from the die. The remaining five extrusions were preheated to 2100°F and performed satisfactorily. All other extrusion parameters were the same as CG-27.

The swaging performance and parameters for the H11 were identical with the CG-27.

The H11 rifled blanks were plugged by welding end caps to them, and evacuated through tubes which were sealed. They were then hardened in an endothermic gas atmosphere by preheating to 1500°F for 45 min, then heating to an austenitizing temperature of 1825°F, followed by an oil quench. They were tempered at 1200°F for 75 min, quenched, straightened, tempered at 1220°F for 75 min and quenched. The resulting hardness was 33-36 Rc. Very little change in bore size occurred during heat treatment.

As with the CG-27, the acceptable H11 rifled blanks were conventionally machined to final configuration. It should be pointed out that they have oversize bores to accommodate chrome plating.

Cobalt-Iron Alloy Processing - The cobalt iron alloy blanks were fabricated by IITRI by extruding rods from canned powder billets. The rod blanks were then gun drilled at Rock Island Arsenal to form the bore.

The first two blanks received were cut in halves to furnish four pieces for establishing swaging parameters. The hardness as measured on the OD of the blanks was 32-33 Rc. The swage dies, shims, and mandrels were the same as used for the CG-27 and H11. The four pieces were welded to handles. Three were preheated for about 45 min in air to 900°F and the fourth to 1100°F. Swaging resulted in fracturing of all blanks. Hardness measurements taken on various as-swaged specimens ranged from 40 to 50 Rc. The material seemed to have high strength but was very brittle as judged from the swaging performance.

The material was reheat-treated as follows: solution treat at 2350°F, water quench, and age 3 hr at 1100°F. This dropped the as-received hardness from 44-49 Rc to 33-39 Rc. After heat treatment the Co alloy was swaged at 1100°F. Swaging of this piece resulted in breaking of the mandrel and the back end of the blank. Work on this alloy was terminated pending additional development on fabrication techniques.

Summary

- Extrusion over a small mandrel is an excellent method of producing gun tube stock of CG-27 for rifling by swaging.
- Extrusion of H11 steel, as conducted in this program, can give tube steels suitable for

further processing by swaging to give a rifled tube. However, other methods of producing such tube stock may be more cost effective and give a product of equivalent quality.

- Swaging is a satisfactory method for rifling CG-27 and H11 7.62mm gun barrels.
- A more rugged and powerful machine is required to rifle the Co-Fe alloy tried in this program.
- Rifling tolerances of ± 0.0002 are easily achieved in rotary swage rifling of 7.62mm bores once the parameters for a given material are established.
- A rifling configuration with a greater number of grooves, with the land and groove width more nearly equal, would be easier to swage-rifle and, therefore, more economical.

Test Firing

The fabrication barrels were chrome-plated by Rock Island Arsenal and test fired there. The following firing schedule was employed for evaluating the chrome-plated CG-27 and chrome-plated H11 barrels:

M134 machine gun firing at a rate of 4000 rounds/min: 500 round burst, cool 10 sec, 500 round burst, cool 10 sec, 500 round burst, cool 10 min in still air. Repeat until 6000 rounds were fired, and cool to room temperature.

Rejection criteria were loss in velocity, yaw, and barrel rupture.

Post Analysis

Bore Measurements - After Rock Island Arsenal completed the firing tests, the rejected barrels were shipped to IITRI for analysis. The rounds to failure for each barrel are listed in Table 18. During the test sequence, silicone impressions of the bore were taken at various intervals. Two bore diameter measurements were taken at 90-degree intervals along the length of each impression. These data are listed in Table 19 for the chrome-plated CG-27 barrels, Table 20 for the chrome-plated H11 barrels, and Table 21 for one of

Table 18

NUMBER OF ROUNDS FIRED ON SCHEDULE I
BEFORE FAILURE WAS OBSERVED

<u>Material</u>	<u>No. of Rounds Fired</u>	<u>Reason for Failure</u>
Chrome-plated CG-27	4,036	Cracked in muzzle area
	7,324	Yaw
Chrome-plated H11	16,291	Yaw
	24,466	Yaw
Standard barrel	12,068	Yaw
	11,283	Crack in breech area

Table 19

**BORE DIMENSIONAL MEASUREMENTS FOR CHROME-PLATED CG-27 BARRELS
AFTER VARIOUS NUMBERS OF TOTAL ROUNDS FIRED ON SCHEDULE I**

Distance from Chamber, in.	Bore Diameter, in.					
	barrel 1, 4,036		Barrel 2			
	Total Rounds		1,016		7,324	
	Posi- tion 1	Posi- tion 2	Posi- tion 1	Posi- tion 2	Posi- tion 1	Posi- tion 2
0	0.307	0.307	0.307	0.307	0.313	0.313
$\frac{1}{2}$	0.307	0.307	0.307	0.307	0.311	0.311
1	0.308	0.309	0.307	0.307	0.314	0.314
$1\frac{1}{2}$	0.310	0.311	0.307	0.307	0.313	0.314
2	0.308	0.308	0.307	0.307	0.311	0.311
$2\frac{1}{2}$	0.308	0.308	0.308	0.308	0.308	0.309
3	0.308	0.308	0.307	0.307	0.308	0.308
4	0.308	0.308	0.307	0.307	0.308	0.308
5	0.308	0.308	0.307	0.307	0.308	0.308
6	0.307	0.307	0.307	0.307	0.308	0.308
7	0.307	0.307	0.307	0.307	0.308	0.308
8	0.307	0.307	0.307	0.307	0.308	0.308
9	0.308	0.308	0.307	0.307	0.308	0.308
10	0.309	0.309	0.307	0.307	0.308	0.308
11	0.309	0.314	0.307	0.307	-	-
12	0.309	0.317	0.307	0.307	0.312	0.313
13	0.312	0.330	0.307	0.307	0.317	0.318
14	0.314	0.340	0.307	0.307	0.317	0.321
15	0.315	0.352	0.307	0.307	0.317	0.322
16	0.320	0.352	0.307	0.307	0.317	0.326
17	0.327	0.362	0.307	0.307	0.322	0.325
$17\frac{1}{2}$	0.331	0.362	0.307	0.307	0.321	0.324
18	Muzzle End Cracked Off		0.307	0.307	0.320	0.322
$18\frac{1}{2}$			0.307	0.307	0.319	0.322
19			0.307	0.307	0.318	0.322
$19\frac{1}{2}$			0.307	0.307	0.310	0.322
20			0.307	0.307	0.311	0.322

Table 20

BORE DIMENSIONAL MEASUREMENTS FOR CHROME-PLATED H11 BARRELS
AFTER VARIOUS NUMBERS OF TOTAL ROUNDS FIRED ON SCHEDULE I

Distance from Chamber, in.	Barrel 1 14,859				Barrel 2 14,167			
	5,074		16,291		1,000		24,466	
	Total Posi- tion	Rounds Posi- tion	Total Posi- tion	Rounds Posi- tion	Total Posi- tion	Rounds Posi- tion	Total Posi- tion	Rounds Posi- tion
0	0.307	0.307	0.307	0.340	0.307	0.307	0.329	0.331
1	0.307	0.307	0.306	0.340	0.307	0.307	0.318	0.340
1½	0.307	0.307	0.307	0.341	0.307	0.307	0.309	0.340
2	0.307	0.307	0.307	0.308	0.307	0.307	0.307	0.324
2½	0.307	0.307	0.307	0.307	0.307	0.307	0.307	0.308
3	0.307	0.307	0.308	0.307	0.307	0.307	0.307	0.307
4	0.307	0.307	0.308	0.307	0.307	0.307	0.307	0.307
5	0.307	0.307	0.308	0.307	0.307	0.307	0.307	0.307
6	0.307	0.307	0.307	0.307	0.307	0.307	0.307	0.307
7	0.307	0.307	0.307	0.307	0.307	0.307	0.309	0.309
8	0.307	0.307	0.308	0.307	0.307	0.307	0.309	0.309
9	0.307	0.307	0.308	0.307	0.307	0.307	0.308	0.308
10	0.307	0.307	0.308	0.307	0.307	0.307	0.308	0.308
11	0.307	0.307	0.308	0.307	0.307	0.307	0.308	0.308
12	0.307	0.307	0.307	0.308	0.307	0.307	0.308	0.308
13	0.307	0.307	0.308	0.308	0.307	0.307	0.308	0.308
14	0.307	0.307	0.308	0.308	0.307	0.307	0.308	0.308
15	0.307	0.307	0.307	0.309	0.307	0.307	0.308	0.309
16	0.306	0.307	0.307	0.309	0.307	0.307	0.308	0.309
17	0.305	0.306	0.306	0.310	0.307	0.307	0.308	0.309
17½	0.305	0.306	0.304	0.311	0.307	0.307	0.308	0.309
18	0.305	0.306	0.303	0.311	0.307	0.307	0.308	0.309
18½	0.305	0.306	0.302	0.311	0.307	0.307	0.308	0.309
19	0.305	0.305	0.302	0.311	0.307	0.307	0.308	0.309
19½	0.305	0.305	0.302	0.310	0.307	0.307	0.308	0.309
20	0.305	0.305	0.302	0.307	0.307	0.307	0.306	0.307
21	0.305	0.305	0.303	0.307	0.307	0.307	0.305	0.307
22	0.305	0.305	0.303	0.307	0.307	0.307	0.305	0.307
23	0.305	0.305	0.303	0.307	0.307	0.307	0.305	0.307
24	0.305	0.305	0.303	0.307	0.307	0.307	0.305	0.307
25	0.305	0.305	0.303	0.307	0.307	0.307	0.305	0.307
26	0.305	0.305	0.303	0.307	0.307	0.307	0.305	0.307
27	0.305	0.305	0.303	0.307	0.307	0.307	0.305	0.307
28	0.305	0.305	0.303	0.307	0.307	0.307	0.305	0.307
29	0.305	0.305	0.303	0.307	0.307	0.307	0.305	0.307
30	0.305	0.305	0.303	0.307	0.307	0.307	0.305	0.307

Table 21

BORE DIMENSIONAL MEASUREMENTS FOR A STANDARD GUN BARREL
AFTER VARIOUS NUMBERS OF TOTAL ROUNDS
FIRED ON SCHEDULE I

Distance from Chamber, in.	Bore Diameter, in.			
	10,065		12,068	
	Total Rounds		Total Rounds	
	Position 1	Position 2	Position 1	Position 2
0	0.321	0.321	0.328	0.328
$\frac{1}{2}$	0.321	0.322	0.338	0.340
$1\frac{1}{2}$	0.310	0.318	0.322	0.339
2	0.305	0.305	0.308	0.309
$2\frac{1}{2}$	0.307	0.307	0.309	0.310
3	0.307	0.307	0.308	0.309
4	0.307	0.307	0.308	0.309
5	0.307	0.307	0.308	0.309
6	0.307	0.307	0.308	0.308
7	0.307	0.307	0.307	0.308
8	0.307	0.307	0.307	0.308
9	0.307	0.307	0.307	0.308
10	0.307	0.307	0.307	0.308
11	0.307	0.307	0.307	0.308
12	0.307	0.307	0.308	0.309
13	0.307	0.307	0.312	0.313
14	0.307	0.307	0.312	0.313
15	0.307	0.307	0.309	0.310
16	0.307	0.307	0.307	0.307
17	0.307	0.307	0.308	0.308
$17\frac{1}{2}$	0.307	0.307	0.307	0.308
18	0.307	0.307	0.307	0.308
$18\frac{1}{2}$	0.307	0.307	0.307	0.307
19	0.307	0.307	0.307	0.307
$19\frac{1}{2}$	0.307	0.307	0.307	0.308
20	0.307	0.307	0.307	0.308

the standard chrome-plated steel barrels. Figures 43 through 47 plot these data and give an excellent representation of what is occurring along the bore surface during the firing schedule.

According to these graphs, with chrome-plated H11 barrels and the standard gun barrels, when failure occurs severe erosion is present in the barrel just forward of the breech area. With the CG-27 chrome-plated barrels, when failure occurs severe erosion is present in the muzzle area of the barrel. Another representation of these data is shown in Figure 48. Here, the maximum bore diameter--regardless of position--is plotted as a function of number of rounds fired. Since two bore measurements were made at each position at 90° intervals, two data points for each measurement are shown.

Metallographic Examination

Metallographic examination was performed with the scanning electron microscope and the optical microscope. These observations revealed that the transverse sections typified the failure mode and that the optical microscope was sufficient for characterization of the failure mode.

Chrome-Plated Gun Steel Barrels - Examination of the bore measurements indicated that for chrome-plated gun steel, the maximum erosion occurs in the area just forward of the breech. Additionally, there appears to be an increase in erosion in the region 11 to 16 inches from the breech. Also revealed in the silicone rubber molds is the general removal of the rifling at the muzzle end of the barrel. To determine changes which were produced by firing until the two steel barrels were unserviceable, transverse metallographic specimens were prepared at 1/2, 1 1/2, 2, 10, 17 1/2, and 19 1/2 inches from the chamber. Photomicrographs taken at these positions on the two chrome-plated gun steel barrels are shown in Figures 49 through 60. Figures 49 through 54 show the structure of the standard chrome-plated barrel which failed after 11,283 rounds by a large crack extending from the bore surface to the outer edge of the barrel. Figure 49 is a transverse section at 1/2 inch from the chamber. It will be noticed that a massive crack is present, and this particular crack typifies many of the cracks in this region: all of the chrome plate has been removed; massive amounts of the steel have been removed by general erosion; the microstructure near the crack and the bore surface appears to be ferrite and carbide; it also appears as though some decarburization along the bore has occurred; and, additionally,

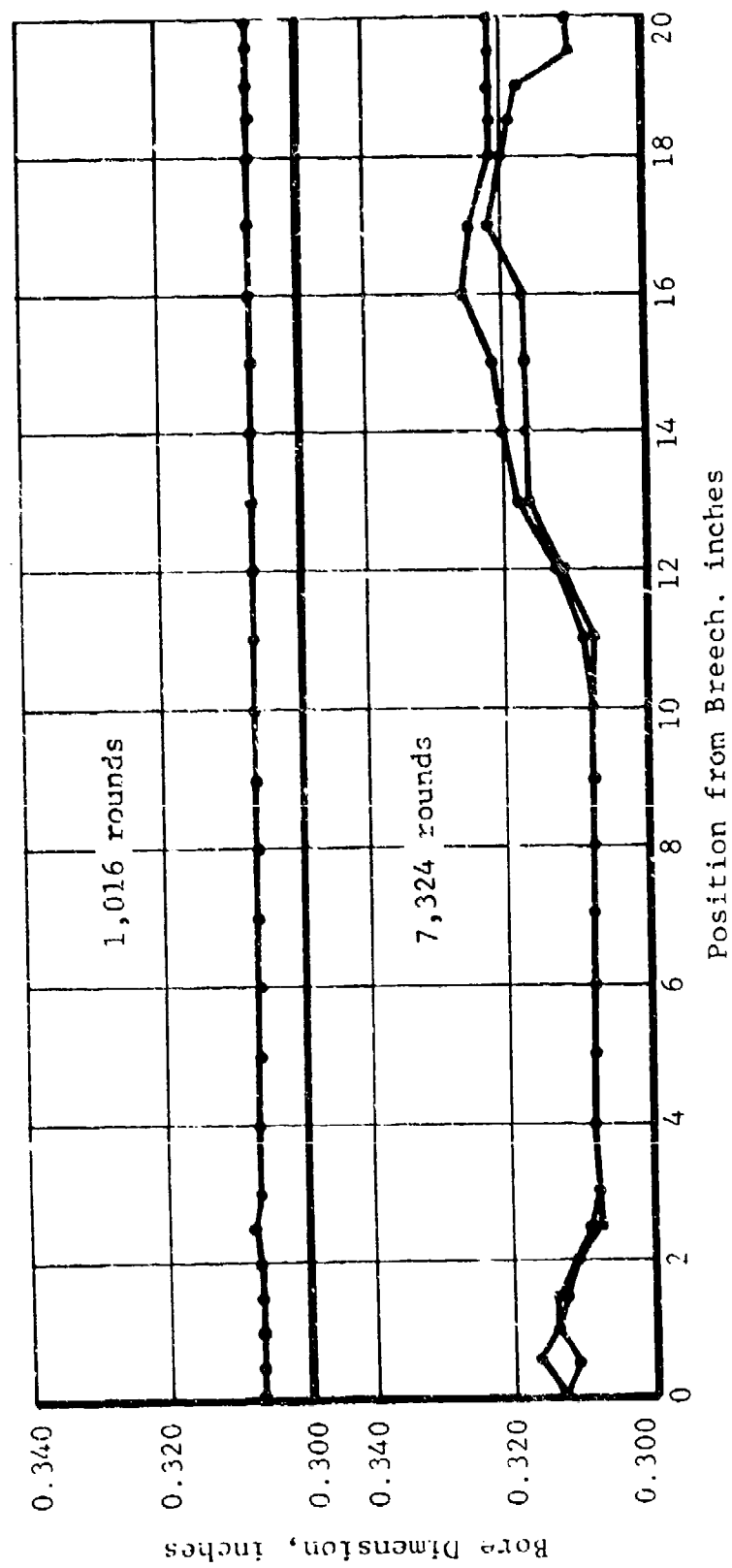


FIGURE 43 BORE PROFILE FOR CG-27 MATERIAL FOR VARIOUS NUMBERS OF TOTAL ROUNDS FIRED.

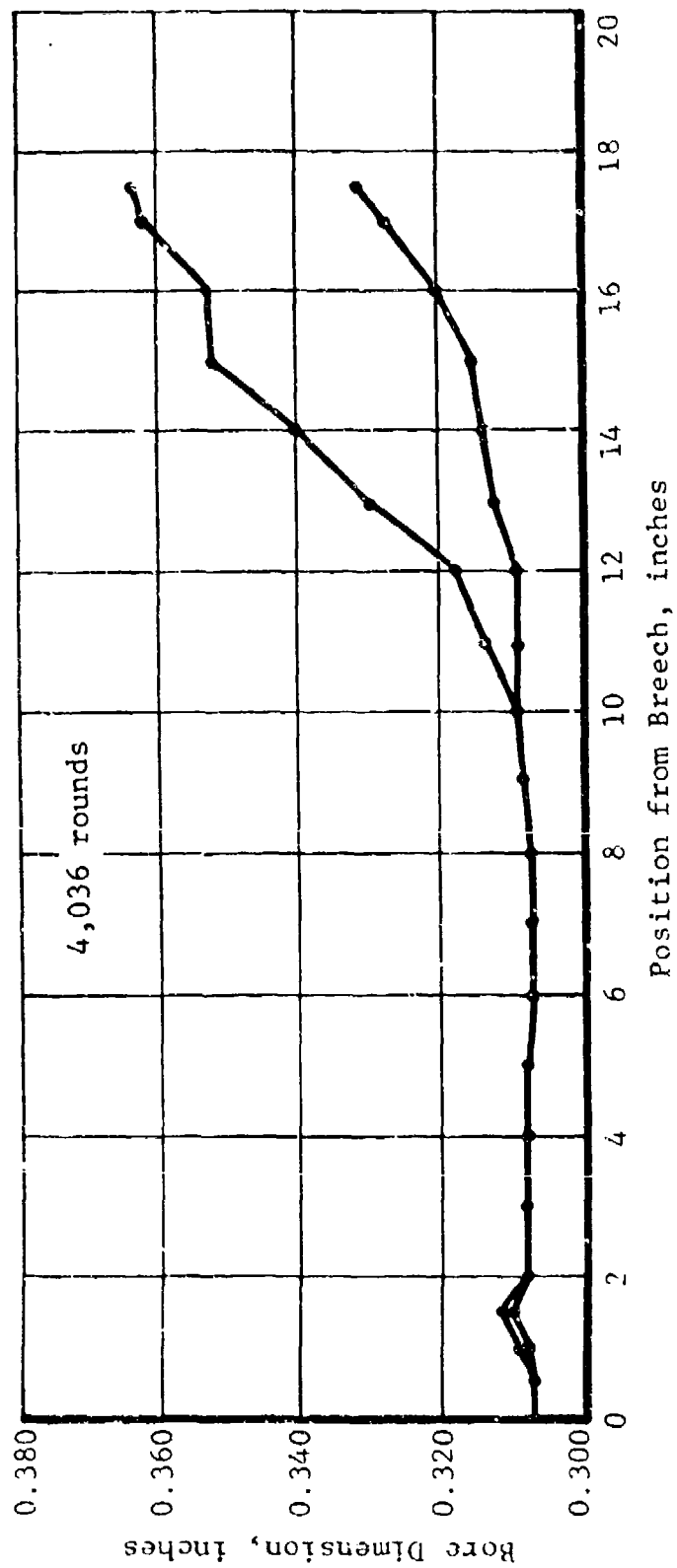


FIGURE 44 BORE PROFILE FOR CG-27 MATERIAL FOR 4036 TOTAL ROUNDS FIRED.

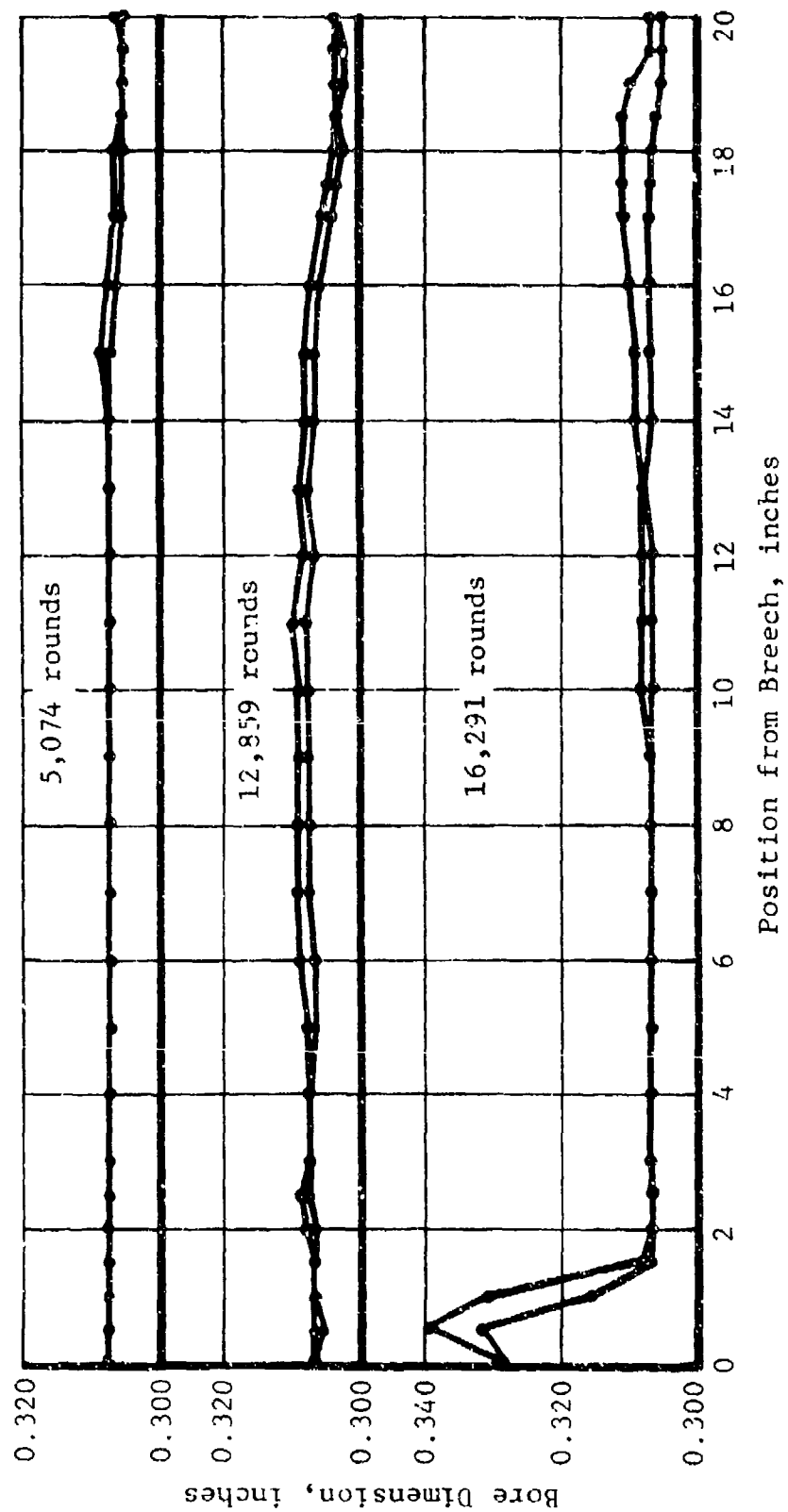


FIGURE 45 BORE PROFILE FOR H11 MATERIAL FOR VARIOUS NUMBERS OF TOTAL ROUNDS FIRED.

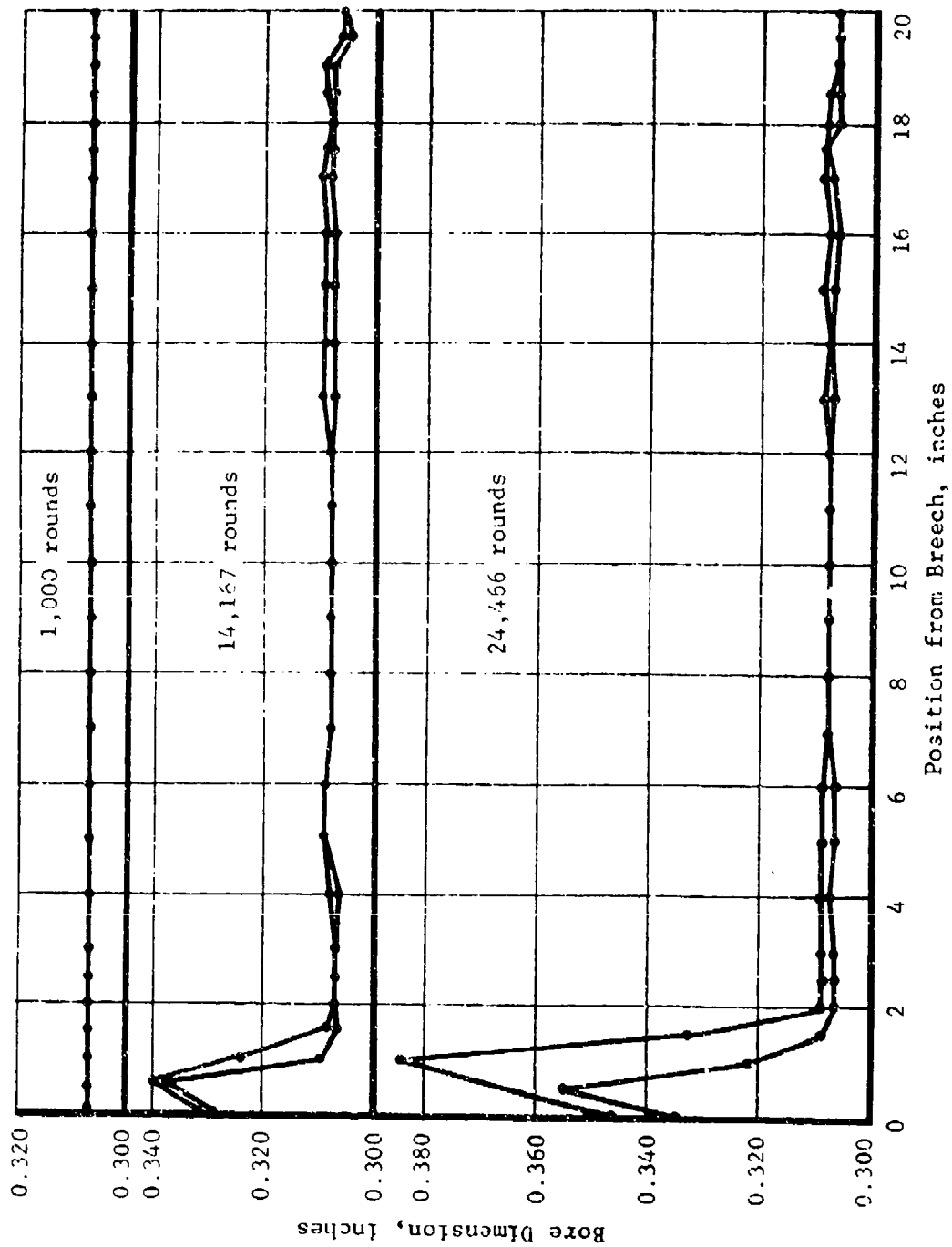


FIGURE 46 BORE PROFILE FOR H11 MATERIAL FOR VARIOUS NUMBERS OF TOTAL ROUNDS FIRED.

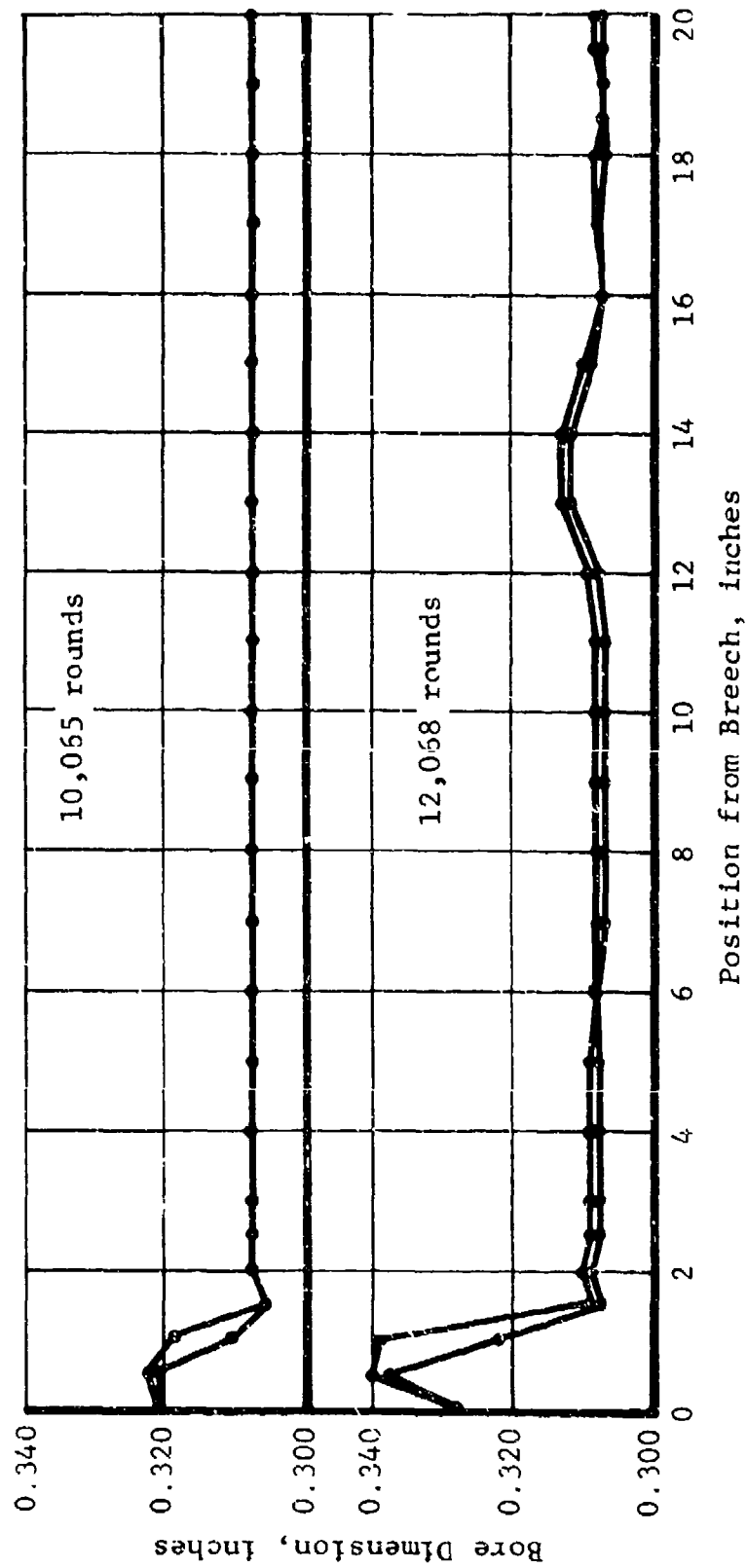


FIGURE 47 BORE PROFILE OF STANDARD STEEL BARREL FOR VARIOUS NUMBERS OF TOTAL ROUNDS FIRED.

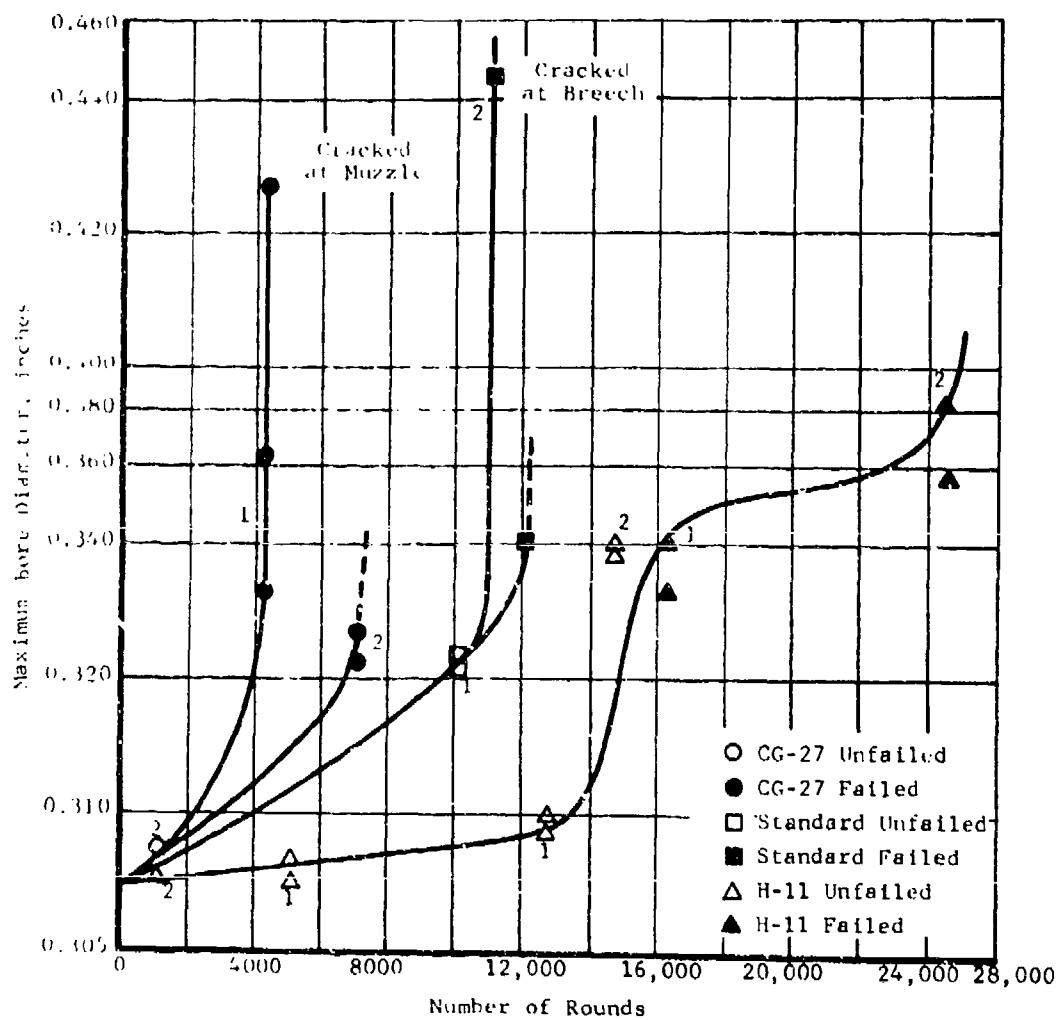


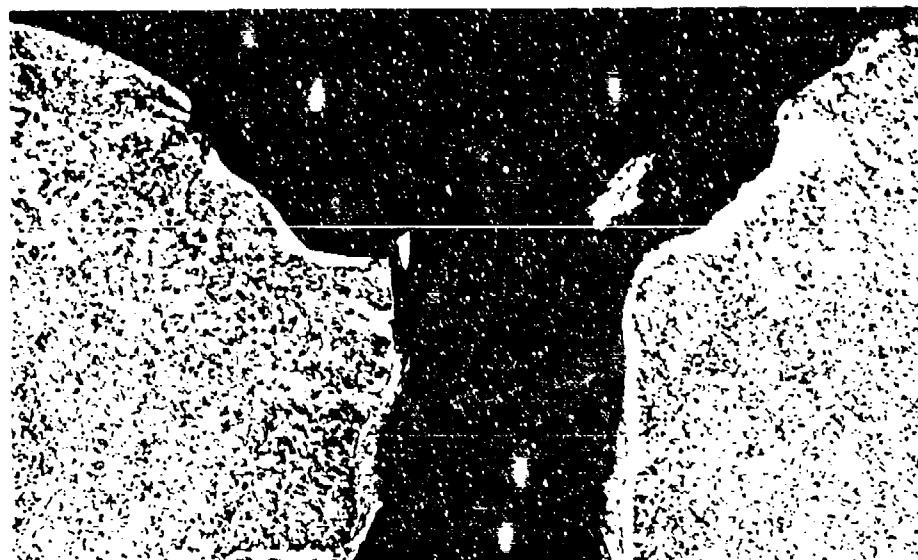
FIGURE 48 MAXIMUM CRACK OR EROSION DEPTH FOR VARIOUS GUN BARRELS AS A FUNCTION OF NUMBER OF ROUNDS FIRED.



Nital Etch

160X

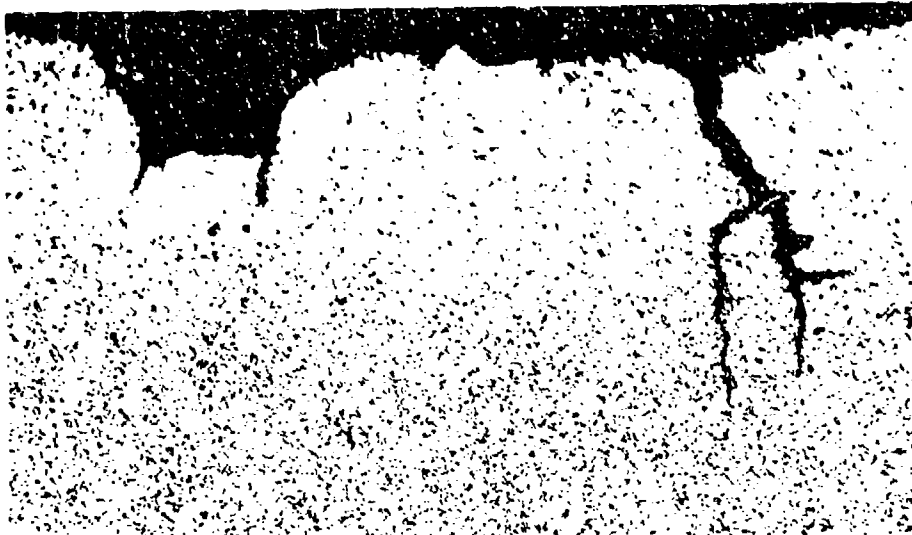
FIGURE 49 TRANSVERSE SECTION AT 1/2 INCH FROM THE CHAMBER OF A STANDARD CHROME-PLATED GUN BARREL AFTER FIRING 11,283 ROUNDS AND BEING DECLARED UNSERVICEABLE.



Nital Etch

160X

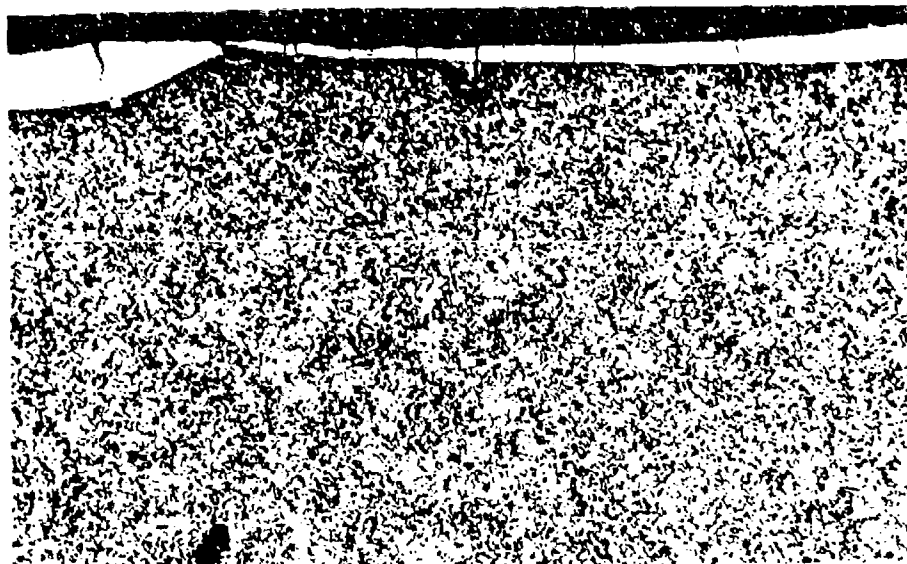
FIGURE 50 TRANSVERSE SECTION AT 1 1/2 INCHES FROM THE CHAMBER OF A STANDARD CHROME-PLATED GUN BARREL AFTER FIRING 11,283 ROUNDS AND BEING DECLARED UNSERVICEABLE.



Nital Etch

160X

FIGURE 51 TRANSVERSE SECTION AT 2 INCHES FROM THE CHAMBER OF A STANDARD CHROME-PLATED GUN BARREL AFTER FIRING 11,283 ROUNDS AND BEING DECLARED UNSERVICEABLE.



Nital Etch

160X

FIGURE 52 TRANSVERSE SECTION AT 10 INCHES FROM THE CHAMBER OF A STANDARD CHROME-PLATED GUN BARREL AFTER FIRING 11,283 ROUNDS AND BEING DECLARED UNSERVICEABLE.



Nital Etch

160X

FIGURE 53 TRANSVERSE SECTION AT 17 1/2 INCHES FROM THE CHAMBER OF A STANDARD CHROME-PLATED GUN BARREL AFTER FIRING 11,283 ROUNDS AND BEING DECLARED UNSERVICEABLE.



Nital Etch

160X

FIGURE 54 TRANSVERSE SECTION AT 19 1/2 INCHES FROM THE CHAMBER OF A STANDARD CHROME-PLATED GUN BARREL AFTER FIRING 11,283 ROUNDS AND BEING DECLARED UNSERVICEABLE.

copper alloy has been deposited in the crack. Microhardness measurements taken from near the bore surface to midway between the bore surface and the outer barrel surface varied from R_C 23 to R_C 30 and confirm the change in metallurgical structure near the bore surface. This hardness difference or softening indicates that the bore material in the steel barrel experienced a temperature excursion in excess of the tempering temperature, about 1200°F, employed in the heat treatment of the barrel.

Figure 50 shows the microstructure near the bore surface of a transverse section at 1 1/2 inches from the chamber. The comments made on Figure 49 also pertain to this photograph.

Figure 51 shows the transverse microstructure at the 2 inch location. The cracks are appreciably smaller; however, the same observations regarding general structure can be made on this section along the bore.

The metallographic structure of the transverse section at the 10 inch location is shown in Figure 52. This particular site is at the intersection of a land and groove. The thickness of the chrome plate on the land has been greatly reduced, whereas very little reduction in thickness has occurred in the groove portion. The metallurgical structure appears to be rather uniform and is quenched and tempered martensite. No appreciable cracking in the steel was observed.

Figure 53 shows the structure of the barrel at 17 1/2 inches from the chamber. The general physical appearance of the structure is similar to Figure 52. However, it does appear that the region directly below the land is ferrite and carbide. The bore surface at 1/2 inch from the muzzle is depicted in Figure 54. Again, it is apparent that the land is completely removed. The material above the steel is copper alloy.

Figures 55 through 60 show the bore at the various sites for the second standard chrome-plated barrel which was declared unserviceable after 12,068 rounds because of yaw.

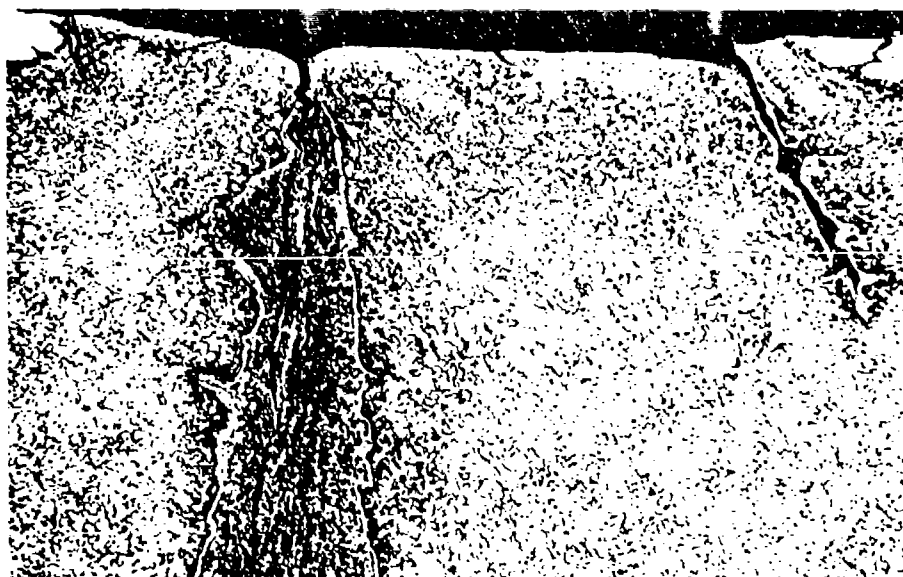
Examination of the transverse section which was cut 1/2 inch from the chamber was very similar to Figure 49. The chrome plating was completely removed, and large cracks with copper alloy in them were present; however, none of the cracks were more than half way through the barrel wall. Figure 55 shows one of the intermediate cracks and typifies the area at the 1/2 inch position.



Nital Etch

160X

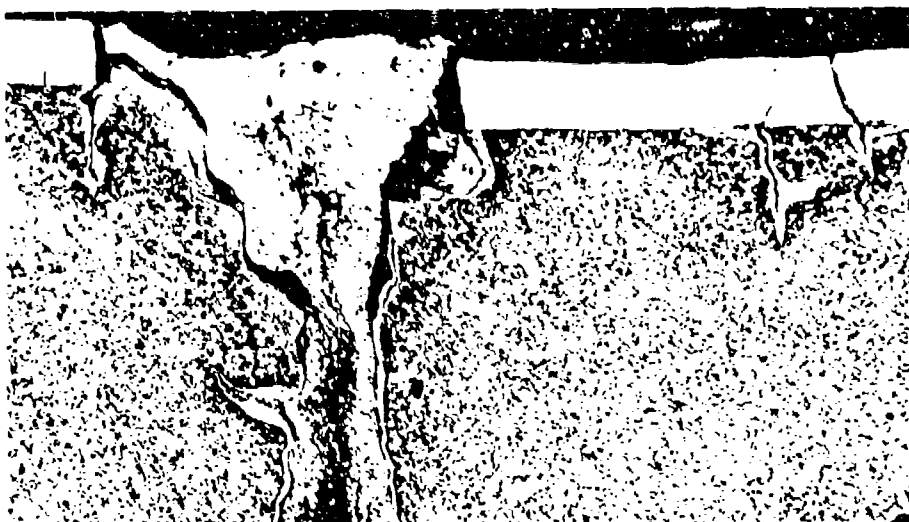
FIGURE 55 TRANSVERSE SECTION AT 1/2 INCH FROM THE CHAMBER OF A STANDARD CHROME-PLATED GUN BARREL AFTER FIRING 12,068 ROUNDS AND BEING DECLARED UNSERVICEABLE.



Nital Etch

160X

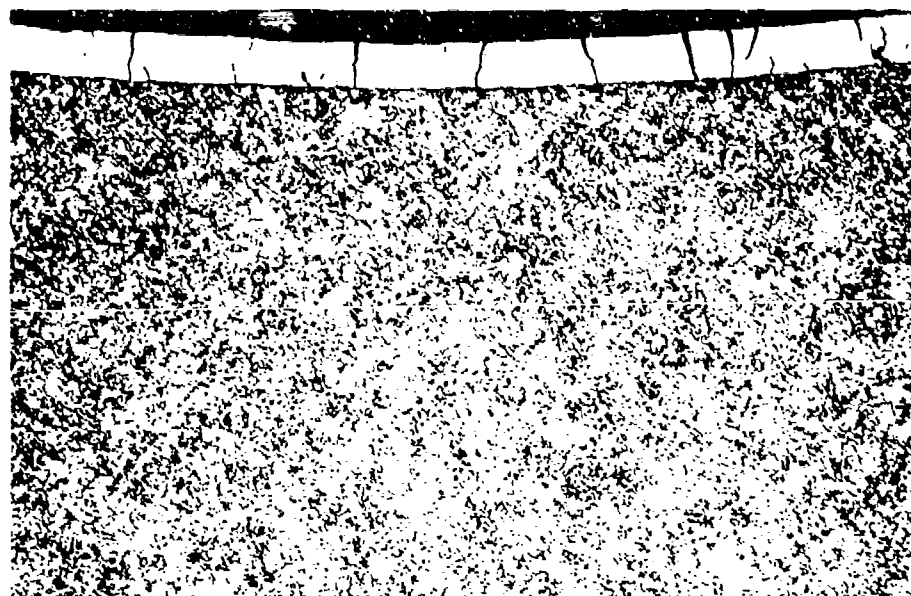
FIGURE 56 TRANSVERSE SECTION AT 1 1/2 INCHES FROM THE CHAMBER OF A STANDARD CHROME-PLATED GUN BARREL AFTER FIRING 12,068 ROUNDS AND BEING DECLARED UNSERVICEABLE.



Nital Etch

160X

FIGURE 57 TRANSVERSE SECTION AT 2 INCHES FROM THE CHAMBER OF A STANDARD CHROME-PLATED GUN BARREL AFTER FIRING 12,068 ROUNDS AND BEING DECLARED UNSERVICEABLE.



Nital Etch

160X

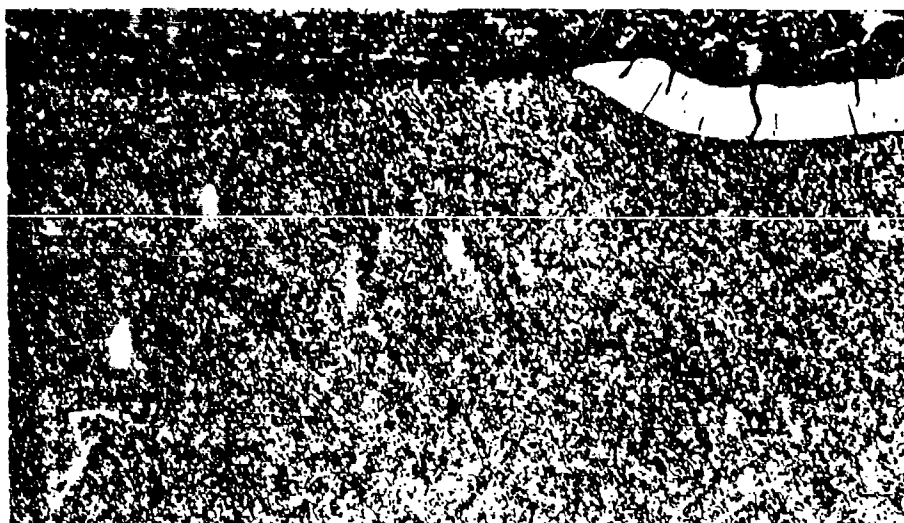
FIGURE 58 TRANSVERSE SECTION AT 10 INCHES FROM THE CHAMBER OF A STANDARD CHROME-PLATED GUN BARREL AFTER FIRING 12,068 ROUNDS AND BEING DECLARED UNSERVICEABLE.



Nital Etch

160X

FIGURE 59 TRANSVERSE SECTION AT 17 1/2 INCHES FROM THE CHAMBER OF A STANDARD CHROME-PLATED GUN BARREL AFTER FIRING 12,068 ROUNDS AND BEING DECLARED UNSERVICEABLE.



Nital Etch

160X

FIGURE 60 TRANSVERSE SECTION AT 19 1/2 INCHES FROM THE CHAMBER OF A STANDARD CHROME-PLATED GUN BARREL AFTER FIRING 12,068 ROUNDS AND BEING DECLARED UNSERVICEABLE.

Figure 56 shows the structure at the bore surface at the 1 1/2 inch site. The land was completely removed; some chrome-plating in the grooves remained; large cracks filled with copper alloy were present; relatively large displacements of the steel can be noted; and the metallurgical structure has been modified from quenched and tempered martensite to ferrite and carbide. The white layer is present and does not appear to be interconnected with the ferrite.

At the 2 inch position, there are relatively large cracks in the chrome plate and the steel. Figure 57 shows a portion of the transverse section. The characteristic features are the presence of the copper alloy in the cracks, the discontinuous white layer, the change in structure to ferrite and carbide near the crack and bore surface, and the presence of most of the chrome plate.

Figure 58 shows the typical appearance of the transverse section at 10 inches. The cracks in the chrome-plate can readily be seen; however, the general integrity of the region is good. Further examination of the sample revealed a thinning of the chrome plate on the barrel similar to that of Figure 52.

Figure 59 shows the transverse section at 17 1/2 inches from the chamber. The lands have been removed, some of the chrome-plate in the grooves remains, the large displacement of steel is apparent, some copper buildup is present, and there is no evidence of a white layer or change in metallurgical structure.

A photomicrograph of the transverse section of the barrel at 1/2 inch from the muzzle end is presented in Figure 60. At this position, the lands have eroded away, the chrome plate in the grooves remains, a copper alloy buildup on the bore surface is present, and no white layer or metallurgical changes in structure have been induced.

From these photomicrographs, it is evident that several events are occurring--the cracking of the chrome plating, the cracking of the steel, the apparent flaking or spalling of the chrome plate, the buildup of copper in the cracks, the presence of white layer, the thinning of the chrome plate toward the muzzle, the removal of the lands, the relative movement of large regions of the steel, and the smearing of copper alloy along the bore surface.

While all of the previously mentioned observations are important in the general erosion of the barrels, it appears that two phenomena are capable of producing an early failure.

These are erosion, by a combination of factors, just forward of the breech and the rapid propagation of a single crack to the outer surface of the barrel to produce catastrophic failure.

With the standard chrome-plated gun steel it appears that a rather rapid deterioration of the chrome plate is achieved in the area just forward of the chamber. The mechanism of erosion is directly related to the chrome plating. As plated, the chrome deposit is extremely brittle and often has cracks present. On firing the barrel, further cracking is produced in the chrome plate and, because of good coupling between the chrome plate and the gun steel, cracks are induced into the steel. As firing continues, the chrome plate flakes off and erosion and cracking continue in the steel.

From this point on, a contest exists as to whether failure will occur due to erosion of the steel or catastrophic failure due to cracks extending through the wall of the barrel. In the erosion process, the steel is removed by reaction with the propellant gas stream and by shallow flaking due to propagation and interconnection of existing cracks in the barrel. The failure is observed by monitoring velocity, accuracy, and yaw. In the catastrophic failure, one of the cracks exceeds the critical flaw size required for rapid propagation under the stress field developed in the firing cycle. In this instance the fracture toughness of the gun steel is sufficiently low that the pressure and thermal gradients can develop a crack of critical size which rapidly propagates to the outer surface of the barrel and results in a catastrophic failure.

Chrome-Plated H11 Steel Barrels - The bore measurements on the two chrome-plated H11 steel barrels indicated that the erosion pattern produced was similar to the one present in the standard chrome-plated gun barrels, the only difference being that significantly more rounds were required before the H11 barrels were declared unserviceable. Transverse metallographic samples were taken at the same distance from the chamber as for the standard barrels. Figures 61 through 72 show the bore area for two H11 barrels. Figures 61 through 66 pertain to the H11 barrel which fired 16,291 rounds before being declared unserviceable.

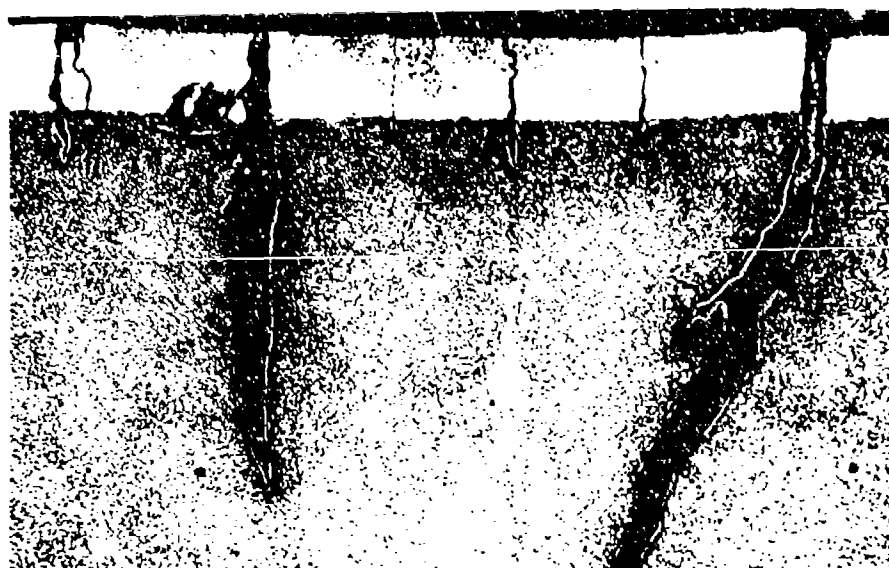
The transverse section at 1/2 inch from the chamber is shown in Figure 61. The removal of the chrome plate, the massive erosion of the steel, the crack in the steel, and the presence of white layer are apparent. The metallurgical



Nital Etch

160X

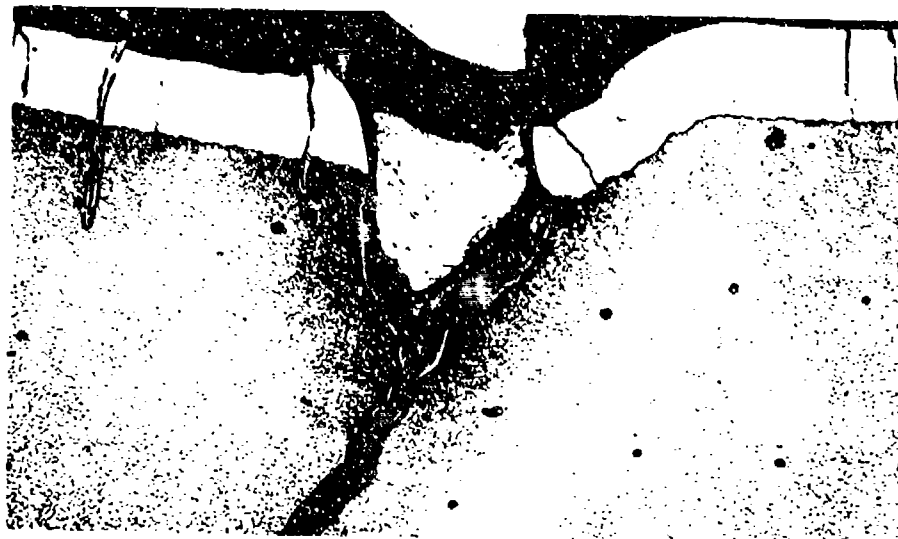
FIGURE 61 TRANSVERSE SECTION AT 1/2 INCH FROM THE CHAMBER OF A CHROME-PLATED H11 STEEL GUN BARREL AFTER FIRING 16,291 ROUNDS AND BEING DECLARED UNSERVICEABLE.



Nital Etch

160X

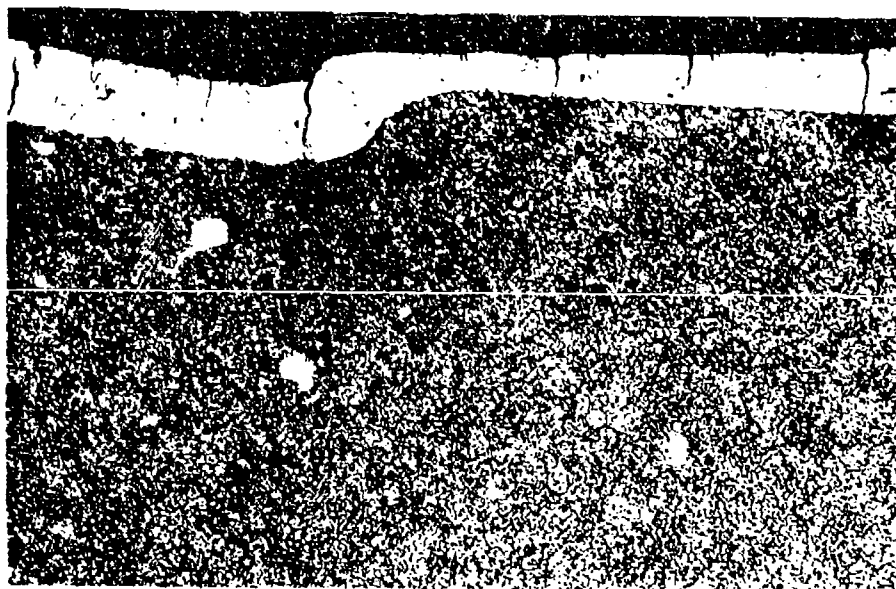
FIGURE 62 TRANSVERSE SECTION AT 1 1/2 INCHES FROM THE CHAMBER OF A CHROME-PLATED H11 STEEL GUN BARREL AFTER FIRING 16,291 ROUNDS AND BEING DECLARED UNSERVICEABLE.



Nital Etch

160X

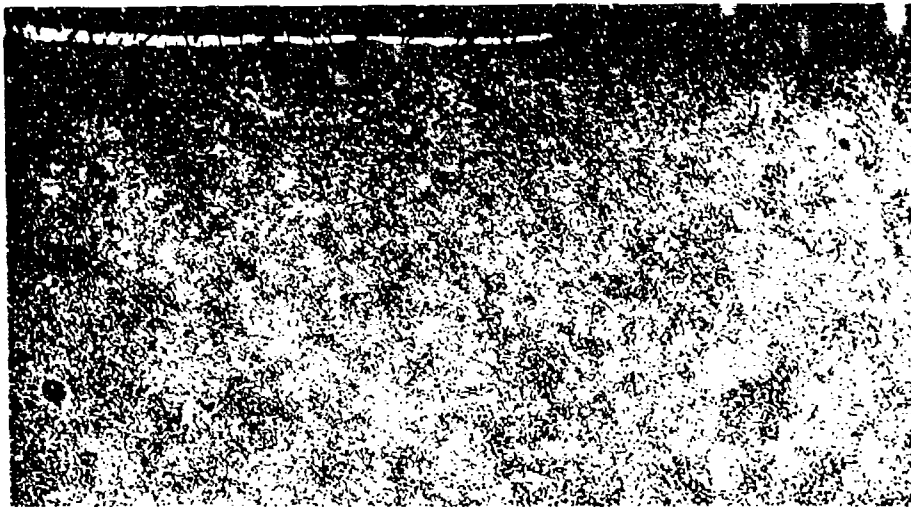
FIGURE 63 TRANSVERSE SECTION A' 2 INCHES FROM THE CHAMBER OF A CHROME-PLATED H11 STEEL GUN BARREL AFTER FIRING 16,291 ROUNDS AND BEING DECLARED UNSERVICEABLE.



Nital Etch

160X

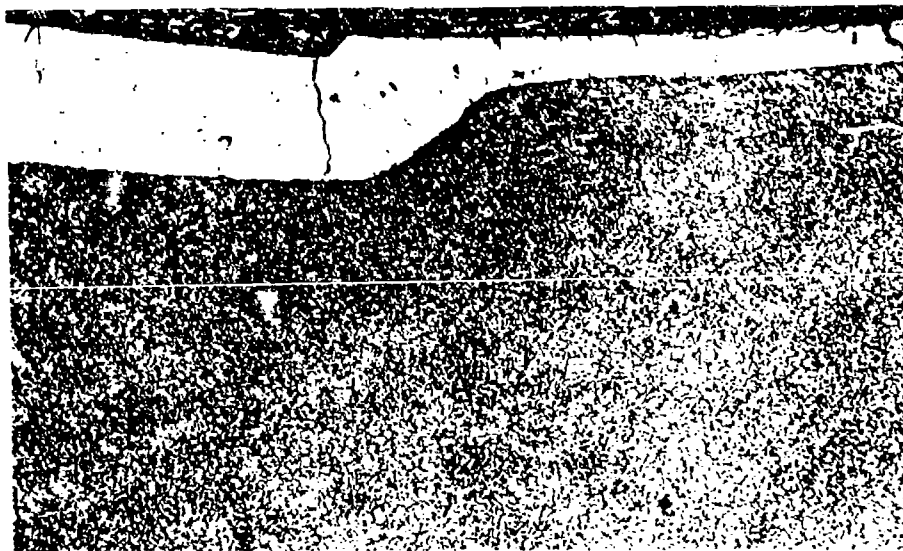
FIGURE 64 TRANSVERSE SECTION AT 10 INCHES FROM THE CHAMBER OF A CHROME-PLATED H11 STEEL GUN BARREL AFTER FIRING 16,291 ROUNDS AND BEING DECLARED UNSERVICEABLE.



Nital Etch

160X

FIGURE 65 TRANSVERSE SECTION AT 17 1/2 INCHES FROM THE CHAMBER OF A CHROME-PLATED H11 STEEL GUN BARREL AFTER FIRING 16,291 ROUNDS AND BEING DECLARED UNSERVICEABLE.



Nital Etch

160X

FIGURE 66 TRANSVERSE SECTION AT 19 1/2 INCHES FROM THE CHAMBER OF A CHROME-PLATED H11 STEEL GUN BARREL AFTER FIRING 16,291 ROUNDS AND BEING DECLARED UNSERVICEABLE.

structure is quenched and tempered martensite with little or no alteration. Microhardness tests were taken along the bore surface to about midway through the barrel. Uniform measurements of R_C 36 were obtained.

Figure 62 depicts the bore surface at 1-1/2 inches. Comparison with Figures 50 and 56, the standard gun steel at a similar location, provides an interesting contrast despite the difference in number of rounds fired. The chrome plate is cracked but still held in place. Examinations in other regions showed the rifling to be present. The cracks are typical, filled with copper alloy and the white layer being present. No other changes in metallurgical structure are apparent.

Figure 63 is the bore region on a transverse section at 2 inches and is very similar to Figure 62. A transverse section at the 10-inch position from the chamber is shown in Figure 64. The reduction of the chrome plate on the land is obvious; however, review of Figure 52 shows that the chrome plate retained on the land of the H11 barrel is thicker than that retained on the standard barrel.

At the 17 1/2 inch position from the chamber the lands are almost completely removed, as can be seen in Figure 65; only scattered thin portions of the chrome plate remain on the land. No copper alloy buildup is present, and the steel microstructure is quencehd and tempered martensite.

Figure 66 shows the transverse section 1/2 inch from the muzzle. Again, chrome plate on the land has been substantially reduced, but all portions of the land are still chrome-plated and copper alloy buildup is present.

Figures 67 through 72 show the transverse sections of the region near the bore surface for the H11 barrel which fired 24,466 rounds before being declared unserviceable. In general, comments made for Figures 61 through 66 apply to these figures. The cracking appears to be more extensive, but this is probably due to the firing of approximately 8,000 more rounds through this barrel. Massive movements of steel are evident at the 1 1/2 and 2 inch regions.

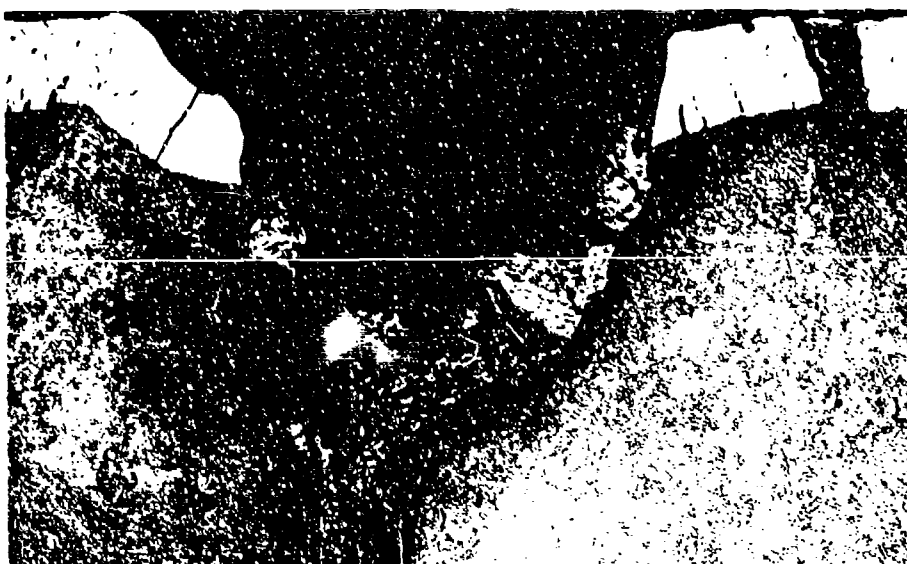
The major difference between the failure mode of the chrome-plated H11 barrels from that of the standard chrome-plated barrels can be attributed to the apparent tenacity of the chrome plate to the H11 steel, the support this steel gives the chrome plate, and the superior high temperature properties of this steel compared to the standard gun steel. Even though both H11 barrels received considerably more



Nital Etch

160X

FIGURE 67 TRANSVERSE SECTION AT 1/2 INCH FROM THE CHAMBER OF A CHROME-PLATED H11 STEEL GUN BARREL AFTER FIRING 24,466 ROUNDS AND BEING DECLARED UNSERVICEABLE.



Nital Etch

160X

FIGURE 68 TRANSVERSE SECTION AT 1 1/2 INCHES FROM THE CHAMBER OF A CHROME-PLATED H11 STEEL GUN BARREL AFTER FIRING 24,466 ROUNDS AND BEING DECLARED UNSERVICEABLE.



Nital Etch

160X

FIGURE 69 TRANSVERSE SECTION AT 2 INCHES FROM THE CHAMBER OF A CHROME-PLATED H11 STEEL GUN BARREL AFTER FIRING 24,466 ROUNDS AND BEING DECLARED UNSERVICEABLE.



Nital Etch

160X

FIGURE 70 TRANSVERSE SECTION AT 10 INCHES FROM THE CHAMBER OF A CHROME-PLATED H11 STEEL GUN BARREL AFTER FIRING 24,466 ROUNDS AND BEING DECLARED UNSERVICEABLE.



Nital Etch

160X

FIGURE 71 TRANSVERSE SECTION AT 17 1/2 INCHES FROM THE CHAMBER OF A CHROME-PLATED H11 STEEL GUN BARREL AFTER FIRING 24,466 ROUNDS AND BEING DECLARED UNSERVICEABLE.



Nital Etch

160X

FIGURE 72 TRANSVERSE SECTION AT 19 1/2 INCHES FROM THE CHAMBER OF A CHROME-PLATED H11 STEEL GUN BARREL AFTER FIRING 24,466 ROUNDS AND BEING DECLARED UNSERVICEABLE.

rounds fired, the complete removal of chrome plate was limited to the 1/2 inch position. In the barrel which fired 16,291 rounds, the size and depth of cracks were quite small. In the barrel which fired 24,466 rounds, the cracking was more extensive but still small in comparison to the standard barrel. The failure of the barrels is probably due to erosion just forward of the breech; however, in comparison to the standard barrels the greater tenacity of the chrome plate to the H11 steel, the better support of the chrome plating, and the better toughness of the H11 steel lead to a longer test life.

Chrome-Plated CG-27 Alloy Barrels - Transverse metalurgical samples were to be prepared for the chrome-plated CG-27 alloy barrels on 1/2, 1 1/2, 2, 10, 17 1/2 and 19 1/2 inch positions from the chamber. However, one of the CG-27 barrels failed by cracking at the muzzle end, and on this particular barrel the transverse specimen was taken at 18 inches from the chamber. Figures 73 through 78 show typical areas near the bore surface.

Figures 73 through 78 pertain to the barrel which failed by cracking near the muzzle after firing 4,036 rounds. The bore area at 1/2 inch from the chamber is shown in Figure 73. Cracking in the chrome plate is present, and associated cracks are also present in the CG-27 alloy. The integrity of the chrome plate is quite good.

Figure 74 shows the microstructure 1 1/2 inches from the chamber. The chrome plate is cracked, and some spalling has occurred.

At the 2 inch site, the chrome plate CG-27 alloy as shown in Figure 75 appears quite similar to that at the 1/2 inch position.

At 10 inches from the chamber, only small amounts of the chrome plate remain on the bore surface. As can be seen in Figure 76, erosion of the CG-27 alloy is present and a scalloping of the surface has occurred.

The structure of the bore at the 17 1/2 inch and 18 inch positions from the chamber is shown in Figures 77 and 78. In both positions it appears that extensive material has been removed from the bore surface. This can be attributed to a gas-metal reaction in which the nickel has probably combined with sulfur in the propellant gases to form a low-melting alloy which has washed away.



Acid Ferric Chloride Etch

160X

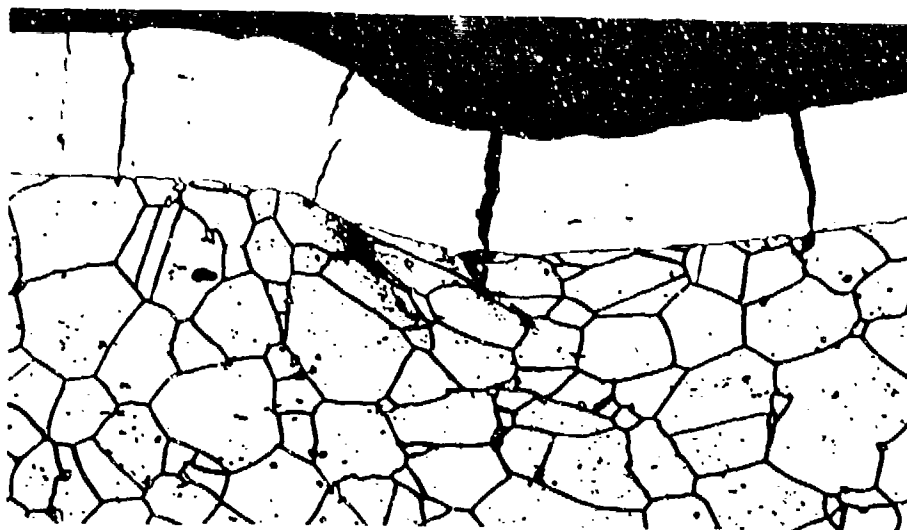
FIGURE 73 TRANSVERSE SECTION AT 1/2 INCH FROM THE CHAMBER OF A CHROME-PLATED CG-27 ALLOY BARREL AFTER FIRING 4,036 ROUNDS AND BEING DECLARED UNSERVICEABLE.



Acid Ferric Chloride Etch

160X

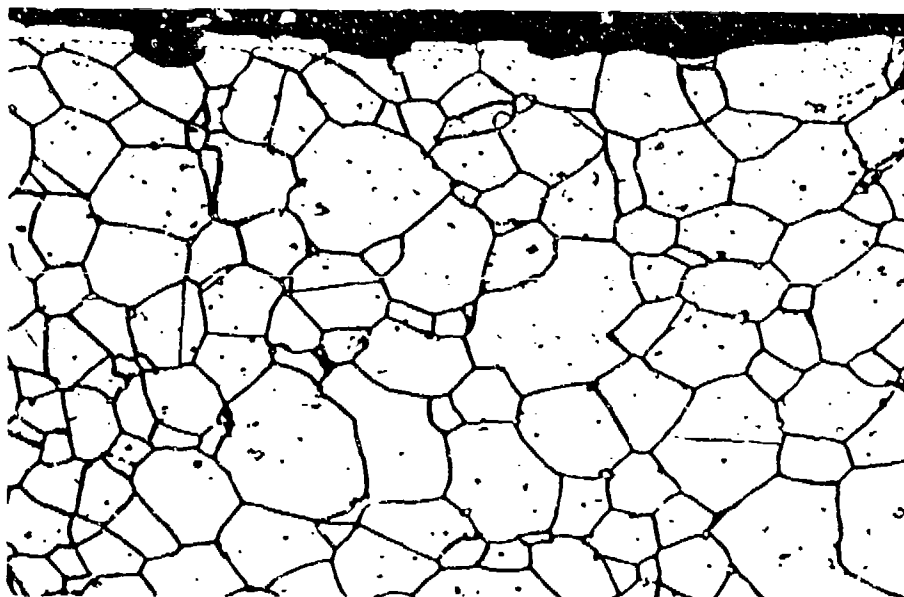
FIGURE 74 TRANSVERSE SECTION AT 1 1/2 INCHES FROM THE CHAMBER OF A CHROME-PLATED CG-27 ALLOY BARREL AFTER FIRING 4,036 ROUNDS AND BEING DECLARED UNSERVICEABLE.



Acid Ferric Chloride Etch

160X

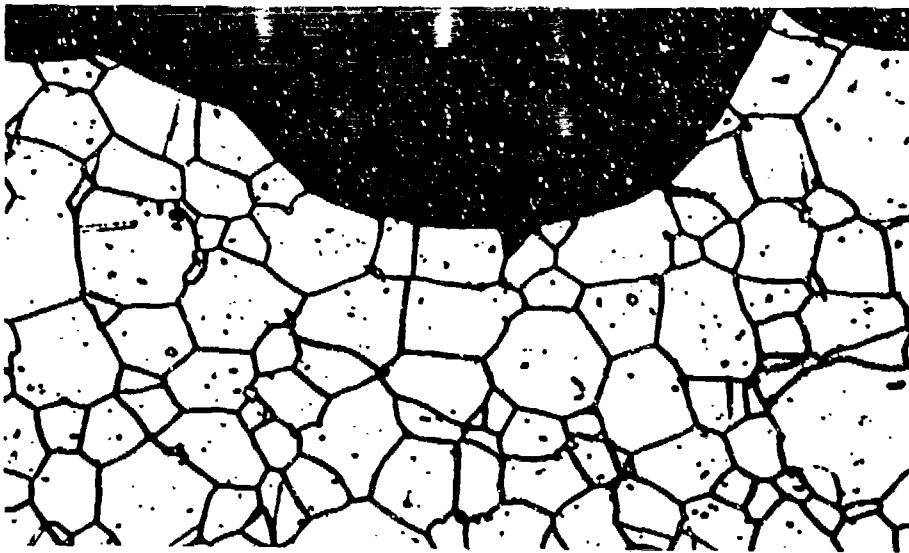
FIGURE 75 TRANSVERSE SECTION AT 2 INCHES FROM THE CHAMBER OF A CHROME-PLATED CC-27 ALLOY BARREL AFTER FIRING 4,036 ROUNDS AND BEING DECLARED UNSERVICEABLE.



Acid Ferric Chloride Etch

160X

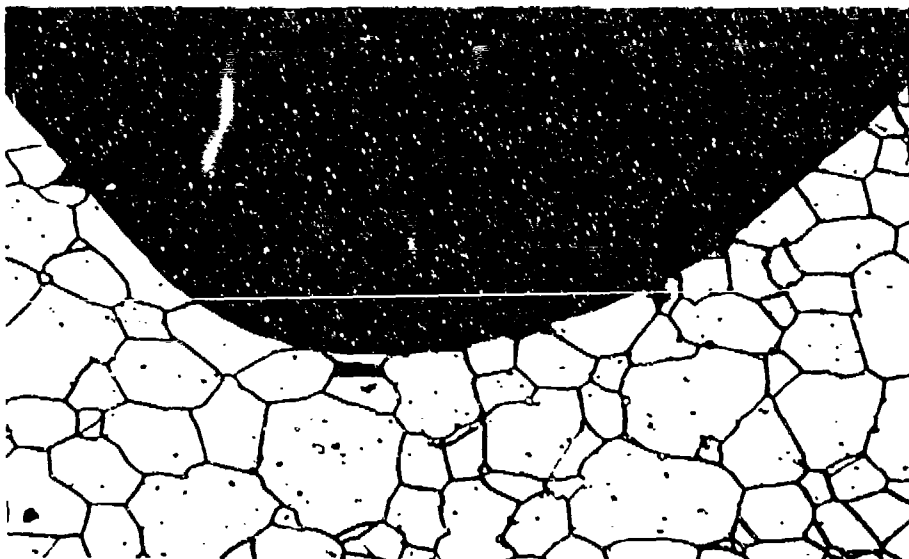
FIGURE 76 TRANSVERSE SECTION AT 10 INCHES FROM THE CHAMBER OF A CHROME-PLATED CG-27 ALLOY BARREL AFTER FIRING 4,036 ROUNDS AND BEING DECLARED UNSERVICEABLE.



Acid Ferric Chloride Etch

160X

FIGURE 77 TRANSVERSE SECTION AT 17 1/2 INCHES FROM THE CHAMBER OF A CHROME-PLATED CG-27 ALLOY BARREL AFTER FIRING 4,036 ROUNDS AND BEING DECLARED UNSERVICEABLE.



Acid Ferric Chloride Etch

160X

FIGURE 78 TRANSVERSE SECTION AT 18 INCHES FROM THE CHAMBER OF A CHROME-PLATED CG-27 ALLOY BARREL AFTER FIRING 4,036 ROUNDS AND BEING DECLARED UNSERVICEABLE.

Figures 79 through 84 are photomicrographs near the bore surface of the second chrome-plated CG-27 alloy barrel after firing 7,324 rounds.

The structure at the 1/2 inch position is shown in Figure 79 and reveals that portions of the chrome plate have been removed, cracking in both the chrome plate and the CG-27 alloy has occurred, and a precipitate having a Widmanstatten pattern is present. The precipitate is probably formed by absorption of interstitial elements such as nitrogen, carbon, hydrogen, or oxygen from the gas stream.

The structures at the 1 1/2 and 2 inch sites from the chamber are shown in Figures 80 and 81. Similar comments to those made for Figure 79 apply.

Figure 82 shows the bore surface of the barrel at the 10 inch position. Portions of the chrome plate have been removed, and intergranular attack has occurred.

The structure of the bore surface at the 17 1/2 inch position from the chamber is revealed in Figure 83. Massive erosion has occurred at this site.

Figure 84 shows the transverse section at the 19 1/2 inch position. The structure present is similar to that observed at the 2 inch position, Figure 81. Figure 85 reveals the structure of the precipitate having the Widmanstatten morphology.

The failure mechanism in the chrome-plated CG-27 alloy barrels can be directly attributed to the particular properties of the chrome plate and the CG-27 alloy. The onset of failure is brought on by the brittle behavior of the chrome plate which cracks and induces cracking in the CG-27 substrate. Once the CG-27 is exposed to the hot propellant gases, a gas-metal reaction, probably nickel plus sulfur, occurs; the barrel becomes "hot short" and barrel material is washed away. The result at approximately 11 inches from the chamber is due to the thermodynamics of the gas stream and the reduction in barrel thickness at that point.

The amount of heat transferred to the barrel from the gas stream is very small compared to the energy in expanding hot gases. Therefore, along the bore surface the temperature is probably reasonably constant and the barrel heats rather uniformly along the length. However, since the last 9 inches of the barrel has a substantial reduction in wall thickness, heating is probably more severe in this region and hence the greater gas-metal reaction.



Acid Ferric Chloride Etch

160X

FIGURE 79 TRANSVERSE SECTION AT 1/2 INCH FROM THE CHAMBER OF A CHROME-PLATED CG-27 ALLOY BARREL AFTER FIRING 7,324 ROUNDS AND BEING DECLARED UNSERVICEABLE.



Acid Ferric Chloride Etch

160X

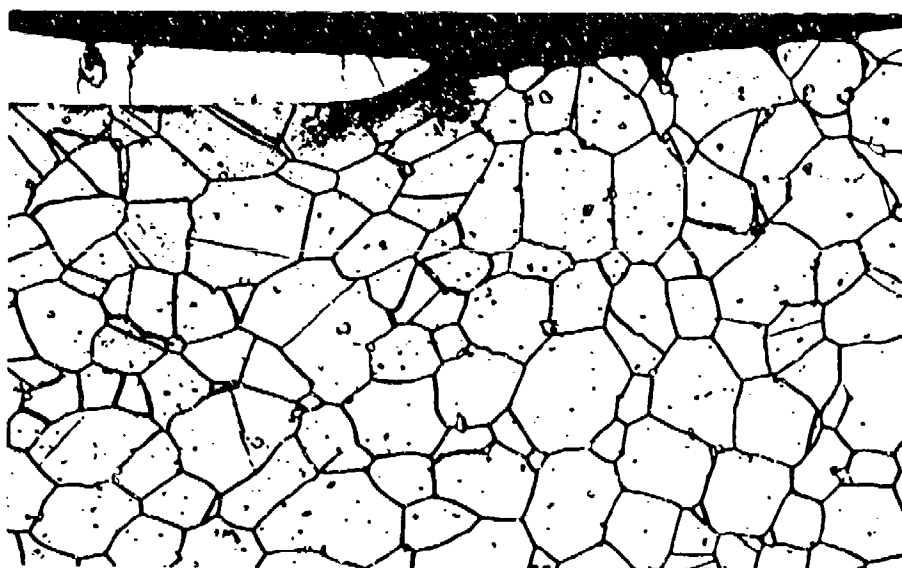
FIGURE 80 TRANSVERSE SECTION AT 1 1/2 INCHES FROM THE CHAMBER OF A CHROME-PLATED CG-27 ALLOY BARREL AFTER FIRING 7,324 ROUNDS AND BEING DECLARED UNSERVICEABLE.



Acid Ferric Chloride Etch

160X

FIGURE 81 TRANSVERSE SECTION AT 2 INCHES FROM THE CHAMBER OF A CHROME-PLATED CG-27 ALLOY BARREL AFTER FIRING 7,324 ROUNDS AND BEING DECLARED UNSERVICEABLE.



Acid Ferric Chloride Etch

160X

FIGURE 82 TRANSVERSE SECTION AT 10 INCHES FROM THE CHAMBER OF A CHROME-PLATED CG-27 ALLOY BARREL AFTER FIRING 7,324 ROUNDS AND BEING DECLARED UNSERVICEABLE.



Acid Ferric Chloride Etch

160X

FIGURE 83 TRANSVERSE SECTION AT 17 1/2 INCHES FROM THE CHAMBER OF A CHROME-PLATED CG-27 ALLOY BARREL AFTER FIRING 7,324 ROUNDS AND BEING DECLARED UNSERVICEABLE.



Acid Ferric Chloride Etch

160X

FIGURE 84 TRANSVERSE SECTION AT 19 1/2 INCHES FROM THE CHAMBER OF A CHROME-PLATED CG-27 ALLOY BARREL AFTER FIRING 7,324 ROUNDS AND BEING DECLARED UNSERVICEABLE.



Acid Ferric Chloride Etch

400X

FIGURE 85 TYPICAL STRUCTURE SHOWING THE MORPHOLOGY
OF WIDMANSTATTEN PRECIPITATE IN CG-27 ALLOY BARREL.

To verify that an increase in sulfur concentration was occurring along the exposed CG-27 bore surface, chemical analysis utilizing X-ray spectrometry was made on the 10 inch transverse sample at a site near the bore surface and at the site midway between the bore surface and the outer diameter of the barrel. Figures 86 and 87 shows the spectrometer readout for the site near the bore surface and away from the bore surface. The sulfur K_{α} and the Mo L_{α} characteristic radiation occur at approximately the same energy level; consequently, the spectrometer analysis causes a reinforcement at approximately the same energy level; however, the S K_{α} and Mo L_{α} peak near the bore surface is higher than that away from the bore surface, indicating a buildup of sulfur near the bore surface. To verify this observation, a digital readout of the S K_{α} and Mo L_{α} peak and the Mo K_{α} peak were made for the two sites of analysis. For the site near the bore surface the peak height for the S K_{α} and Mo L_{α} line was 1683 counts, and the background radiation level was about 750 counts; this yields a peak height to background of 833 counts. For the Mo K_{α} lines the peak height was 86 counts and the background was approximately 75; this gives a count difference of peak to background of 11. The ratio of the S K_{α} and the Mo L_{α} peak to the Mo K_{α} peak is 833 to 11 or about 75 to 1.

At the site away from the bore surface, the combined peak for the S K_{α} and the Mo L_{α} was 1034 counts, and the background was about 530 counts or a difference of 504 counts; whereas for the Mo K_{α} peak the height was 163 counts and the background was approximately 80 counts, or a difference of 83 counts. The ratio of the S K_{α} and Mo L_{α} peak height to the Mo K_{α} peak height is 504 to 83 or about 6 to 1.

Since the site away from the bore surface represents the base material, the ratio of 6 to 1 for the S K_{α} and Mo L_{α} peak to the Mo K_{α} peak typifies the proportion of S to Mo in the base material. The determination near the bore surface shows a ratio of 75 to 1 for the two peaks. Since it can be assumed that the ratio of the Mo L_{α} peak (alone) to the Mo K_{α} peak should be constant, it can be concluded that the increase in the ratio from 6:1 to 75:1 is due to a buildup of sulfur near the bore surface, and the hypothesis that the CG-27 alloy is failing by a sulfur reaction is verified.

SUMMARY AND CONCLUSIONS

A multiphase program has been conducted with the objective of determining materials which would be capable of

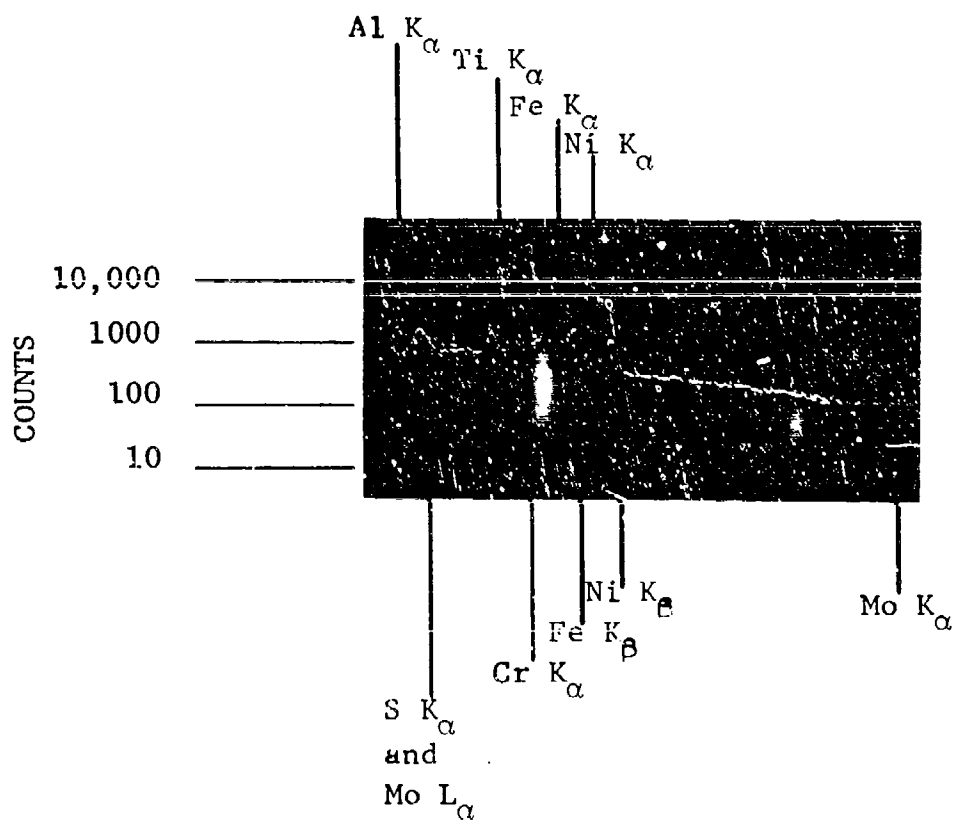


FIGURE 86 X-RAY PATTERN REVEALING CHARACTERISTIC RADIATION OF ELEMENTS AND THEIR RELATIVE CONCENTRATION NEAR THE BORE SURFACE OF A CG-27 ALLOY BARREL.

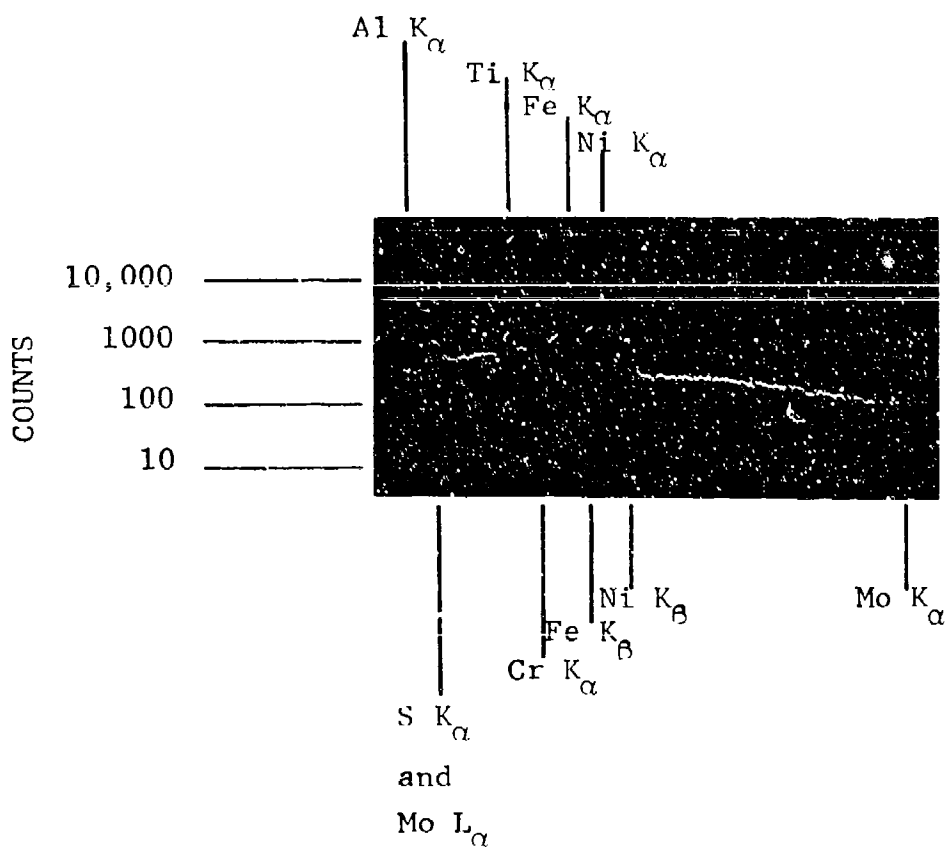


FIGURE 87 X-RAY PATTERN REVEALING CHARACTERISTIC RADIATION OF ELEMENTS AND THEIR RELATIVE CONCENTRATION IN THE BASE MATERIAL OF A CG-27 ALLOY BARREL.

providing extended life and improved performance when employed as 7.62mm Minigun barrels. The specific phases were:

- I. Characterization of erosion/corrosion in the 7.62mm standard steel barrel. A literature review of the general subject of gun barrel erosion in high-performance small caliber weapons.
- II. Materials evaluation, involving vented bomb tests, thermal fatigue, hot hardness, and other mechanical properties of fifteen materials and correlation with gun tests of some alloys.
- III. The selection of three materials from those evaluated in Phase II for evaluation in gun tests.
- IV. Fabrication and gun testing of barrels to failure.
- V. Post analyses of fired barrels after being declared unserviceable.

In Phase I, to determine the mode of failure of standard Minigun barrels, a controlled firing schedule was applied to both plated and unplated barrels to establish the onset of failure. Metallographic examination and X-ray spectrographic analyses were performed on sections from the several barrels. In the chrome-plated barrels, it can be postulated that relatively large cracks are developed in the chrome plate after one shot. These cracks reach the steel substrate in less than 300 rounds and, because of the mechanical coupling, propagate into the steel. Further firing causes crack growth in the steel substrate; as the cracks meet, a portion of the chrome plate and steel flake off. Invariably associated with the cracks is an envelope of the well observed "white layer." Evidence indicates that the white layer is produced after cracking, and spectrographic analyses shows that it is deficient in iron and chromium and probably contains light elements. Additionally, copper was frequently observed within the cracks. In the unplated barrels, very little cracking was observed and the prime mode of failure appeared to be washing away of metal.

In the literature review it was difficult to make comparisons between various materials, inserts, coatings, etc., because of the wide range of propellants, firing schedules,

calibers of weapons, velocities, and material conditions which were reported. However, some general trends were discerned. Steels or special iron-base alloys have not shown outstanding promise as bore surface materials. Chrome plating these materials markedly improves their erosion resistance. Certain cobalt alloys have shown satisfactory performance as liners in guns when single-base propellants were employed. It appears that molybdenum or tungsten base materials with optimized mechanical properties would offer an improvement over cobalt base alloys in the environment created by a double-base propellant. However, the cost and fabrication difficulties associated with these refractory metals could present a problem.

In Phase II, a comparison was made of A286, CG-27, X-15, iron-base alloys, high temperature alloys, 22-4-9 austenitic valve alloy, and plated and unplated Cr-Mo-V gun steel in gun tests and vented bomb tests. The gun tests, employing a particular firing schedule, showed that the CG-27 barrel had approximately a 25 percent longer life than the other materials in the unplated condition, but the chrome-plated gun steel barrel had more than twice the life of the unplated CG-27 barrel. The vented bomb tests with WC846 propellant ranked the erosion resistance of the materials (in decreasing order) as follows: chrome-plated gun steel, X-15 alloy, unplated gun steel, 22-4-9 alloy, A286 alloy and CG-27 alloy. Hot hardness and thermal fatigue tests were also conducted. The hot hardness at 1600°F, in decreasing order, is CG-27 alloy, 22-4-9 valve steel, X-15 alloy, A286 alloy, and Cr-Mo-V steel. The thermal fatigue tests ranked the materials, in descending order, as CG-27 alloy, A286 alloy, X-15 alloy and 22-4-9 valve steel. In gun tests with WC846 propellant the ranking was determined to be chrome-plated gun steel and unplated CG-27 alloy, A286 alloy, X-15 alloy and 22-4-9 valve steel.

Examinations of inserts and barrels after firing showed that a correlation in the mode of failure in gun tests could be predicted by the vented bomb. The vented bomb erosion tests showed that CG-27 alloy will fail by reaction with the propellant gas stream if the firing sequence and barrel dimensions are such that sufficient heat is generated to allow the nickel in the CG-27 to react with the sulfur in the gas stream. Sulfur attack of nickel at high temperatures (above 1300°F) is exothermic and is predominantly intergranular in nature. Once attack begins, the metal lattice is opened as the sulfur penetrates the alloy and a low-melting eutectic (about 1170°F) sulfide is formed. The reaction of nickel alloys is somewhat similar; however, it is known that the

increasing chromium content does somewhat retard the sulfur attack. The other alloys will fail by either cracking or flattening of the lands if the conditions of the firing test are such that the barrels attain high temperature.

Using the correlation study as a basis, a variety of steel and superalloys which could offer potential as gun barrels were selected:

1. A286, an iron-nickel-chromium-molybdenum alloy.
2. 22Cr-4Ni-9Mn, an austenitic valve alloy
3. CG-27, an iron-base superalloy
4. X-15, an iron-base alloy
5. Cr-Mo-V steel, the current gun steel
6. Chromium-plated gun steel
7. Haynes Stellite 21, a cobalt alloy
8. 50Co-29Fe-20W-1C, a cobalt alloy
9. H11, a chromium hot work tool steel
10. D2, a high-carbon, high-chromium cold work steel
11. H26, a tungsten hot work tool steel
12. 446, a ferritic stainless steel
13. L605, a cobalt superalloy
14. HS-31, a cobalt-chromium-nickel-iron superalloy
15. S-590, a cobalt superalloy

All materials were tested in the unplated condition except for the gun steel, which was evaluated plated and unplated.

Metallographic examination of the fired vented bomb inserts revealed that:

1. The cobalt-base superalloys tend to fail by cracking.
2. The austenitic valve alloys, typified by 22-4-9 alloy, exhibit brittle behavior in the vented bomb.

3. With the exception of D2 (a high-carbon, high-chromium cold work) steel and 446 stainless steel, steel alloys do not fail by cracking.
4. Chrome plate on steel produces crack starters which propagate into the steel substrate.
5. The 50Co-29Fe-20W-1C alloy and the CG-27 alloy do not appear to fail by cracking in the vented bomb.

In Phase III, materials selection, the 50Co-29Fe-20W-1C alloy, chrome-plated CG-27 alloy, and chrome-plated H11 alloy were selected for evaluation in gun tests because of their mechanical properties and economic considerations.

In Phase IV, barrels of CG-27 and H11 were fabricated utilizing improved hot extrusion and cold swaging methods. The 50Co-29Fe-20W-1C alloy barrel could not be fabricated by this technology. The hot extrusion process reduced a 4-inch round billet to a 1.35 inch diameter rod containing a mild steel sacrificial mandrel. After extrusion, straightening and cutting operations were conducted to obtain true rods. The sacrificial mild steel core was removed either by machining or acid dissolving to produce a barrel blank. The bore surface was honed to prepare a barrel blank suitable for rifling. Rifling was performed by swaging the barrel blank over a tungsten carbide mandrel to produce a premium-quality finished rifled bore surface. The dimensions of the bore diameter were slightly oversize to allow for chrome plating. The swaging operation to produce a rifled barrel required approximately 40 seconds. Chrome-plated barrels of each of the two candidate materials were fired with chrome-plated standard steel barrels in complement in a six-barrel Minigun weapon. The chrome-plated CG-27 alloy barrels were declared unserviceable in the firing tests at 4036, 7200, and 7324 rounds, the standard barrel at 11,283, 11,605, and 12,068 rounds, and the chrome-plated H11 steel barrels after 16,291, 24,466, and 24,583 rounds. Thus on this particular firing schedule the chrome-plated H11 steel barrel showed an improvement of approximately 33 to 100 percent the service life over the standard gun barrel, whereas the chrome-plated CG-27 barrels were inferior to the standard barrel.

Phase V, post analyses, revealed that the chrome-plated CG-27 alloy barrel failed by massive erosion which was probably induced by a high-temperature nickel/sulfur reaction of the CG-27 alloy. This behavior was indicated by the vented bomb tests; the chrome plate should prevent it from occurring.

The chrome-plated standard barrel failed in the classic manner. The outstanding performance of the chrome-plated H11 alloy was due to the high tenacity of the chromium plate to the H11, the hot strength and temper resistance of the H11, and the toughness of the H11 steel when heat treated to medium hardness levels for hot-work die steels. Additionally, examination of the failed barrels indicated that an excellent metallurgical product was produced by the manufacturing technology employed. The quality of the product so produced contributed significantly to the excellent performance of the chrome plate H11 barrels.

RECOMMENDATIONS

Chrome plating is good on a suitable substrate--meaning one which produces high tenacity and has a similar coefficient of thermal expansion, high hot strength, and good toughness.

Cost-effective ferrous alloys appear to offer potential for improved performance with firing schedules used in this work. Hot hardness - high strength steels containing appreciable chromium and carbon, preferably with low nickel content, would be appropriate. Typical of the family are H11, H13, H23, and H26 steels.

The 50Co-29Fe-20W-1C type alloys could offer good potential as barrel materials in the chrome-plated or unplated condition. However, the carbon content should be adjusted below the one percent employed in this study to approximately the 0.5 percent region. This should give increased toughness and a more fabricable alloy without the loss of other essential properties.

The utility of the hot extrusion/cold swaging technology for the manufacture of 7.62mm barrels has been demonstrated. If cost analysis shows this production scheme to be viable then the hot extrusion/cold swaging production method for the manufacture of 7.62mm barrels should be adopted.

REFERENCES

1. "Barrel (D-7161814) for Gun, Machine, Browning, Cal .50, M2, Heavy Barrel-Recommended for Adoption," Ordnance Committee, Minutes 27817, OCD, (Approved) May 1945.
2. H. N. Smith, "The Behavior of Gun Liners and Coatings Tested under Conditions of Hypervelocity," OSRD 6475, Rep. No. A-404, Franklin Institute, Oct. 1945.
3. "Investigation of Gun Erosion at the Geophysical Laboratory," Vol. III, Jan. 1944-July 1944, OSRD 4354, Rep. No. A-300, Geophysical Laboratory, C/W, Nov. 1944.
4. E. F. Osborn, "The Testing of Erosion-Resistant Materials and the Development of Improved Machine Gun Barrels," OSRD 6480, Rep. No. A-409, Geophysical Laboratory, CIW, Nov. 1945.
5. T. H. Gray, "Refractalloy 70 as a Liner Material for Cal .50 Barrels," OSRD 6491, Rep. No. A-420, Westinghouse Electric and Mfg. Co., Inc., Jan. 1946.
6. J. Wulff, "Erosion Tests of Materials in the Form of Short Liners in a Cal .30 Machine Gun Barrel," OSRD 6477, Rep. No. A-406, Johnson Automatics Inc., April 1944.
7. "Investigation of Gun Erosion at the Geophysical Laboratory, Vol. 1, July 1941 to July 1943," OSRD 3448, Rep. No. A263, Geophysical Laboratory, C/W, March 1944.
8. R. M. Parke and F. P. Bens, "Development of Chromium-Base Hot-Hard Alloys as Gun Liner Materials," OSRD 6486, Rep. No. A-415, Climax Molybdenum Co., Jan. 1946.
9. P. H. Brace and J. W. Marden, "Preliminary Report on Molybdenum as a Material for an Erosion-Resistant Gun Liner," OSRD 3700, Rep. No. A-233, Westinghouse Electric and Mfg. Co., Inc., May 1944.
10. J. W. Marden, "Fabrication of Molybdenum for Use as a Gun Liner Material," OSRD 6494, Final Rep. No. A-423, Westinghouse Electric and Mfg. Co., Inc., Oct. 1945.
11. P. H. Brace, "Development of Molybdenum for Gun Liners," OSRD 6495, Rep. No. A-425, Westinghouse Electric and Mfg. Co., Inc., Feb. 1946.

REFERENCES (Continued)

12. S. Breitbart, "On the Erosion of Metallic Nozzles by Powder Gases," BRL Memorandum Rep. No. 533, Aberdeen Proving Ground, Md., April 1951.
13. "Improved Fabrication Technology for 7.62mm Gun Barrels for High Strength Iron, Nickel, and Cobalt Base Alloys," BNPG-1830-563, Battelle-Northwest, Richland, Wash., Dec. 29, 1971.